Research Department Report 48/2006

Dungeness, SE England, UK Palaeomagnetic Secular Variation (PSV) Dating and Environmental Magnetic Properties of Late Holocene Marsh Sediments

Andy Plater, Paul Stupples, John Shaw, and Sigrid Hemetsberger

ISSN 1749-8775

Research Department Report 48/2006

Dungeness, SE England, UK Palaeomagnetic Secular Variation (PSV) Dating and Environmental Magnetic Properties of Late Holocene Marsh Sediments

Andy Plater, Paul Stupples, John Shaw, and Sigrid Hemetsberger

Summary
Palaeomagnetic Secular Variation (PSV) ages were determined for a series of six late Holocene marsh sediment cores from Dungeness Foreland, south-east England, UK. The PSV ages are indicative of an extensive phase of rapid marsh sedimentation during the period of *c* 1100 to 500 years ago. Coupled with an apparent eastward-younging trend in the marsh sedimentation, these chronological data agree well with evidence of late Holocene foreland progradation and storm-induced changes in coastline. The PSV approach, which has relied on the interpretation of palaeoinclination alone, has proved successful even though the high rate of sedimentation limits the resolution of the preserved PSV trends. However, mean whole-core values coupled with a consideration of the temporal trends in palaeoinclination at each site enable effective dating with reference to the Paris archaeomagnetic secular variation calibration curve. Despite clear evidence of diagenetic and pedogenetic overprinting of the NRM and sedimentary evidence of tidal current influences on sedimentation, a cleaned PSV record may be obtained from back-barrier and marsh sediments to provide a chronology for late Holocene coastal minerogenic sequences.

Keywords
Archaeomagnetism
Geochronology
Medieval

Authors' addresses
Andy Plater and Paul Stupples : Department of Geography, University of Liverpool, P.O. Box 147, Liverpool, L69 7ZT. Tel: 0151 794 2843. e-mail: gg07@liv.ac.uk

John Shaw, and Sigrid Hemetsberger : Geomagnetism Laboratory, Oliver Lodge Laboratories, University of Liverpool, P.O. Box 147, Liverpool L69 3BX. Tel: 0151 794 3463. e-mail: shaw@liv.ac.uk

Palaeomagnetic Secular Variation (PSV) Dating and Environmental Magnetic Properties of Late Holocene Marsh Sediments, Dungeness, SE England, UK

1. Introduction

This report describes the results of palaeomagnetic and environmental magnetic measurements undertaken as part of a project funded by English Heritage, through the Aggregate Levy Sustainability Fund, on the late Holocene depositional history of Dungeness Foreland.

The extensive sand and gravel beaches of Dungeness Foreland are a spectacular sedimentary monument to the long-term effects of sea-level change, storms, coastal erosion, and sediment accumulation during the Holocene period (Fig 1). They are unparalleled in the UK and are known internationally as *the* type-site for cuspate gravel foreland environments. The beaches have long attracted humans, with the oldest evidence for human activity being a group of five bronze low-flanged axes recovered from the Lydd quarry in 1985 (Needham 1988). Fire-cracked and worked flints, as well as some Bronze Age pottery, have also been identified as surface scatters on the gravel near Lydd. During the Romano-British period saltworking developed as an important local industry, with saltwater trapped between the shingle beaches and evaporated over fires positioned on the higher beach crests (Barber 1998a). There follows a gap in activity until the onset of land claim from the twelfth century AD which continued through until the early-sixteenth century (Barber 1998b). Today, these beach deposits are attractive as a major source of aggregate for UK industry, and a long history of sand and gravel extraction has resulted in the partial destruction of the beach ridges and their associated palaeoenvironmental and archaeological resource.

Remarkably little is known about the age and depositional history of the 500 or so beach ridges that comprise Dungeness Foreland. Existing models suggest that the earliest beaches were in place by at least 4000 cal years BP, but thereafter our chronology is reliant on limiting radiocarbon dates and archaeological finds on the gravel surface (see above), as well as palaeoenvironmental and historical records relating to the age of marshland landscapes which abut the gravel. Consequently, we have struggled to understand how the foreland developed, and also the impacts which the evolution of the Dungeness Foreland had on the wider landscape history of the Romney Marsh depositional complex (Lewis 1932; Lewis and Balchin 1940; Eddison 1983; Long and Hughes 1995; Long and Innes 1995; Plater 1992; Plater and Long 1995; Plater *et al* 2002). This report is based on research completed as part of a much larger project funded by English Heritage – *The Evolution and Landscape History of Dungeness Foreland* – the aims of which were to establish the age, depositional origin, and landscape history of Dungeness Foreland, and to place this work in the wider setting of the Romney Marsh depositional complex. Development of a macroscale chronology for storms, sediment supply, and landscape change during the mid- to late Holocene is locally important for informing models of coastal evolution and human activity, regionally significant in developing a chronology for sea-level change, storm incidence and sediment processing in the English Channel, and of wider international significance to those with an interest in the sedimentary response of cuspate gravel forelands to environmental changes.

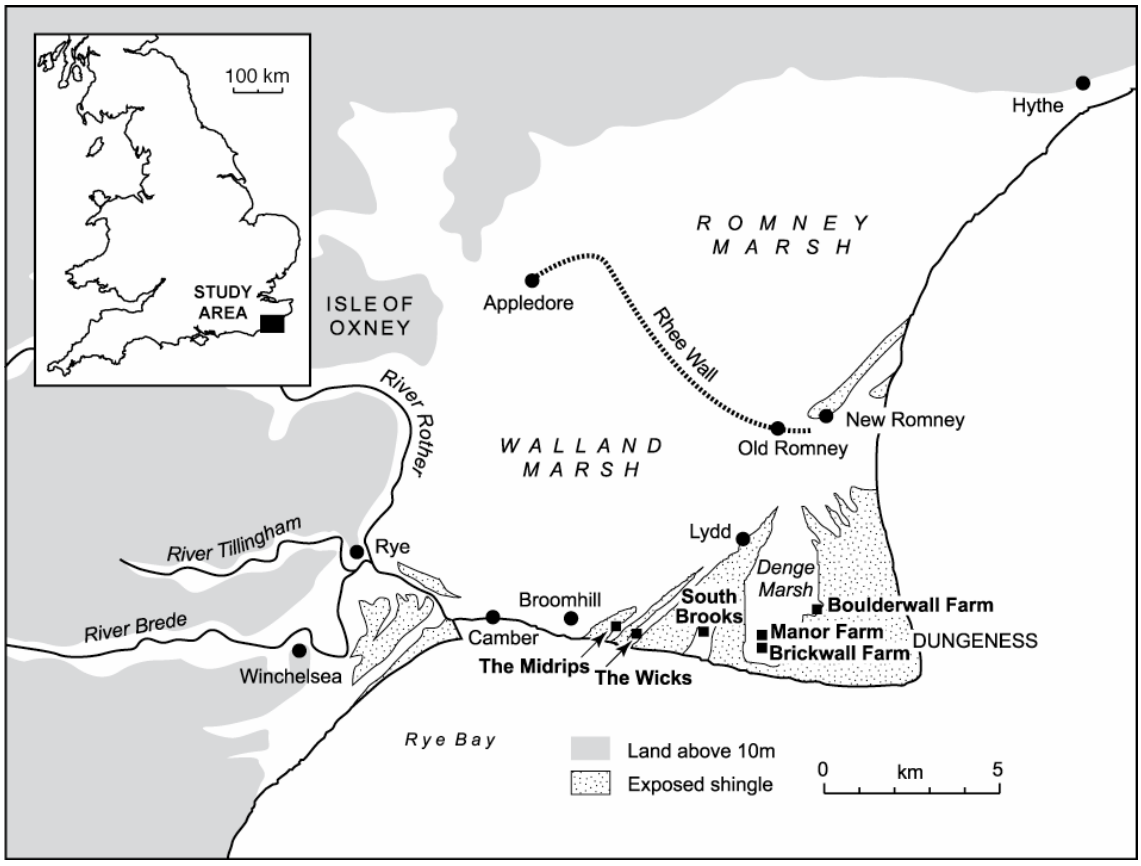

Figure 1 Dungeness Foreland site map, showing the location of the marshland core sites referred to in this report.

1.1. Post-gravel lithostratigraphy

The simplified lithostratigraphy of the six marsh sites is summarised here (Figs 2, 8, and 9) and this sequence, and its subtle variations, is closely comparable to the findings of the more extensive surveys completed previously (Plater 1992; Long and Hughes 1995; Plater *et al* 1999; 2002). The base of the sequence at five of the six sites is defined by the sharp upper contact with the gravel. However, at Manor Farm, a saturated silty sand forms the basal deposit (unit 1) and gravel was not proved here. Overlying the gravel or silty sand is a variably laminated sandy mud to muddy sand (units 2 and 3). These laminated sediments tend to constitute half to two-thirds of the post-gravel marshland sediment sequence and fine-upwards slightly before grading into a heavily mottled clay silt (unit 4) with little structure other than a few sandy lenses or partings. The modern vegetation roots into this mottled sandy mud and forms the thin soil (unit 5) typical of the marsh. Transitions between units are invariably gradational. With one or two exceptions the key feature of the sedimentary sequences recovered from the post-gravel marshland sites is how remarkably consistent they are both temporally and spatially.

1.2. Depositional palaeoenvironments

The principal control on deposition of the post-gravel marshland sediments was the eastward progradation of the Dungeness foreland and the concomitant creation of sheltered back-barrier environments, the morphology of which reflects the varying storm intensity through the mid- to late Holocene (Long and Hughes 1995). The rolling topography of the gravel surface (Fig 2) provided both the protection and accommodation space required for the accumulation of the finer grained fill sequences recovered in the six marshland cores (Plater 1992; Plater *et al* 1999; 2002). The longer sequence recovered at Manor Farm reflects its

location on the bank of a former marsh creek where the gravel was either very deep, removed by the creek, or not deposited in the first instance.

The depositional environments which led to the infill of these openings within the gravel have been determined from litho-, bio- and magnetostratigraphic studies of the marsh sediments (Plater 1992; Long and Hughes 1995; Plater *et al* 1999; 2002). The openings developed into blind tidal channels, open to the sea at one end, but also protected so that tidal flooding was the only source of sediment and wave action was limited. The tidal dominance led to the formation and preservation of the laminated sediments (units 2 and 3) and the extent of their development was restricted by the availability of accommodation space, ie the depth of the gravel surface. Variations in particle size and layer thickness (Stupples and Plater forthcoming) can be related directly to the regular cycles of the tidal energy which cover periods ranging from days to many years. The effects of storms and changing barrier integrity must also be cited as possible explanation for occasional coarser phases in the marsh sediments, eg the Wicks (Fig 9).

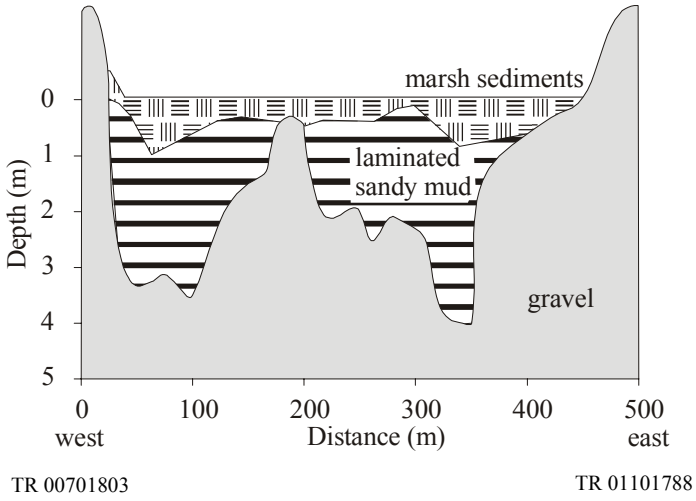

Figure 2 Schematic lithostratigraphic section across The Wicks study area showing gravel topography infilled with finer muddy marshland sediments. The marsh surface is at an elevation of around 2±0.5m OD and the main gravel ridges to east and west rise to an elevation of around 4m OD. The Wicks sample core was taken around 200m north of this section (based on Long and Hughes (1995), figure 4b, p260). See Figures 8 and 9 below for detailed lithostratigraphy and particle size profiles from each of the six marshland core sites.

1.3. Research approach

Amongst the wider project aims, optically stimulated luminescence (OSL) and palaeomagnetic secular variation (PSV) dating were used to constrain the timing of gravel deposition. These techniques were selected due to shortcomings identified in the earlier use of ^{14}C-dated material contained within the gravel complex and the minerogenic sediments both below and above. With the exception of *in situ* peat deposits which abut and overlie the gravel in main back-barrier environment (the former inter- and supratidal areas which were deposited behind the increasing protection of the gravel barrier) and the natural pits (small naturally occurring depressions in the main gravel mass, now partially or completely infilled with marine and freshwater deposits), respectively, these chronological data have been shown to give the age of the contained detrital organic material rather than the timing of sediment deposition. Indeed, ^{14}C dating was applied to date the most recent phase of gravel beach deposition in the region of Dungeness Nuclear Power Station (Greensmith and

Gutmanis 1990), but all ages here are based on reworked sediment and many are chronologically reversed within individual boreholes. Both OSL and PSV dating have the potential to provide information on the timing of the depositional event, assuming effective bleaching on deposition in the case of OSL, or alignment of magnetic particles in the prevailing geomagnetic field during, or soon after, sedimentation in the case of PSV.

Previous work suggests that the marsh sediments which overlie much of the foreland gravels contain no *in situ* organic material suitable for ^{14}C dating (Plater and Long 1995). In addition, these sediments are not well-suited to OSL dating as they are generally fine-grained, occasionally finely-laminated and show evidence of considerable post-depositional changes in water content (ie oxidation/reduction mottling). Some success has been achieved in applying PSV dating approaches to Holocene tidal and subtidal sediments (Maher 1997; Long *et al* 2002). This is despite potential over-printing of the original magnetic signature, the possibility of selective sediment processing by currents, and potentially variable sedimentation rates. The six marshland sample areas (Fig 1) were initially selected on the basis of previous work in the area (Plater 1992; Long and Hughes 1995; Plater *et al* 1999; 2002) and the desire to sample the post-gravel sediments from each of the well-defined areas of marshland which interdigitate with the gravel. Further investigations in the field identified the final coring locations as being representative of the stratigraphy occupying the deeper swales which lie between the gravel ridges (Fig 2) and which consequently record as complete a sedimentary record as possible.

The specific objectives of the phase of the project covered by this report were:

1. to recover replicate sample cores from each of the spatially (and possibly temporally) distinct areas of former marshland across Dungeness;
2. to extract and interpret the record, if any, of PSV within the marsh deposits and to compare this with established PSV master curves in an attempt to define the period of post-gravel marshland sedimentation at each site and so test the validity of the proposed model of very rapid sedimentation based on interpretation of the laminated sediments as tidal rhythmites (Stupples and Plater forthcoming);
3. to measure a series of environmental magnetic properties and develop an understanding of the driving mechanisms of temporal and spatial change in magnetostratigraphy across Dungeness with particular reference to the implications for the integrity of the PSV signal and also to augment other work which focussed on the broader implications for sediment processing and depositional palaeoenvironment as recorded in the lithology, texture, structure, and chemical properties of the marshland sands and muds.

This report details below the principles of PSV dating and interpretation of environmental magnetic data; the results of both palaeo- and environmental magnetic measurements; interpretation of down-core trends in magnetic concentration, mineralogy, and grain-size; assessment of post-depositional geochemical alteration of the magnetic record and, hence, the integrity of the PSV record; and the validity, precision, and accuracy of the PSV ages.

2. Palaeomagnetic Secular Variation Dating

As a consequence of instabilities within the Earth's core, long-term or secular variations in the direction and strength of the Earth's magnetic field take place over periods ranging from 10^4 to a few years. Palaeomagnetic secular variation (PSV) offers an established approach for dating Holocene lake sediments and, by association, lagoonal or tidal sediments laid down in a low energy back-barrier depositional environment. Here, the alignment of fine magnetic particles in the Earth's magnetic field, ie the detrital remanent magnetisation or

DRM, preserves a record of the geomagnetic field's declination, inclination and intensity at the time of deposition (Tarling 1983; Butler 1992; Barendregt 1998).

2.1. PSV Dating of Lake Sediments

Early palaeomagnetic studies included the investigation of secular variations preserved in annually laminated postglacial varved clays (McNish and Johnson 1938; Ising 1943; Granar 1958). These studies revealed the lake-based natural remanent magnetisation (NRM) record to be unreliable due to mechanical reworking by bottom currents. However, Mackereth (1971) was successful in obtaining a record of palaeomagnetic secular variation from the Holocene sediments of Lake Windermere. Here, the necessary conditions for PSV dating were considered to be:

- sediment acquires a measurable intensity of magnetisation at, or close to, the time of deposition;
- magnetic remanence is aligned with the Earth's magnetic field at, or close to, the time of deposition;
- detrital magnetic remanence is sufficiently stable to retain its direction despite subsequent changes in the Earth's magnetic field; and
- sediment samples are collected without significant disturbance of their preserved magnetic orientation.

Despite both major and minor post-depositional disturbances of the sedimentary record introducing some degree of scatter, Mackereth (1971) identified a recognisable and reproducible down-core pattern of directional change. Indeed, the pattern of declination in the upper part of the lake sedimentary record was observed to be in good agreement with the early British archaeomagnetic record (Aitken *et al* 1963) (see Section 2.2). From the PSV record in Windermere, both age and sedimentation rates were obtained which were in good agreement with an established ^{14}C chronology.

Turner and Thompson (1981, 1982) produced a 'master curve' of PSV for Britain over the last 7000 years or so by averaging dated core records from a number of lakes in Scotland, the English Lake District, and north Wales. However, the efficacy of this approach is thought to be limited by the size, shape, and nature of the geomagnetic carrier component as well as the porosity of the sediment. Furthermore, post-depositional changes in the remanence carrier *via* diagenesis introduce a potential complication of the PSV record in that the down-core trends may not be a faithful record of DRM. In direct contrast, however, Snowball *et al* (1999; 2002a; 2002b) and Snowball and Sandgren (2002) have been successful in developing a PSV chronology over the period of AD 1500 to 6500 BC for two lakes in northern Sweden where stable single domain magnetite resulting from authigenic bacterial magnetosomes dominates the magnetic characteristics of the sedimentary record.

A further complication of the sediment-based PSV is that a time delay may be observed between sedimentation deposition and its subsequent alignment in the ambient magnetic field. This aspect of 'lock-in depth' clearly introduces a lag between the sediment deposition and the alignment events.

Holocene PSV has been employed successfully in the study of lake sediments from Ireland (Thompson and Edwards 1982), Fenno-Scandia (eg Tolonen *et al* 1975; Stober and Thompson 1977; 1979; Huttunen and Stober 1980; Saarinen 1994; 1998; 1999; Ojala and Saarinen 2002), Sweden (Morner and Sylwan 1987; Snowball *et al* 1999; 2002a; 2002b; Snowball and Sundgren 2002), Spitzbergen (Løvlie *et al* 1991), Iceland (Thompson and Turner 1985), western Canada (Turner 1987), and southern Argentina (Gogorza *et al* 2000).

2.2. Archaeomagnetic Dating

Archaeomagnetism refers to the magnetisation of archaeological materials. This was first observed in the magnetisation of bricks (Boyle 1691) and volcanic building blocks (Melloni

1853), and subsequently in pottery (Folgheraiter 1899a; 1899b; Mercanton 1918). However, the foundations of archaeomagnetic dating are based on measurements of kilns and hearths of baked clay. Clay commonly contains sufficient ferromagnetic iron oxides which have the potential to acquire a measurable thermo-remanent magnetisation (TRM) induced by the ambient magnetic field as the clay cools (Aitken 1974; Tarling 1983). This archaeomagnetic record can then be based on either the strength or direction of the preserved remanence (Clark *et al* 1988).

For dating over the last two millennia, the archaeomagnetic dating approach (Aitken 1990) makes use of the geomagnetic field data recorded in volcanic lava and speleothem. In Britain, the archaeomagnetic record may be established back to AD 1576 using direct observations (Malin and Bullard 1981). Beyond this date, field directions are inferred from the remanence of features dated by other means, eg pottery, coins, etc, providing the foundation of the early British reference curve covering the period from the Roman period to the present with a gap from about AD 350–1000 (Aitken 1970). Being cyclic, the archaeomagnetic calibration curve is characterised by loops and overlaps from short-term to millennial scales, leading to ambiguities which can only be resolved by independent means (Clark *et al* 1988). However, unlike the sediment-based PSV record, there is no uncertainty of a time lag between the time of formation and the acquisition of remanent magnetisation. Hence, archaeomagnetism has proved effective from about AD 850 to the present with a dating accuracy of ±20 years (at 68% confidence), although this precision decreases for the Dark Ages or the early Medieval period. For regions of limited precision, the current British archaeomagnetic reference curve makes use of lake sediment data from Loch Lomond and other lake records (Turner and Thompson 1979; 1982).

The dating of fine grained minerogenic sediments by archaeomagnetism is considered to be problematical due the relative shallowness of such records making them susceptible to weathering and diagenesis or physical disturbance and bioturbation (Clark *et al* 1988). However, silts from a millpond at Wharram Percy have been dated with some success (Tarling 1983) where the depositional context resembles that of a lake environment. Similarly, well-drained sandy-silts from an Iron Age hillfort at Holmbury have been dated archaeomagnetically (Clark 1979). Significantly, the stability of the DRM is enhanced where the post-depositional environment is either wet and aerobic or, in contrast, dry. Between these two end-members lies a post-depositional setting characterised by significant diagenesis and, hence, chemical overprinting of the DRM – particularly where oxidation mottling is observed (Clark *et al* 1988).

2.3. PSV Dating of Coastal Sediments

Palaeomagnetic studies have been undertaken on Baltic Sea deep water sediments (Rother 1989; Abrahamsen 1995; Kotilainen *et al* 2000), from which a temporal resolution of ±50 years has been achieved for sediments deposited during the last 3000 years (Kotilainen *et al* 2000). Indeed, this recent study concluded that observed disturbances of the sediment cores limited the full use of PSV for dating and core correlation, with declination being particularly sensitive to disturbance, possibly due to changes in depositional conditions. However, the inclination data were considered to be reliable in all cores analysed, and were used to determine sedimentation rates of the order of 0.1–1.0mm/yr.

As mentioned above, some success has been achieved previously in using PSV to date Holocene tidal and subtidal sediments, eg Maher (1997) and Long *et al* (2002). This is encouraging considering that the deposition of fine-grained mineral matter in low-energy coastal settings is subject to potential mechanical reworking by tidal currents, waves, and/or storm surges, particularly on open tidal flat environments. In addition, both tidal and wave conditions exhibit marked temporal variability on scales of seconds to years which, when coupled with aperiodic storms and changing coastal morphology, may result in significant variations in sedimentation rate and preservation potential. Furthermore, the preservation of such tidal and back-barrier deposits at altitudes above mean sea-level, ie those deposited in

upper mudflat and saltmarsh settings, leaves the sedimentary record subject to both diurnal and seasonal changes in water table elevation, sequential oxidation and reduction and, hence, over-printing of the original DRM.

3. Environmental Magnetism

Iron (Fe) and iron-bearing minerals are common in the natural environment, and their presence may be diagnostic of source lithology, soil processes, sediment pathways, pollution, and biological conditions. Differences in the way Fe is structured at the atomic level allow these minerals to be studied and classified according to their magnetic properties. The environmental magnetic properties of sedimentary records may be employed to address a range of palaeoenvironmental questions and issues. Fundamentally, such studies interpret temporal changes in sedimentation, sediment provenance, and past environment and climate from down-core trends in magnetic concentration, mineralogy, and grain-size. For example, depth profiles of sediment magnetic parameters and quotients are increasingly used in palaeoenvironmental work to aid interpretation of lithostratigraphy and correlation between sites (see Thompson and Oldfield 1986; King and Channell 1991; Oldfield 1991; Verosub and Roberts 1995; Dekkers 1997; Walden *et al* 1999 for reviews and examples). Such profiles may identify subtle changes to the lithostratigraphy not always detected by other techniques. Changing magnetic properties may imply a change in source or depositional environment (Nichol *et al* 2000) or a time gap caused by erosion in the sedimentary sequence (Ridgway *et al* 2000). In addition, correlation of the magnetic signatures from different cores may be possible, allowing a degree of relative dating between sites (eg Manley *et al* 1993). Studies have shown magnetic susceptibility to be a useful means of core correlation in lakes (eg Thompson 1973; Thompson *et al* 1975; Oldfield *et al* 1978; Bloemendal *et al* 1979; Thompson and Oldfield 1986) and in the deep sea (eg Robinson 1982; 1986; Thompson and Oldfield 1986). Magnetic susceptibility has also been shown to be related to variations in sediment particle size (Thompson and Oldfield 1986; Oldfield 1999). This raises the potential for magnetic susceptibility to act as a proxy for particle size, although the exact nature of this relationship varies and, therefore, requires some degree of empirical ground-truthing (eg Oldfield and Yu 1994; Wheeler *et al* 1999).

A potential problem with environmental magnetism is that the detrital magnetic signal may be obscured by magnetic components derived from a combination of physical, chemical or biological, diagenetic or authigenic processes, the main source and cycles of which are summarised by Smith (1999). For example, soil formation is well known to lead to the formation of secondary iron oxides which are often amorphous in structure. Pedogenetic processes of particular significance are the oxidation and reduction processes which may occur repeatedly *in situ* in a soil horizon (Maher 1986). In addition, reduction in the presence of organic material also tends to result in the formation of iron sulphides, in particular pyrite and greigite (Snowball 1991). More recently, it has been recognised that biological activity may result in the bacterial formation of ultra-fine magnetite in soils (Fassbinder *et al* 1990), lakes (Snowball 1994), and marine sediments (Petersen *et al* 1986). However, these magnetosomes may degrade rapidly in the surficial sedimentary record. Consequently, the identification of a detrital or depositional natural remanent magnetisation (NRM) requires careful consideration of the sedimentary context and the observed environmental magnetic properties.

3.1. Interpretation of Environmental Magnetic Properties

The interpretation of environmental magnetic properties may focus on different forms of magnetic behaviour or, alternatively, magnetic concentration, grain size, and mineralogy. In terms of magnetic behaviour, ferromagnetism is the spontaneous magnetisation that occurs where the spins of unpaired adjacent atoms become aligned in the absence of an applied magnetic field. Different forms of ferromagnetism include anti-ferromagnetic, ferrimagnetic (eg magnetite, maghemite, titanomagnetite, greigite), and imperfect (or canted) anti-

ferromagnetic (eg goethite, haematite) behaviour, whilst other forms of magnetism include paramagnetism (eg ferrihydrite, lepidocrocite, ilmenite) and diamagnetism (eg carbonate and organic matter) – a review of which is given in Thompson and Oldfield (1986) and Smith (1999). Rather than focussing on magnetic behaviour, the interpretative model employed here centres on the second of the approaches identified above, following the principles outlined in Table 1.

The environmental magnetic properties that correlate positively with magnetic concentration include magnetic susceptibility (χ), normalised anhysteretic remanent magnetisation (or susceptibility of ARM) (χ_{ARM}), and saturated isothermal remanent magnetisation (SIRM).

Ferrimagnetic materials can be divided into different regions of cells of magnetisation known as domains. Above *c* 110µm, grains are referred to as multi-domain or MD because it is energetically favourable to have more than one magnetic domain. In small grains <0.2µm only one domain will form, leading to single domain (SD) or stable single domain grains (SSD). Grains between 0.2 and 110µm are large enough to have more than one domain but exhibit the magnetic properties of SD grains and are known as pseudo-single domain (PSD) grains. Very small (<0.03µm) ferro- or ferromagnetic grains have thermal vibrations at room temperature which are of the same order of magnitude as their magnetic energies. These superparamagnetic (SP) grains do not, therefore, exhibit stable remanent magnetisation. Primary minerals derived from igneous and metamorphic rocks are predominantly MD, PSD and SSD, whilst secondary minerals produced biogeochemically in soils and sediments, or through fire, are mainly SSD and SP grains. In terms of magnetic grain size, whilst χ increases with higher contributions from larger MD grains and very fine SP grains, both χ_{ARM} and SIRM increase with the proportion of fine SSD grain sizes (Maher 1988). The quotients of χ_{ARM}/χ and χ_{ARM}/SIRM also correlate positively with the presence of finer SSD grains (King *et al* 1982). Frequency-dependent susceptibility (χ_{fd}%) is indicative of very fine-grained ferromagnetic grains lying within the SP domain size. Here, χ_{fd}% values range from zero in samples containing no SP grains to *c* 15% where SP grains completely dominate the magnetic mineral assemblage.

Table 1 Magnetic parameters and quotients and their interpretation (adapted from Matthews *et al* 2000, after Stoner *et al* 1996)

Magnetic Property	Interpretation
Volumetric magnetic susceptibility (k) and specific magnetic susceptibility (χ) (measured at low and high frequency).	A first-order measure of the amount of ferromagnetic material (eg magnetite). Susceptibility is enhanced by superparamagnetic (SP) magnetite (<0.03μm) and by large magnetite grains. When the concentration of ferromagnetic material is low, susceptibility responds to antiferromagnetic (eg haematite), paramagnetic, and diamagnetic materials.
Frequency-dependent magnetic susceptibility, χ_{fd} (or k_{fd}), is the difference between low frequency and high frequency susceptibility expressed as a percentage of the low frequency susceptibility.	χ_{fd} indicates the presence of ultra-fine ferromagnetic (superparamagnetic) material, produced by bacteria or by chemical processes mainly in soil. Superparamagnetic material in high concentrations complicates the grain size interpretations using interparametric ratios.
Isothermal remanent magnetisation (IRM), commonly expressed as a saturation IRM (or SIRM) when a field of 1T is applied. A backfield IRM is that magnetisation acquired in a reversed field after SIRM acquisition.	SIRM depends primarily on the concentration of magnetic, mainly ferromagnetic, material. It is grain size dependent, being particularly sensitive to magnetite grains smaller than a few tens of μm.
Anhysteretic remanent magnetisation (ARM), commonly expressed as susceptibility of ARM (χ_{ARM}) when normalised using the biasing DC field.	χ_{ARM} is a measure of the concentration of ferromagnetic material but is also strongly grain size dependent. χ_{ARM} is highly selective of stable single domain (SSD) ferromagnetic grains in the range of 0.02–0.04μm.
The 'hard' IRM (HIRM) is derived by imparting a backfield IRM, typically 100–300mT, on a sample previously given a SIRM.	HIRM is a measure of the concentration of magnetic material with a higher coercivity than the backfield, which commonly gives the concentration of antiferromagnetic (eg haematite and goethite) or very fine grained ferromagnetic grains.
χ_{ARM}/χ	Providing the magnetic mineralogy is dominated by magnetite, χ_{ARM}/χ varies inversely with magnetic grain size, particularly in the size range of 1–10μm.
SIRM/χ	Again, when the magnetic mineralogy is dominated by magnetite, SIRM/χ varies inversely with magnetic grain size. SIRM/χ is more sensitive to changes in the proportion of large (>10μm) grains.
SIRM/ χ_{ARM}	SIRM/ χ_{ARM} increases with increasing magnetic grain size.

Magnetic mineralogy may also be determined through the interpretation of both parameters and quotients. For example, SIRM increases in proportion to the presence of minerals with high magnetisation, eg magnetite, whilst χ may, in addition, reflect the presence of diamagnetic and superparamagnetic minerals (Peck *et al* 1994). Similarly, hard isothermal remanent magnetisation (HIRM) is a measure of the contribution of higher coercivity magnetic minerals, eg goethite and haematite (Robinson 1986). The presence of iron

sulphides in the form of greigite may be interpreted from divergence of the -40 and -100mT backfield isothermal remanent magnetisations and/or a SIRM/χ quotient value in excess of *c* $40x10^3$ Am^{-1} (Snowball 1991).

4. Methods

4.1. Recovery of sample cores

Duplicate and overlapping (in terms of sampling breaks) cores of 65mm diameter were recovered at six sites (Fig 1) using a Stitz piston corer to sample sediments from the base of the sequence to around the upper limit of the laminated units (tidal rhythmites) characteristic of the post-gravel marshland deposits (Fig 8). The elevation of the top of the laminated units varied but the remaining upper section of the sequence in each case was sampled with a combination of gouge corer and/or auger as these subsurface sediments are typically too compact for recovery with the piston corer. These cores were sampled in order to investigate the stratigraphy, palaeoecology, grain-size, sedimentation rate, and sediment provenance of the marsh sediments that post-date the gravel deposits of Dungeness Foreland. A second set of overlapping piston cores were also recovered from each site for PSV dating – the compact nature of the near surface sediments imposing a practical upper limit to the extent of the sequence which could be sampled for this purpose. In this case, the coring location was first orientated relative to magnetic north using a compass and a marker placed on the ground. Core sections were drilled vertically using the piston corer, and the outside of each sampling tube was orientated north on extraction from the borehole. Following decoupling from the corer, *c* 1m core sections were extruded horizontally into PVC gutters from the sampling tubes with their north arrow facing skyward. During this process, the north arrow was translated onto the outer surface of the sediment core using a thin wooden marker. Given the potential for error propagation during sampling, it is acknowledged that whilst cores were drilled vertically with an uncertainty of ±2%, the orientation relative to magnetic north was achieved with an uncertainty of, at best, ±5–10%. A greater uncertainty in core orientation was generally associated with coarser-grained, more saturated sediment cores.

4.2. PSV laboratory sampling

Cores from the six marshland study sites were refrigerated on return to the laboratory to prevent oxidation and ingrowth of magnetic minerals which would adversely affect or 'overprint' the PSV. Palaeodeclination and palaeoinclination data were obtained from 23 cores with typically 10–14 sub-samples (N) measured, these being recovered in 18mm plastic cubes evenly spaced along the nominal metre length of each core. Several cores were sampled at a greater frequency but preliminary results indicated that a lower resolution approach was suitable in that rapid sedimentation rates, perhaps up to 0.5m/y, were implied by the laminated character of the cores (Stupples and Plater forthcoming). Consequently, it was thought unlikely that the individual cores would record any significant secular variation along their length, and this assumption was supported by the results from the cores on which a contiguous sampling regime was applied. Cores were first aligned horizontally in a jig with the north marker facing upward (Fig 3). The uppermost third of the core was then cut away cleanly from this north side as a longitudinal section. Samples were taken along the centre of the core, with their 'up' and 'north' faces being recorded, to minimise the risk of sampling sediment which may have been disturbed or contaminated during coring and extrusion. Samples were then returned to the fridge prior to measurement.

4.2.1. Measuring the NRM

The natural remanent magnetisation (NRM) of the samples was measured in a zero field using a FIT Liquid Nitrogen SQUID Magnetometer, following a minimum of three cleaning steps using alternating field (AF) demagnetisation performed using the University of Liverpool Geomagnetism Laboratory's Tumble-AF Demagnetiser. The cleaning steps (Fig 4) were used to remove any post-depositional and/or post-sampling contamination of the NRM, isolating the dominant detrital remanence component vector (As and Zijderveld 1958;

Zijderveld 1967; Tarling 1983; Butler 1992; Tauxe 2002). Here, the soft remanence component is susceptible to overprinting by both soil-forming and diagenetic processes (see Section 3.0) or, indeed, storage in the laboratory. This overprint may be removed by subjecting the sample to an increasing alternating field with a net zero vector to isolate the high coercivity, hard NRM whose vector passes through the origin of the Zijderveld plots (Clark *et al* 1988; Butler 1992; Borradaile *et al* 1999; Yamazaki *et al* 2003); this is the characteristic NRM of the sample formed during or soon after deposition (Fig 4).

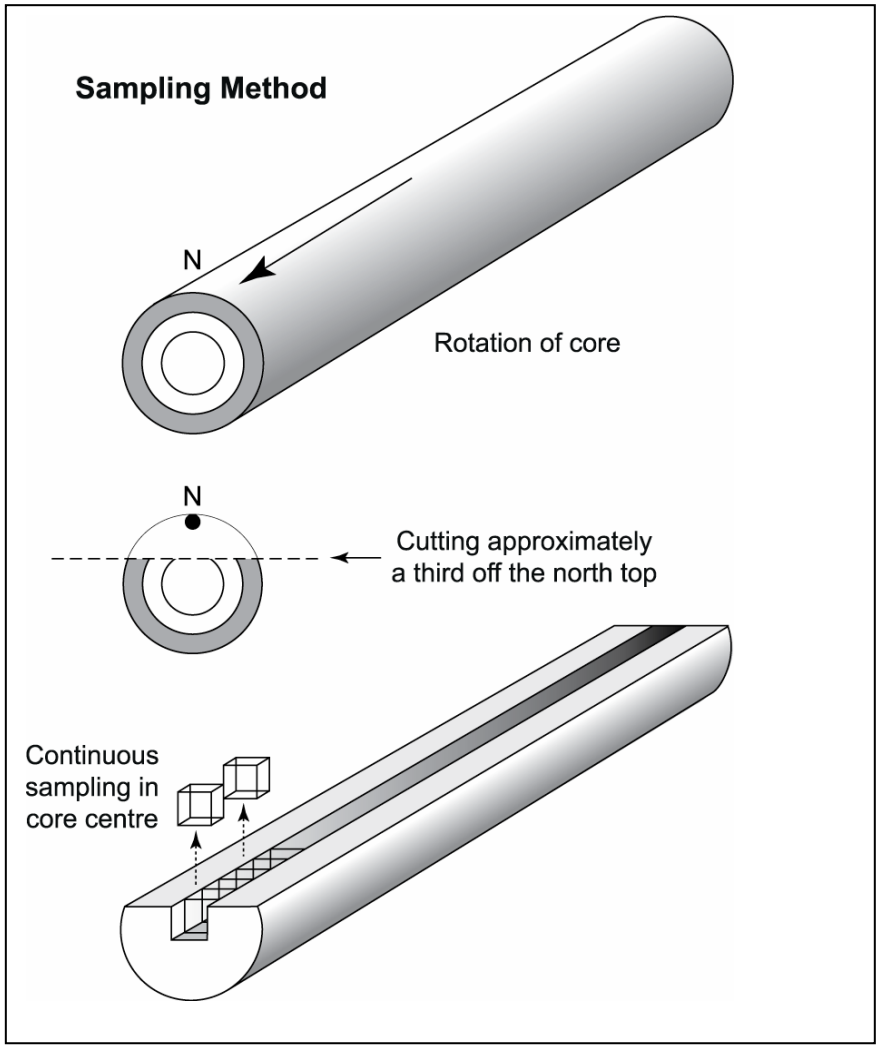

Figure 3 Sampling of orientated core section for PSV measurement.

Pilot samples were cleaned with alternating fields ranging from 0 to 100mT (Fig 4), with increments of 3 to 20mT, but it was established that samples with low initial NRM intensities were typically suitable for cleaning with peak alternating fields of 10, 20, and 30mT, whilst those sediments with higher NRM intensities were cleaned by AF intensities of 20, 40, and 60mT. Occasional variations were made to these steps according to the observed behaviour of individual samples.

4.3. PSV data analysis

Declination and inclination for each sample were determined from the characteristic NRMs by vector-fitting using the program PLOTCORE (Department of Earth Sciences, University of Liverpool) to generate Zijderveld plots (Zijderveld 1967; Tarling 1983; Butler 1992; Borradaile *et al* 1999; Tauxe 2002) which convert the 3D change in the total magnetisation vector onto a 2D plane (Figs 4a and d). Given the proposed rapid sedimentation rates of the laminated

post-gravel marshland sediments (Stupples and Plater forthcoming) data from each core were averaged to generate mean palaeoinclination and palaeodeclination values for each (nominally) one metre core section. Between 6 and 37 samples (N) were taken from each core (Table 2) and the Fisher Distribution (Fisher 1953; Tarling 1983; Butler 1992; Tauxe 2002) was used to calculate mean directions and associated confidence intervals – comparable to those associated with normally distributed planar data – from these spherically distributed palaeomagnetic directions.

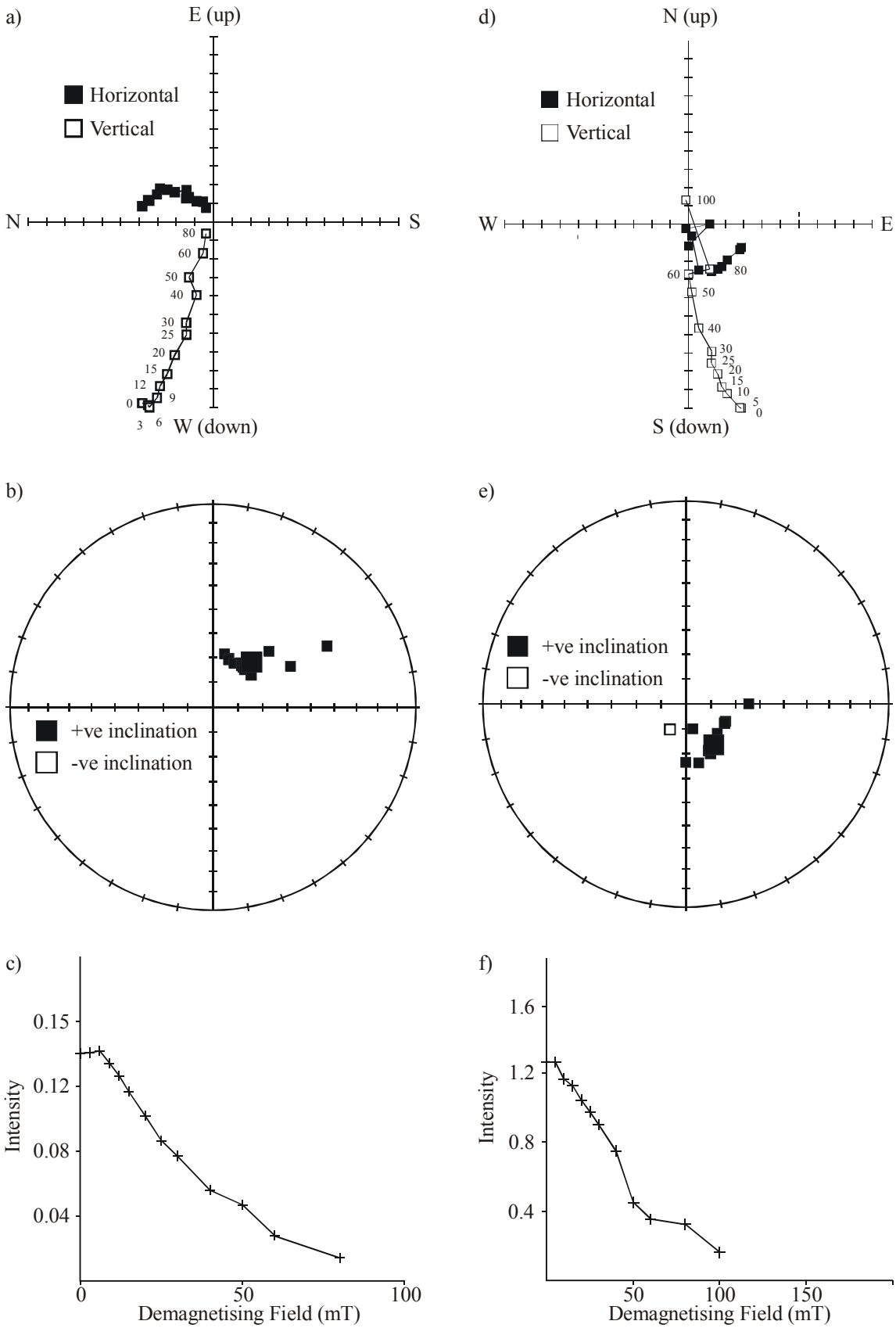

Figure 4 Results of pilot AF demagnetisation for low initial NRM (a-c, core Bould1, 17–19cm depth) and high initial NRM (d-f, core Bould2, 43 to 45cm depth) samples from Boulderwall Farm: Zijderveld plots (a, d), stereographic projections (b, e) and intensity plots (c, f).

4.3.1. Analysis of palaeodirection data: the Fisher Statistics

The software PMAG Tools version 3.2 (Hounslow 2003) was used to calculate the Fisher statistics, namely:

- the mean palaeodirections for each core section recovered,
- an estimate of the precision (k) of these sample means which provides an indication of the degree of scatter about the mean and is analogous to the standard deviation of the normal distribution (Butler 1992),
- a confidence limit (α_{95}) which indicates how likely these sample mean directions are to represent the true population mean directions, which is comparable to the standard error of a Gaussian mean (Butler 1992). The α_{95} statistic is the angular radius of a cone, centred on the sample mean, in which there is a 95% probability that the true mean direction lies therein.

Tests were also applied to ensure that the data were randomly distributed and to confirm that the spherical Fisher Distribution was an appropriate model for the data (see Tauxe 2002). A small number of outliers were removed prior to calculation of the Fisher statistics.

Higher values of k and N accompanied by lower values of α_{95} indicate increasing confidence in how representative the resultant mean directions are of the actual declination and inclination encoded within the sedimentary record of each core. As a general rule Fisher statistics of the order N>7, k>10 and $\alpha_{95}<5°$ can be considered acceptable (Tarling 1983; Butler 1992; Noel and Batt 1990). However, higher (less precise) values of α_{95} do not necessarily invalidate a particular datum (Butler 1992), especially in situations where the number of available samples is small, and applying a strict upper limit to the value of α_{95} may be unnecessarily restrictive (Clark *et al* 1988; Tarling and Dobson 1995; Borradaile *et al* 1999; Gallet *et al* 2002). In addition, a high degree of scatter may, in fact, reflect a period of rapid PSV rather than poorly constrained sample data (Batt 1997). Table 2 contains the mean palaeodirections from each core and the associated Fisher statistics.

4.3.2. Deriving the PSV ages: comparing sample data to the master curve

Having obtained the mean inclination and declination of each core, PSV dates are derived by comparison with a calibration curve (of which there are several) compiled primarily from dated archaeological artefacts (archaeomagnetic dates) and, over the past few hundred years, historical records of direct measurements of changes in the Earth's magnetic field (Clark *et al* 1988; Tarling and Dobson 1995; Batt 1997; 1998; Gallet *et al* 2002; Le Goff *et al* 2002; Linford and Welch 2004). The complexity (Fig 10) of the palaeodirection data used to generate archaeomagnetic calibration curves for a particular location, driven by the natural variability of the Earth's magnetic field, and the difficulties inherent to the acquisition and dating of archaeological materials, led initially to these Master curves being hand-drawn, with sample palaeodirections fitted by eye to obtain the PSV dates.

Various approaches to the statistical smoothing of palaeodirection data have been developed to improve on this initial graphical method (Tarling and Dobson 1995; Batt 1997; 1998; Borradaile *et al* 1999; Gallet *et al* 2002; Le Goff *et al* 2002; Linford and Welch 2004). They have the advantage of impartial reproducibility and can incorporate estimates of errors attached to the palaeomagnetic dataset from which the curves are derived. However, such smoothing techniques, whether a simple fixed width moving window or something more sophisticated, also risk the potential loss of important detail during the averaging process and must tackle the associated problem of how to select the most appropriate width smoothing window (and any associated weightings) – different widths (and/or weighting formulae) will clearly generate subtly different calibration curves (eg Borradaile *et al* 1999). A further advance circumvents the need to fit the sample data to the Master curve by eye and applies an extension of Fisher's distribution to identify the 'best-fit' of sample data to the reference curve and assigns a percentage probability estimate of the reliability of this match between sample palaeodirections and calibration curve to the dates obtained (Batt 1998; Le Goff *et al* 2002).

4.3.3. The Paris calibration curve

The selection of which calibration curve to use is based primarily on proximity to the sample site as the reference curves are site-specific and also, where applicable, sensitive to the quality of the calibration data covering the likely periods of interest in the samples (Clark *et al* 1988; Tarling and Dobson 1995; Borradaile *et al* 1999). Previous direct dating of organic and inorganic sediments from Romney Marsh, and complementary historical and archaeological evidence, indicate a likely time frame of deposition for the post-gravel marshland sediments of Dungeness of no more than 2000y bp in the west and most likely <1000y bp for the central and eastern sites (Plater 1992; Plater *et al* 1999; 2002; Roberts and Plater 2005). Both the UK and Paris calibration curves cover these periods, and are roughly the same distance from the marsh sites, but the latter was selected here as it offered the possibility of applying the method of Le Goff *et al* (2002) with its sophisticated approach to the creation of the calibration curve (Fig 10) and subsequent derivation of the PSV ages from the palaeodirections obtained from the marshland sediment cores.

To compare sample palaeodirections to a calibration curve, and so derive the PSV ages, the sample data must first be adjusted to a central location that is the location on which the Master curve is based (Clark *et al* 1988; Tarling and Dobson 1995). In this case the Dungeness data from the study sites (for simplicity we used the location of South Brooks in the middle of the field area: latitude 50.925519 north, longitude 0.882959 east) were corrected to the baseline location of Paris (latitude 48.9 north, 2.3 east) – the site of the archaeomagnetic Master curve used to date these sediments. This conversion, using the virtual geomagnetic pole (VGP) method (Shuey *et al* 1970; Noel and Batt 1990) adjusts the data to effectively normalise (with respect to Paris in this instance) the systematic variation of inclination and declination, at any particular time, with location on the Earth's surface. Finally, the palaeodirection data and associated Fisher statistics for each core were tested against the Paris Master curve using the method from Le Goff *et al* (2002) to determine the most likely period of deposition. However, only those cores where the results were sufficiently precise (high k, low α_{95}) were tested in this way.

4.4. Environmental Magnetism Sampling and Data Processing

In the laboratory 20mm (occasionally 30mm) sub-samples were removed at regular intervals along the cores with the sample resolution determined by the requirement to limit the total number of samples to 80 per core. Greater attention was paid to the deeper, generally laminated sections, with the sampling frequency reduced in the upper metre or so of structureless muds. Samples were freeze dried, disaggregated, tightly packed with clingfilm into 10ml plastic pots, and weighed. A suite of environmental magnetic measurements was then completed on the samples using the following:

- Bartington MS2 Magnetic Susceptibility Meter (frequency-dependent magnetic susceptibility)
- KLY-3 Kappabridge Susceptibility Facility (magnetic susceptibility)
- DTech Precision Instruments AF demagnetiser with ARM capability (applies fields for susceptibility of anhysteretic remanent magnetisation)
- Magnetic Measurements MMPM9 Pulse Magnetiser (applies fields for saturation and backfield isothermal remanent magnetisation)
- Molspin Spinner Fluxgate Magnetometer (measurement of susceptibility of anhysteretic remanent magnetisation, and saturation and backfield isothermal remanent magnetisation)

Data were processed and graphically presented using *Excel 2000* and *OriginPro 7*. Data are presented as a series of depth profiles and biplots with the magnetic properties expressed on a mass specific basis and as quotients derived from these parameters. Appendix II contains the complete dataset.

5. Environmental Magnetism: Results and Interpretation

Results of the environmental magnetic analyses are presented in Figures 5 to 8. The general magnetostratigraphy can be defined simply as a tripartite division which is applicable to all six sites and this is evident in both the down core plots of magnetic properties (Fig 5) and the biplots (Fig 6). This broad structure will be described first before discussing any prominent trends and/or anomalies within and between sites, and considering the potential grain size influence and post-depositional alteration of the magnetic components preserved in the sedimentary record.

5.1. Magnetostratigraphy

5.1.1. Magnetostratigraphic Zone 1

Magnetostratigraphic zone 1 (Figs 5 and 8) extends from the base of the cores to an altitude of *c* +1.0m OD and is characterised by the predominance of Soft IRM and relatively high concentrations of magnetic minerals (Figs 5 and 6) as defined by high values of magnetic susceptibility (χ_{kappa}), saturation isothermal remanence magnetisation (SIRM) and susceptibility of anhysteretic remanence magnetisation (χ_{ARM}). Values of χ_{ARM}/SIRM, and χ_{ARM}/χ_{lf} are also at their greatest in zone 1 whilst the percentage of hard remanence (Hard%) carried by the samples tends to be the lowest (<5–10%) recorded at each site. The depth profiles of the magnetic parameters in zone 1 (Fig 5) are characterised by a cyclical variation in the concentration of magnetic minerals, although the amplitude and frequency of these cycles varies temporally through each core and spatially between sites. The variability is driven by a relative concentration effect related to the laminated character (see particle size profile in Fig 9) of these deeper sediments, whereby the coarser sandier layers are relatively poor in magnetic minerals compared to the intercalated finer grained silts. The texture and structure of the laminations is highly variable, temporally and spatially, and this is reflected in the magnetic profiles. In addition, these laminae recur at millimetre to centimetre scale, but the sampling resolution of the magnetic measurements is approximately 3cm, and this has a smoothing effect on the underlying cyclicity.

Whilst there are no strong linear trends moving up-core through zone 1 (Fig 5), there is typically a broad peak in magnetic concentration, Soft IRM and SIRM/χ_{lf} around the middle of the zone. This horizon of relatively enhanced values broadly coincides with (or at least overlaps with, eg the Midrips Fig 5a) a divergence in backfield IRMs (Fig 7) and the extent of the latter is indicated by the grey shading in Figures 5, 7, and 8. Biplots of SIRM against χ_{lf} (Figs 6a–f) show a curvilinear expression of zone 1, and whilst this is not directly depth-related, the subset of points in the high SIRM and high χ_{lf} quadrant of each graph represent the sections of each core where the defining characteristics of zone 1 are at their maximum values. These maxima correlate with loss on ignition values which approached, or slightly exceeded, 4% – the highest values recorded (other than in the well-rooted surface samples) – but are inversely related to particle size (Fig 9), ie there is a concentration of magnetic particles in the relatively muddier, finer grained samples. This particle size relationship is further demonstrated in the occurrence of occasional outliers to the main zone 1 groups (Fig 6). The coarser, basal sands from South Brooks (Figs 6c and 9c) and Manor Farm (Figs 6e and 9e) plot to the low magnetic concentration side of the group whereas the muddy samples from the base of the Boulderwall Farm (Figs 6f and 9f) core plot to the high concentration side.

Manor Farm is something of an exception to this general description. Not only is the area of backfield IRM divergence (-1.2 to +0.6m OD, Fig 7) and higher organic content (loss on ignition around 4%) more extensive than elsewhere, but the cluster of samples with the highest values of the defining zone 1 properties (Figs 5 and 6) are restricted to a narrow band between 0 and +0.6m OD which coincides with a brief, *relatively coarser* phase of sedimentation (Fig 9). This apparent anomaly is more likely to be driven by the overall finer particle size of the Manor Farm sediments compared to the other site, indicating a distinct sediment processing regime (or perhaps source) in this former tidal creek, in contrast to the

gravel swale environments at the other five sites. Previous work on Romney Marsh has indicated a high concentration of magnetic minerals in the coarse silt to fine sand grades and the appearance of these grades as relatively fine or coarse material in a down-core plot of mean particle size is obviously dependent upon the ambient sediment pool at a particular site (Stupples 2002b).

5.1.2. Magnetostratigraphic Zone 2

The boundary between zones 1 and 2 is well-defined and occurs at approximately +1.0 ±0.2 m OD in all cores (Figs 5 and 6). The defining characteristics of zone 2 are a sharp relative increase in the contribution of the hard remanence component to the total magnetic signal, expressed as Hard% up to 25–30%, and an accompanying marked decrease in magnetic concentration where χ_{kappa}, SIRM, and χ_{ARM} are all lower than in zone 1. Whilst the absolute amount of high coercivity minerals tends to remain reasonably stable up-core, as shown by the HIRM trend, the proportion of hard remanence is certainly enhanced in zone 2. There is also a much reduced degree of variability in the depth profiles (Fig 5) and scatter plots (Fig 6) of the magnetic parameters in zone 2, with each recording relatively constant values throughout, or at least values within a tightly restricted range. Consequently, the quotients derived from the basic parameters are generally lower and less variable than zone 1. Given the relative uniformity in the altitude of the zone1/zone 2 transition across the marshland sites (Fig 8), a post-depositional influence from water table depth is favoured in preference to a change in magnetic properties resulting from sediment provenance and/or processing during deposition. Zone 2 extends to around +1.7 to +2.0m OD before a less clearly defined transition to the zone 3 which extends to the surface.

5.1.3. Magnetostratigraphic Zone 3

In the near-surface zone 3 (Fig 5) the proportion of hard remanence-carrying minerals declines to values intermediate to those seen in zones 1 and 2. The other properties of this zone are comparable to zone 2 – hence, there is some overlap between zones 2 and 3 in the biplots from the Midrips, Wicks, and South Brooks (Figs 6a–c) – with the addition of a weak trend of increasing magnetic concentration towards the surface and, occasionally, a somewhat sharper increase in the uppermost 30cm or so. The zone 2/zone 3 transition occurs at an altitude of *c* 1.85 ±0.25m OD (Figs 5 and 8), and is at a lower elevation at the Midrips and Wicks compared to the four eastern sites. Again, a pedo/diagenetic control is interpreted from the observed uniformity in the altitude of this transition, and the extension of zone 3 at the two western-most sites may be driven by disturbance of this upper section by military activity.

Figure 5a-f (following 3 pages) Down-core plots of environmental magnetic properties and selected ratios from the six marshland sediment core sites. The three zones are defined on the basis of breaks in these depth profiles, particularly changes in the concentration of magnetic minerals and the relative importance of the contribution high coercively minerals (hard and soft IRM). These zones are also seen in the well-defined groupings in biplots of the same magnetic properties (Fig 6). The grey band identifies the section of core where backfield IRM plots diverge (Fig 7) and SIRM/χ_{lf} is elevated, suggesting the presence of authigenic greigite.

a) The Midrips

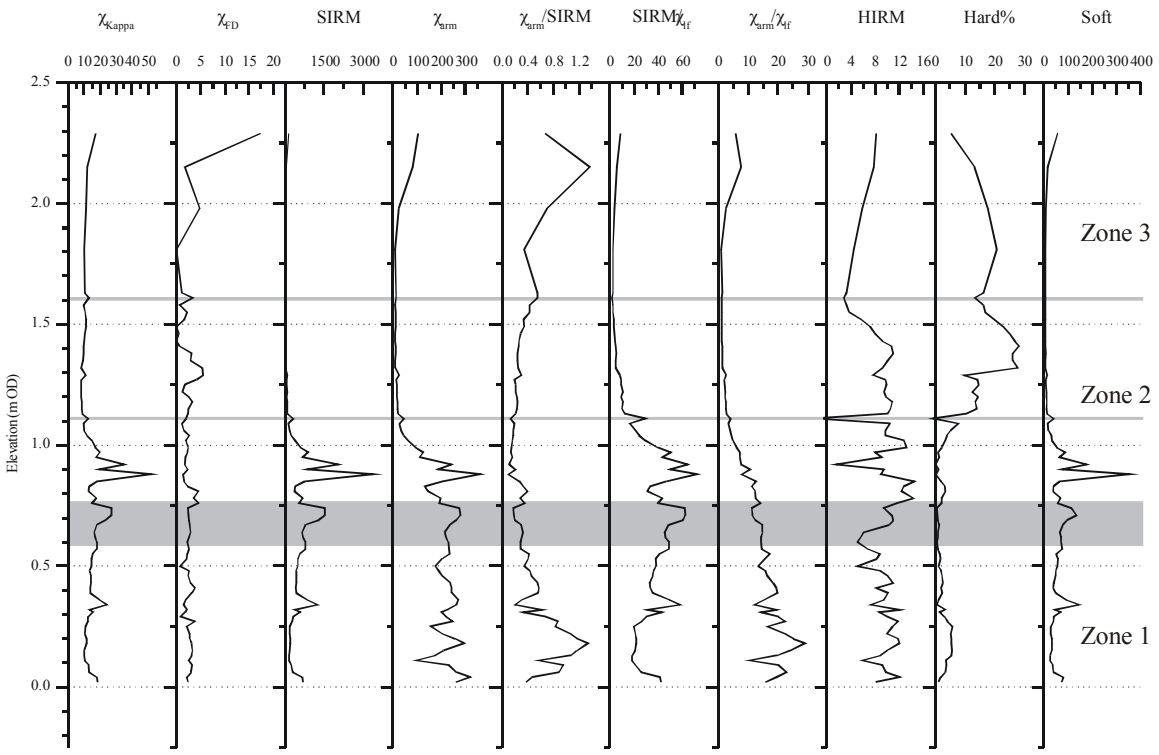

b) The Wicks

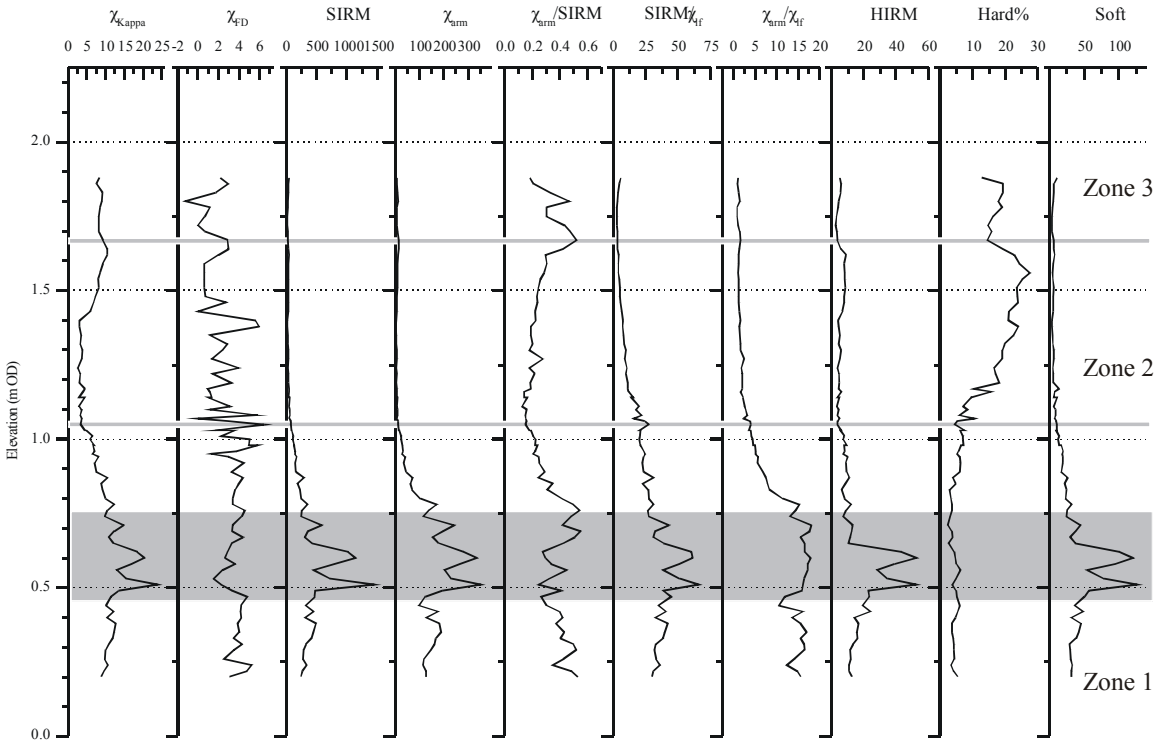

c) South Brooks

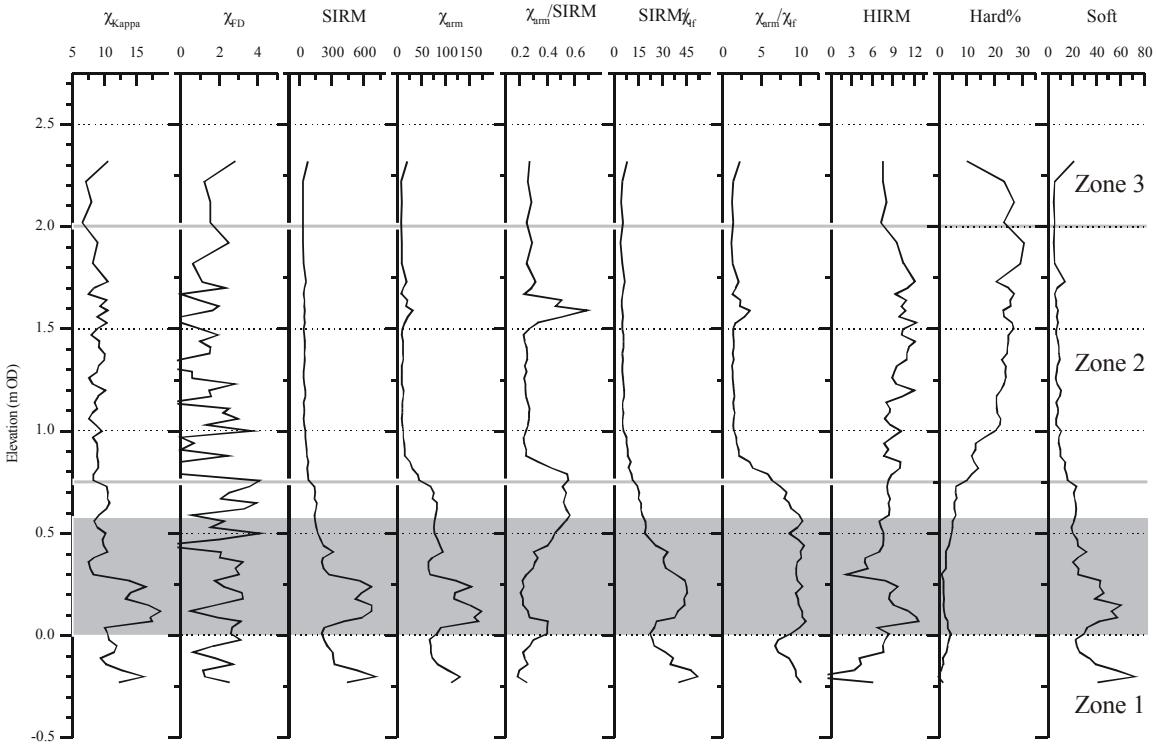

d) Brickwall Farm

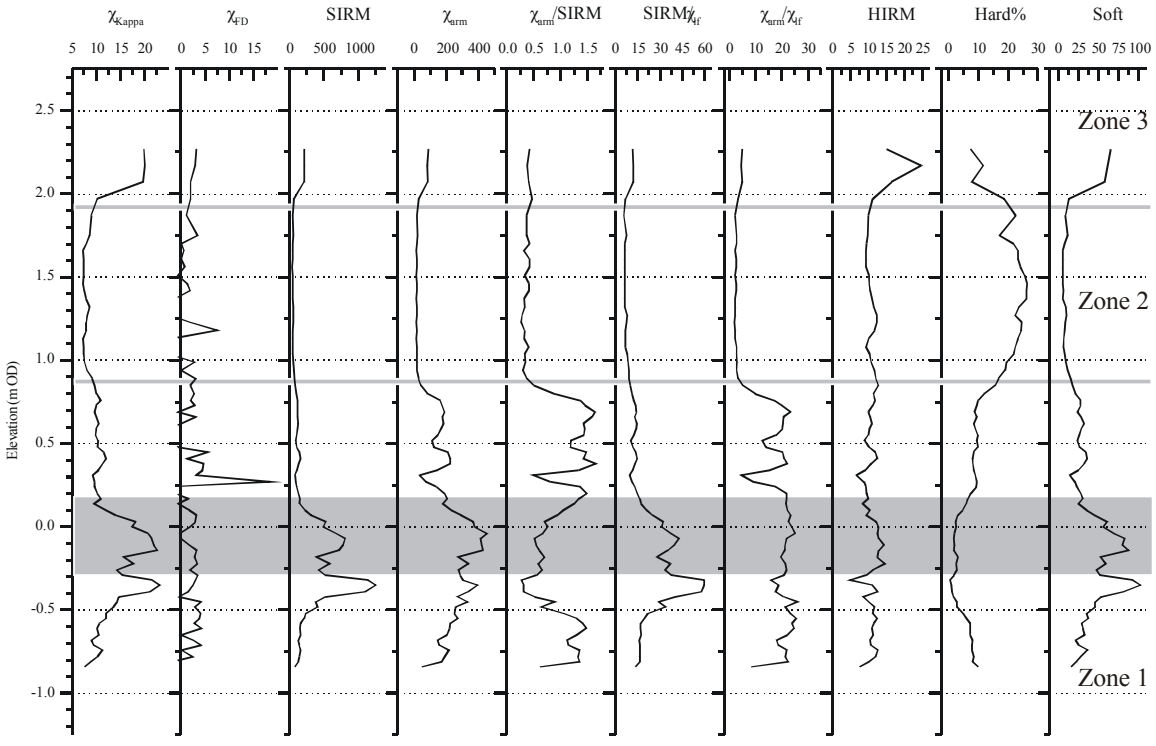

e) Manor Farm

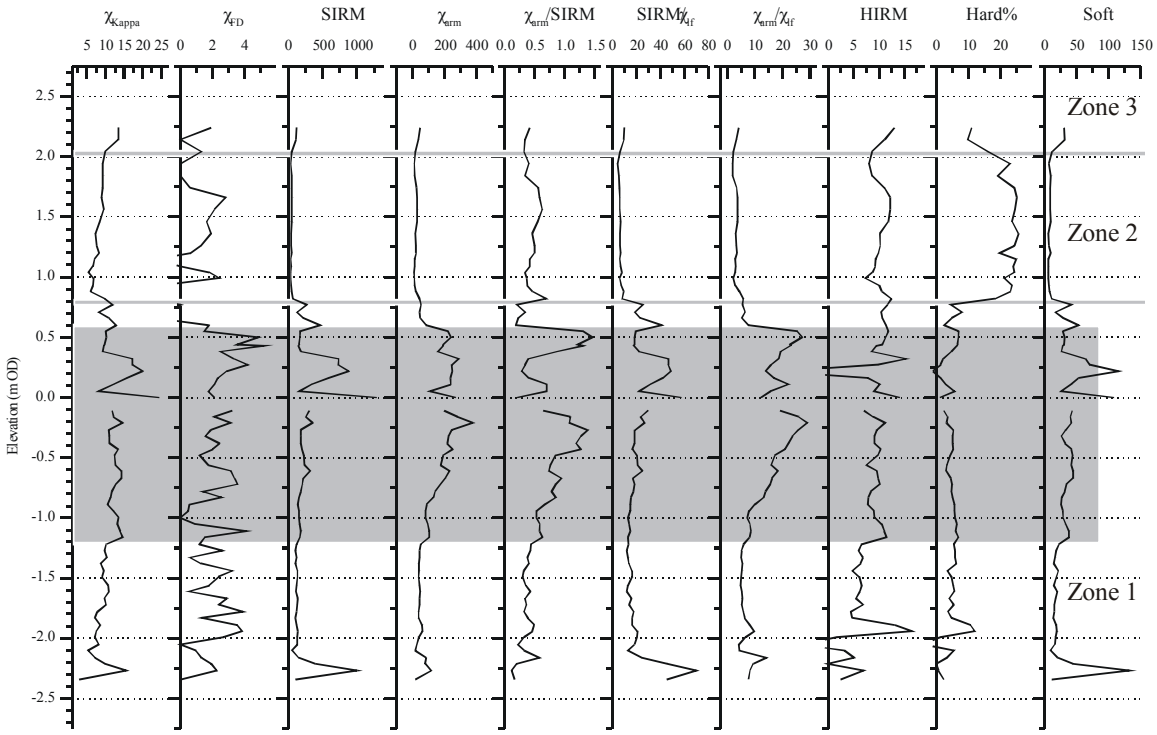

f) Boulderwall Farm

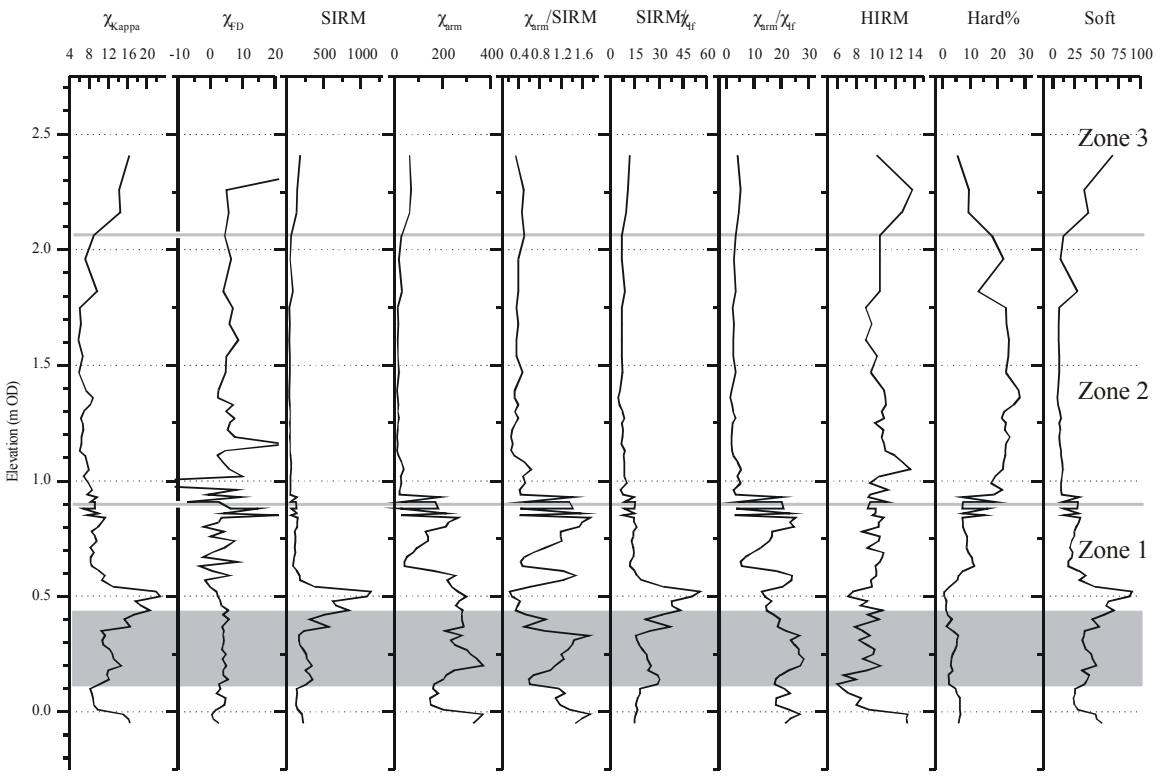

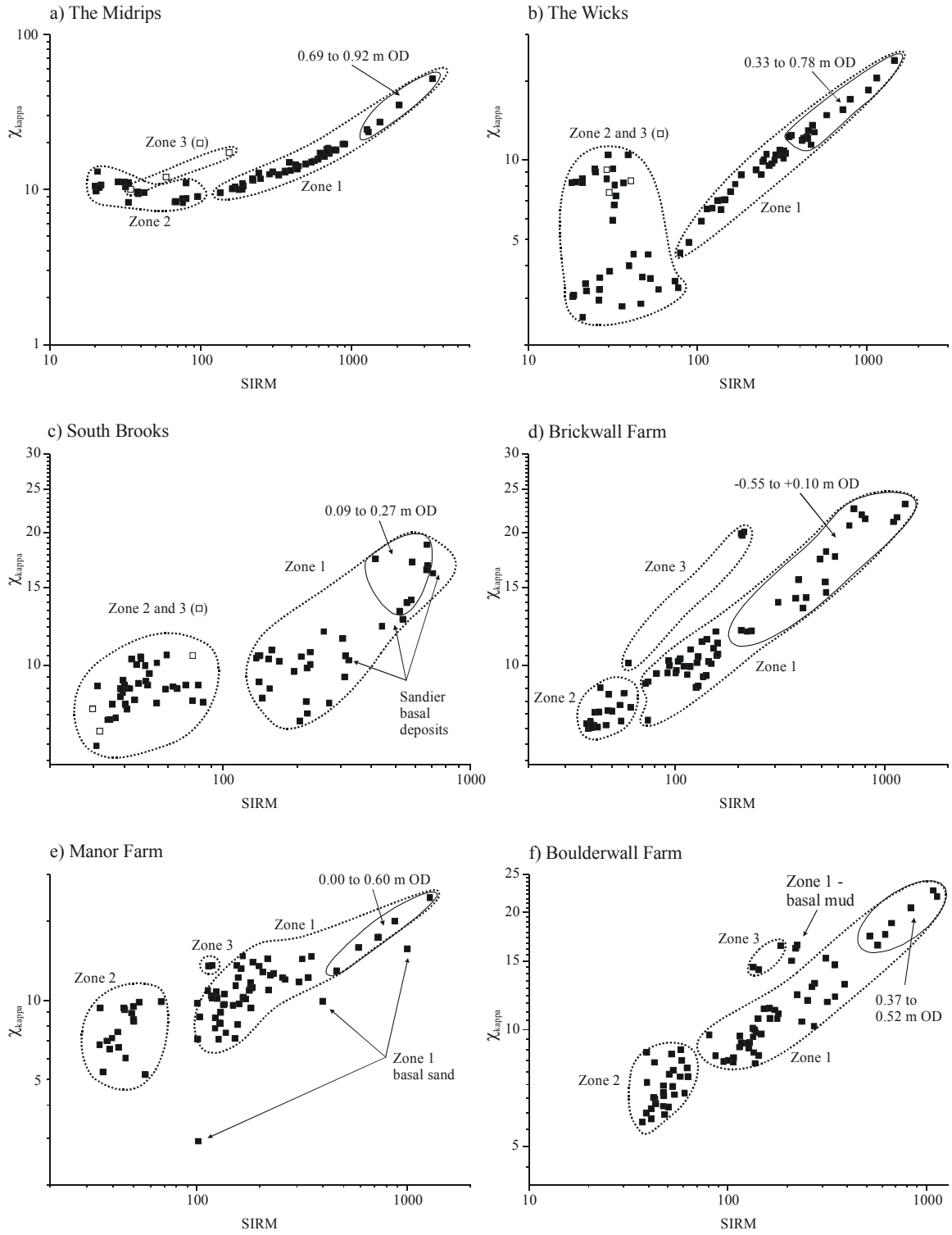

Figure 6a-f Biplots of SIRM against χ_{lf} for the six marshland sediment core sites showing generally good separation of the three zones identified on the depth profiles of magnetic properties in Fig 5. The subset of points identified in zone 1 defines the region of peak magnetic concentration in Fig 5. Basal sands (c, e) and muds (f) plot as outliers to the main distribution. Note the expanded zone 3 at the Midrips (a) and the Wicks (b) and that zone 2 and the surface samples (zone 3) overlap at South Brooks (c).

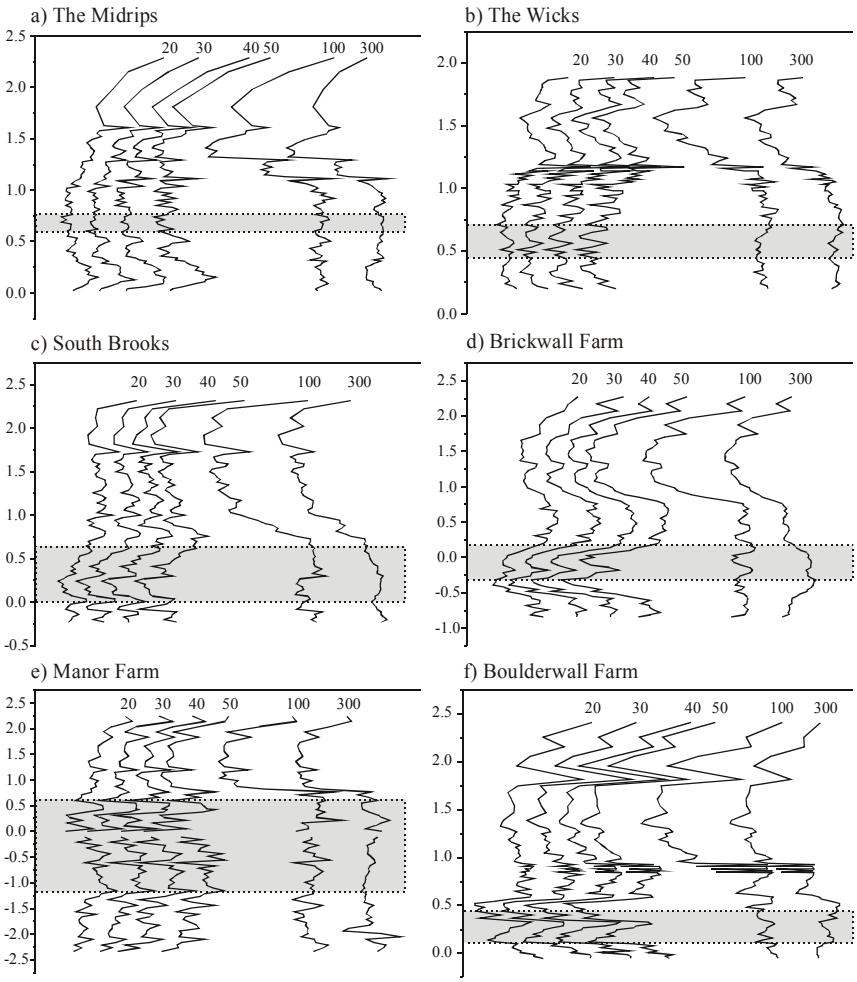

Figure 7 Depth profiles of backfield IRMs at 20 to 300mT showing divergence of high- and low-field IRM in the grey band indicating authigenic greigite formation.

5.2. Interpretation of Magnetostratigraphy

The lithostratigraphy (Figs 8 and 9) in these marshland cores can also be represented by a simplified tripartite sequence of variably laminated silty sands to sandy clay silts at depth (units 2 and 3), grading up to a mottled sandy mud (unit 4), which is increasingly structureless, and topped by the well-rooted sandy silty clay soil (unit 5). With the exception of Manor Farm, where an impenetrable silty sand (unit 1) was the basal unit, all cores were underlain by gravel which was not recovered. However, the reasonably well-defined lithostratigraphic boundaries were not mirrored in the magnetostratigraphy (Fig 8). This observation, coupled with the relative uniformity in the altitudes of the magnetostratigraphic boundaries, suggests that a post-depositional control on the magnetic properties of the sediments over-rides any clear expression of the detrital magnetic signature. Comparable 'overprinted' magnetostratigraphic sequences have been reported from other sites on Romney Marsh (Plater and Long 1995; Long *et al* 1996; Spencer 1997; Plater *et al* 1999), as well as lake and marine sediments from other areas (eg Snowball and Thompson 1988; Roberts and Turner 1993; Verosub and Roberts 1995; Nolan *et al* 1999; Wheeler *et al* 1999).

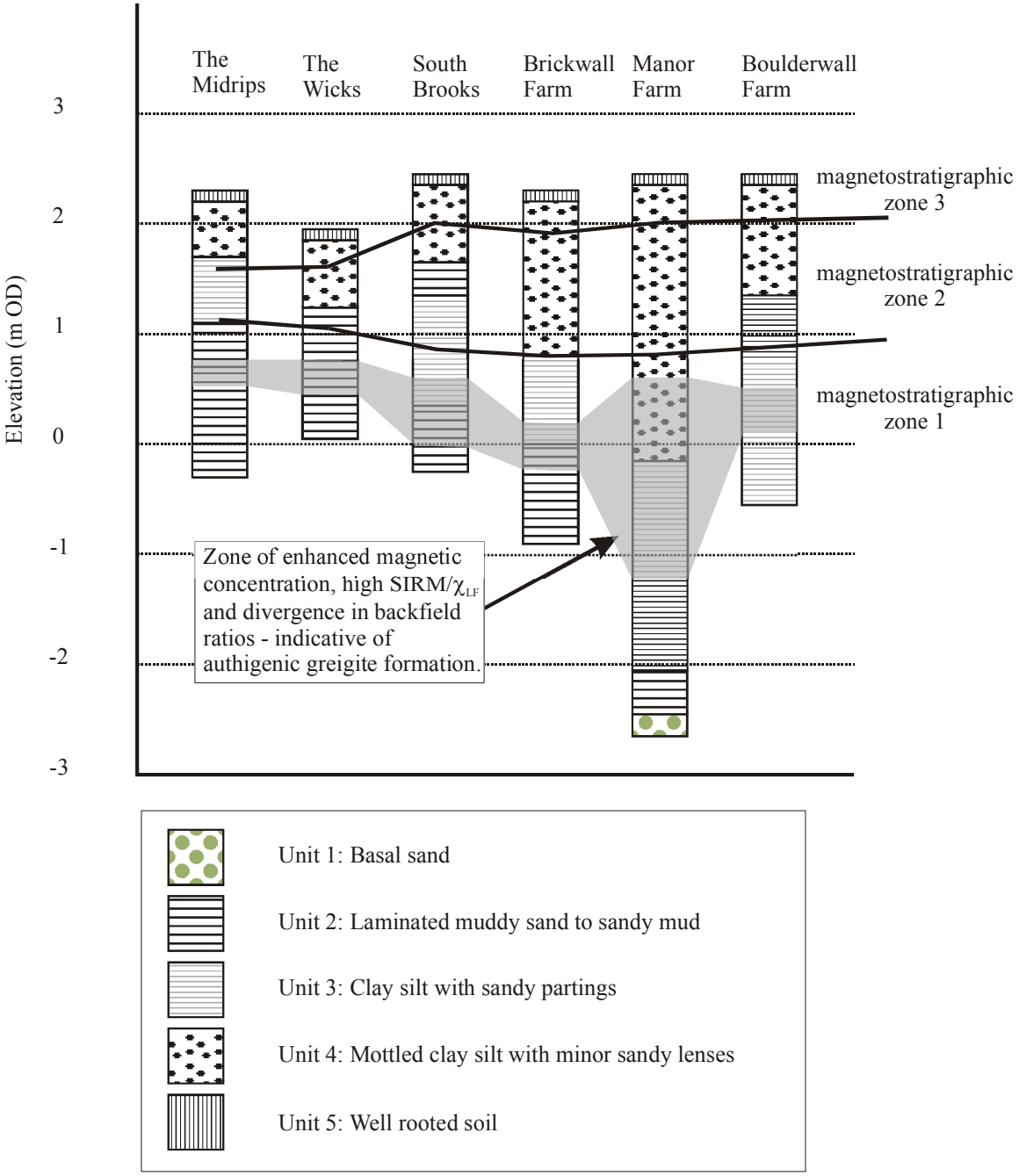

Figure 8 Relationship between lithostratigraphy and magnetostratigraphic zones in the post-gravel marshland deposits of Dungeness.

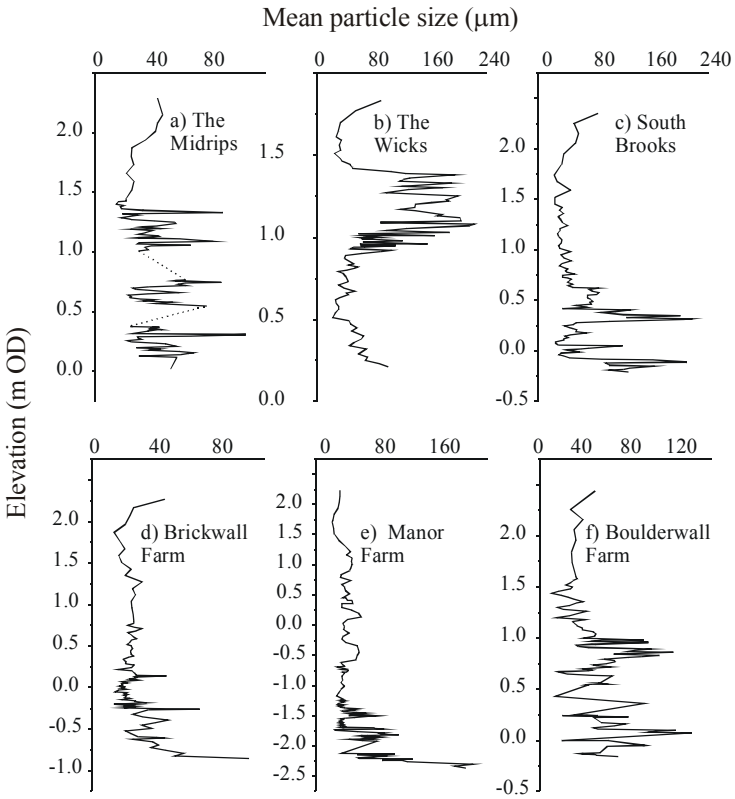

Figure 9 Mean particle size profiles from the six marshland sediment cores highlighting cyclical variation in sediment texture, as well as basal sands at South Brooks, Manor, and Boulderwall Farms.

In zone 1 there are generally high concentrations of magnetic minerals and there is an enhanced relative and absolute contribution from low coercivity minerals (Fig 5). In addition, there is a region towards the centre of zone 1 where high values of SIRM/χ_{lf} (Figs 5 and 6) and a divergence in the backfield IRM ratios (Fig 7) are indicative of the authigenic formation of greigite. Greigite develops under reducing conditions, often in the presence of organic matter, as part of a reaction series, which given time and suitable conditions, converts magnetite (typically the principal source of the detrital magnetic signal) into pyrite (Roberts and Turner 1993; Verosub and Roberts 1995; Dekkers 1997; Maher and Hallam 2005). The sediments of zone 1 tend to be dark in colour, indicative of their position below the water table. Whilst organic content was generally low (2 to 4%), occasional intercalated organic layers were recorded and the highest values (*c* 4%) of loss on ignition were recorded in this section of the cores. Both these factors would encourage the formation of greigite.

The variable, perhaps cyclical, nature of the magnetic properties in zone 1 (Fig 5) is primarily a function of grain size variation within the laminated sediments (Fig 9). Here, magnetic minerals tend to be concentrated in the finer-grained muddy layers. This effect seems to be accentuated by the greigite formation process which appears to be most strongly developed in a zone of between 0.2 and 0.8m thickness where peak values of the diagnostic parameters and quotients are observed. Outside of this zone the values decline both up- and down-core, grading into zone 2 upwards.

Overprinting of the detrital magnetic signal may also be driven by bacterial production (and subsequent dissolution) of very fine-grained magnetite, or the preferential leaching of certain species under reducing conditions (eg Verosub and Roberts 1995; Wheeler *et al* 1999; Snowball *et al* 1999). The latter process may be applicable to zone 2 in the post-gravel marshland deposits, whilst the former is likely to contribute to the enhanced concentration of magnetic minerals in zone 3. The delineation of zone 2 (both upper and lower zone

boundaries) is based on the relative increase of the hard remanence component (Hard%), although the absolute contribution from higher coercivity minerals, eg haematite and/or goethite, remains fairly consistent in all cores. This may be interpreted as the preferential loss of bacterial fine-grained magnetite with depth (and age) from the core surface. This appears to be enhanced by the seasonal wetting and drying as the watertable rises and falls between winter and summer, hence the consistent elevation of the base of zone 2 (+1.00 ± 0.25m OD) and the top (+1.85 ± 0.25m OD). Below the summer season watertable, here reductive diagenesis is maintained and, hence, the soft remanence component increases relative to the hard remanence.

Zone 3, typically the uppermost 30–50cm of each core, exhibits a relative reduction in the hard remanence contribution and an increase in the concentration of magnetic minerals. This can be related to the biological production of fine-grained secondary ferrimagnets, although several mechanisms have been proposed for its occurrence during the soil formation, and is consistent with the widely reported enhancement of magnetic properties in the soil zone (Thompson and Oldfield 1986; Oldfield 1999).

5.3. Intra- and Inter-site Trends in Magnetic Properties

The Midrips (Fig 5a) shows the highest values of χ_{kappa}, SIRM and χ_{ARM} and, hence, the highest concentration of magnetic minerals of the six marshland sediment sites. In contrast, the sediment sequence from South Brooks (Fig 5c) has the lowest values for the concentration-related parameters. Values from the four remaining sites are fairly consistent. In all cases concentration values are generally higher in zone 1 whereas zone 2 and 3 are lower – typically χ_{kappa} is twice as large in the deepest sediments whilst SIRM and χ_{ARM} are up to an order of magnitude greater (Fig 5).

5.3.1. Magnetic Grain Size

Some indication of the likely particle size of the magnetic components of the sediment can be derived from a consideration of the quotients derived from the magnetic parameters (see Section 3.1).

Frequency-dependent susceptibility (χ_{FD}%) becomes increasingly unreliable when magnetic susceptibility is low, which may explain some of the more extreme (both high (>15%) and low (~0%)) values recorded here. However, the majority of the sites have χ_{FD}% in the range 0 to 5–6%. χ_{ARM}/SIRM is less than $1x10^{-3}$ mA^{-1} throughout zones 2 and 3, and also through zone 1 at the Wicks and South Brooks (Figs 5b and 5c, respectively). At the Midrips (Fig 5a), apart from isolated peaks near the surface and base of the core, χ_{ARM}/SIRM also remains below $1x10^{-3}$ mA^{-1}. The profile through zone 1 at the remaining 3 sites (Brickwall Farm, Manor Farm and Boulderwall Farm, ie the Denge Marsh sites) is a little more complicated with alternating bands showing values both above and below $1x10^{-3}$ mA^{-1}. At Brickwall and Manor farms (Figs 5d and 5e, respectively) the most intensely diagenetically-overprinted greigite zone has χ_{ARM}/SIRM values $<1x10^{-3}$ mA^{-1} but is flanked by sediments where the value is in excess of this. At Boulderwall Farm (Fig 5f) χ_{ARM}/SIRM is variable throughout the deepest magnetostratigraphic zone.

Where χ_{ARM}/SIRM is greater than $1x10^{-3}$ mA^{-1} and χ_{FD} is <5%, a dominance of the magnetic grain size population by stable single domain grains is implied (Thompson and Oldfield 1986; Walden *et al* 1999). Low values of χ_{FD} may also be driven by the very finest superparamagnetic grains of <0.005µm diameter, and this may be the case in the upper sediments of zones 2 and 3 where χ_{ARM}/SIRM are typically less than $0.5x10^{-3}$ mA^{-1}.

SIRM/χ_{LF} is greatest at depth (zone 1) with the highest values overall recorded in the Midrips core (up to $70x10^{-3}$ mA^{-1}). The overlying zones have uniformly low values: less than $15x10^{-3}$ mA^{-1} at all sites apart from the Midrips where $<40x10^{-3}$ mA^{-1} was recorded. χ_{ARM}/χ_{LF} follows a similar pattern with highest values (up to 30) in zone 1 generally, and peaking again in sediments from the Midrips; consistently lower values are present in the upper zones

(typically <5 but <10 at the Midrips). Both quotients are inversely proportional to the grain size of magnetite, particularly larger multi-domain grains. However, some complication arises in this simple relationship if very fine-grained material is present. In general, however, a fining-upward trend is indicated; a trend supported by the magnetic properties discussed previously (χ_{ARM}/SIRM and χ_{FD}).

Table 2 Mean declination and inclination with associated Fisher (1953) statistics, and mean inclination after McFadden and Reid (1982) for the post-gravel marshland cores. Declination and inclination are adjusted to the latitude and longitude of Paris from the location of the South Brooks sampling site by the VGP method. The age (and estimated error) associated with each core section was derived by comparison of sample palaeoinclinations (and α_{95}) with the Paris calibration curve (Fig 12).

					Fisher Statistics					McFadden and Reid			
	Piston	Elevation (m OD)			Degrees					Degrees			
Site and Grid Ref	Core	Top	Base	Mid	Dec	Inc	α_{95}	k	N	Inc	α_{95}	k	Age (AD)
The Midrips	Mid1	2.31	1.31	1.81	34.9	61.4	7.5	38	10	60.1	6.6	41	1175 ±100
TR 00466 18271	Mid2	1.31	0.31	0.81	30.4	62.7	4.4	77	14	62.2	4.1	66	1100 ±50
	Mid3	1.94	0.94	1.44	82.2	63.9	11.9	19	10	60.5	10.6	17	1175 ±200
	Mid4	0.94	-0.06	0.44	31.7	71.2	2.2	200	35	70.3	1.8	173	875 ±25
The Wicks	W2	1.94	0.94	1.44	38.8	60.1	9.9	39	6	59.2	9.1	46	1200 ±200
TR 00888 18004	W1	1.19	0.19	0.69	-5.3	60.6	2.7	282	10	60.4	2.5	287	1175 ±25
South Brooks	SB1	1.75	0.75	1.25	1.2	47.7	8.5	25	12	46.8	8.0	22	1375 ±200
TR 02786 17815	SB2	1.25	0.25	0.75	0.4	58.1	6.3	49	11	57.0	4.7	72	1300 ±75
	SB3	0.75	-0.25	0.25	31.3	64.0	3.8	131	11	63.5	2.5	250	1025 ±25
Brickwall Farm	Brick1	1.8	0.8	1.3	-43.7	54.8	14.5	15	9	51.4	11.8	15	1375 ±200
TR 05050 18290	Brick2	0.8	-0.2	0.3	-12.5	62.8	3.2	203	10	62.5	2.7	255	1075 ±25
	Brick3	1.15	0.15	0.65	-10.0	57.6	2.9	273	9	57.5	3.0	218	1175 ±25
	Brick4	0.15	-0.85	-0.35	3.5	68.3	2.5	516	7	68.2	2.7	394	900 ±25
Manor Farm	MF1	0.96	-0.04	0.46	6.0	63.4	3.8	148	10	63.0	3.2	172	1500 ±25
TR 05928 18077	MF2	-0.04	-1.04	-0.54	18.1	65.5	3.5	175	10	65.3	3.6	134	1525 ±50
	MF3	-1.04	-2.04	-1.54	9.8	59.6	2.7	286	10	59.4	2.2	372	1425 ±25
	MF4	0.46	-0.54	-0.04	3.7	64.5	7.2	41	10	62.7	4.6	81	1500 ±50
	MF5	-0.54	-1.54	-1.04	20.1	65.5	2.3	395	10	65.4	2.4	322	1525 ±25
	MF6	-1.54	-2.54	-2.04	28.9	57.7	4.5	106	10	57.3	3.7	125	1400 ±50
Boulderwall Farm	Bould1	1.34	0.34	0.84	5.4	63.4	2.5	87	37	63.0	2.5	60	1500 ±25
TR 06181 19231	Bould2	0.34	-0.16	0.09	-24.3	57.4	8.5	23	13	55.5	7.6	24	1400 ±100
	Bould3	1.84	0.84	1.34	4.9	56.2	17.9	5	17	44.2	11.8	8	n/a
	Bould4	0.84	-0.16	0.34	-11.5	53.4	2.0	139	37	53.1	1.6	146	1400 ±25

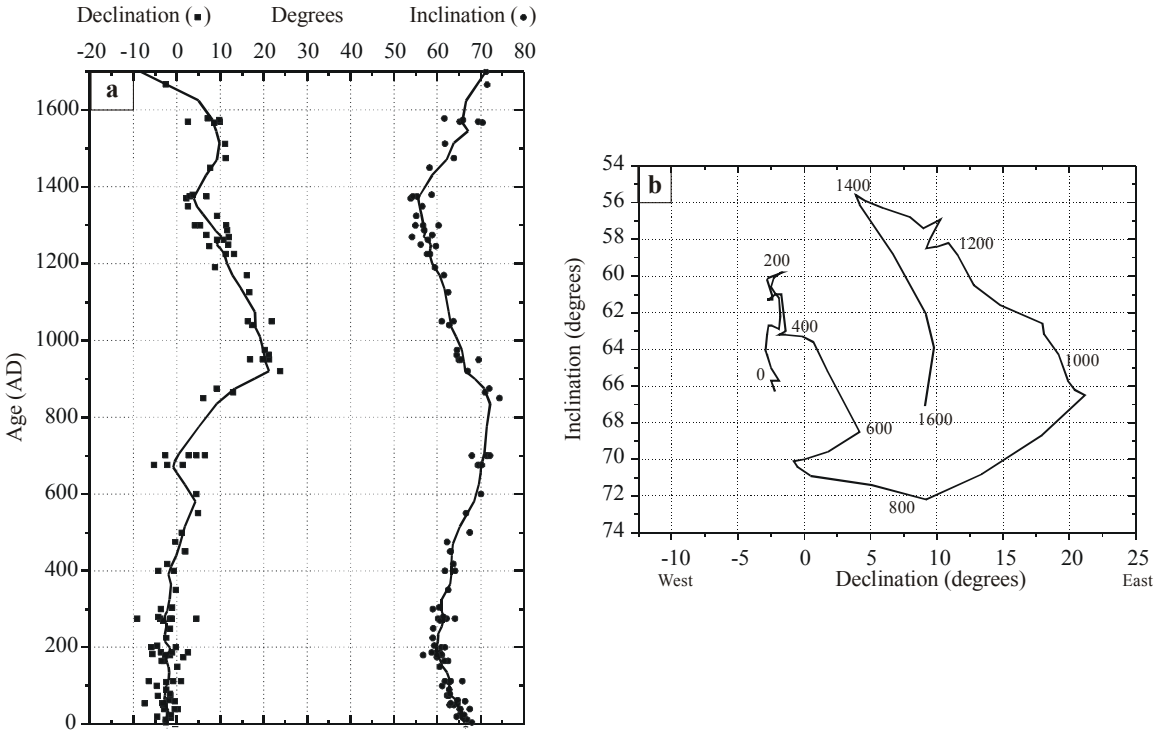

Figure 10 PSV calibration data for Paris over the past 2000 years (after Le Goff *et al* 2002).
a) Plot of smoothed declination and inclination with raw data points. Note the variation in the number of datums available for a particular period and also the scatter around the smoothed curve.
b) Bauer plot (Clark *et al* 1988) of the Paris Master Curve with selected ages (years AD) indicated.

6. PSV Dating: Results and Interpretation

From the environmental magnetic data, evidence of diagenetic and pedogenic overprinting of the NRM is apparent, *via* reductive diagenesis (iron sulphide formation) in the lower parts of the cores and the formation, and subsequent dissolution, of biogenic magnetite in the upper part (Yamazaki *et al* 2003; Maher and Hallam 2005). Despite this post-depositional addition to the detrital magnetic properties, it is also apparent that this overprinting is expressed mainly in the soft remanence and that the hard remanence (HIRM) varies to a much lesser degree down-core in the late-Holocene marshland sediments (Fig 5 and see Yamazaki *et al* 2003). It is this high coercivity, hard remanence component of the samples' magnetic properties which is identified and isolated as the characteristic NRM by the AF demagnetisation cleaning process described previously (section 4.2) and from which the palaeodirections are derived (Table 2, Figs 11 and 12).

Results of the statistical analysis of the palaeodirection data from the six marshland core sites are shown in Table 2 and include mean declination and inclination for each piston core together with associated values of k, N, and α_{95}. All palaeodirections are geo-referenced to Paris and so can be compared directly to the Le Goff *et al* (2002) Paris calibration curve (Figs 10 and 12). An initial inspection of the Fisher statistics from the Dungeness cores (Table 2) suggested that values of declination cover a much wider range than those on the Paris calibration curve (Fig 10), whilst inclination is consistently within the bounds of the secular variation at Paris. Assuming, on the basis of evidence cited previously, that these sediments are less than 2000 years old then this variability in declination must be attributed to errors in measurement of the original orientation of the cores to north in the field, or more likely, maintaining this orientation during coring and subsequent extrusion of the sediments.

The potential impact of an error of even ±5° of declination on a date derived from the Paris Master Curve (Fig 10) is obvious. The declination errors reduced the number of cores that could be dated using the Le Goff *et al* (2002) method, which evaluates the most statistically likely fit of the palaeodirections to the Paris calibration curve. Indeed, this renders the resulting dates of little or no value as the occurrence and degree of error in declination can not be quantified.

Despite the above, previous studies have relied on only one of the two available palaeodirections (eg Mackereth 1971 – declination only; Borradaile *et al* 1999; Yamazaki *et al* 2003 – inclination only) as a dating tool, and this approach can be applied here by comparing palaeoinclinations from the Dungeness marshland sediments to the Paris calibration curve. Consequently, mean *inclination only* values (Table 2, Figs 11 and 12) were recalculated using PMAG Tools and applying the approach of McFadden and Reid (1982) to exclude the likely random and unquantifiable errors in declination, although the difference in mean palaeoinclination from the two methods is small *c* 1°. These whole core mean palaeoinclinations and, importantly, the associated temporal (ie down-core) trends at each site (Table 2, Figs 11 and 12), were visually compared to the Paris calibration data (Fig 12; Le Goff *et al* 2002) and the most likely ages were identified for each sample. Batt (1997, pp163–4 and fig 4 therein) demonstrates this simple, but significant, use of superposition in constraining possible ages where a clear temporal relationship exists between samples, which can in turn be related to marked trends in palaeoinclination and palaeodeclination. Possible age ranges were further refined in light of previous work on the chronostratigraphy of Dungeness.

This pragmatic balance of direct PSV dating constrained and refined by additional archaeological or other chronologically relevant data is common to most (if not all) palaeomagnetic dating whether in the construction of the various calibration curves or the subsequent dating of material of unknown age (see for example Batt 1997; Borradaile *et al* 1999; Linford and Welch 2004). Whilst it was not possible to apply the Le Goff *et al* (2002) method to test the reliability of the dates generated here, and we acknowledge the need to apply a more rigorous statistical approach to PSV dating whenever possible (Batt 1997; 1998), we also note the potential for successful dating using the more straightforward graphical approach. The latter is perhaps only appropriate when clear temporal trends in palaeodirections are dominant during the period of interest (as is the case here) and there is good quality supporting evidence which can be used to aid a sensible interpretation of the results of the PSV dating process. Furthermore, some indication of the errors associated with the ages can still be derived from an examination of the slope of the *smoothed* Paris calibration curve (Fig 12) in light of the respective α_{95} values of the sample inclinations (Table 2, Fig 11). Dates with values of α_{95} of around 2° equates to an error of the order of ±25y, 4° to ±50–75y and 6° to around ±100y.

A semi-quantitative feel for the errors associated with the Master curve itself is provided by a consideration of the scatter of data points around the smoothed calibration curve, and the uneven spread of these points through time (Figs 10a and 12). In addition, any date based on the smoothed curve can be stated no more precisely than the width of the window used to smooth the data in the first place (Batt 1997). The width of smoothing windows used to construct the Paris Master curve was variable (Le Goff *et al* 2002) and depended upon the amount of data available for a particular time frame but ranged (approximately) from 20 to 140 years, giving a precision range of ±10 to ±70y with the lowest precision period being around 600 to 1000 AD due to the paucity of dateable material currently available for this period (Figs 10a and 12).

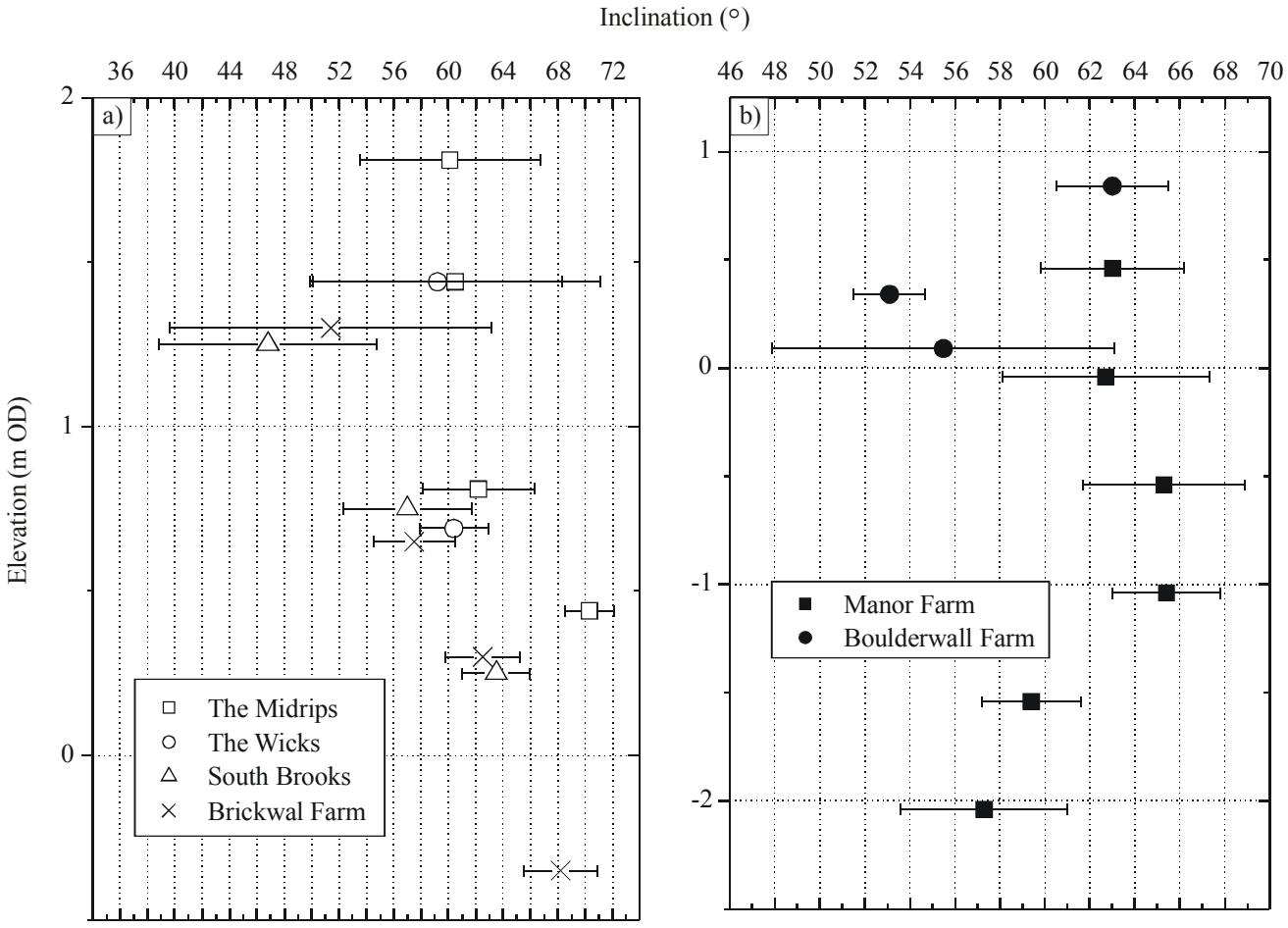

Figure 11 Comparison of palaeoinclination and associated α_{95} error bars from the older western marshland core sites (a) and the younger eastern sites (b). Sample Bould3 is omitted from (b) due to high α_{95} and low k. Two samples with mean values which are bracketed by the error bars of one (or both) of the samples are not distinguishable at the 95% level of significance.

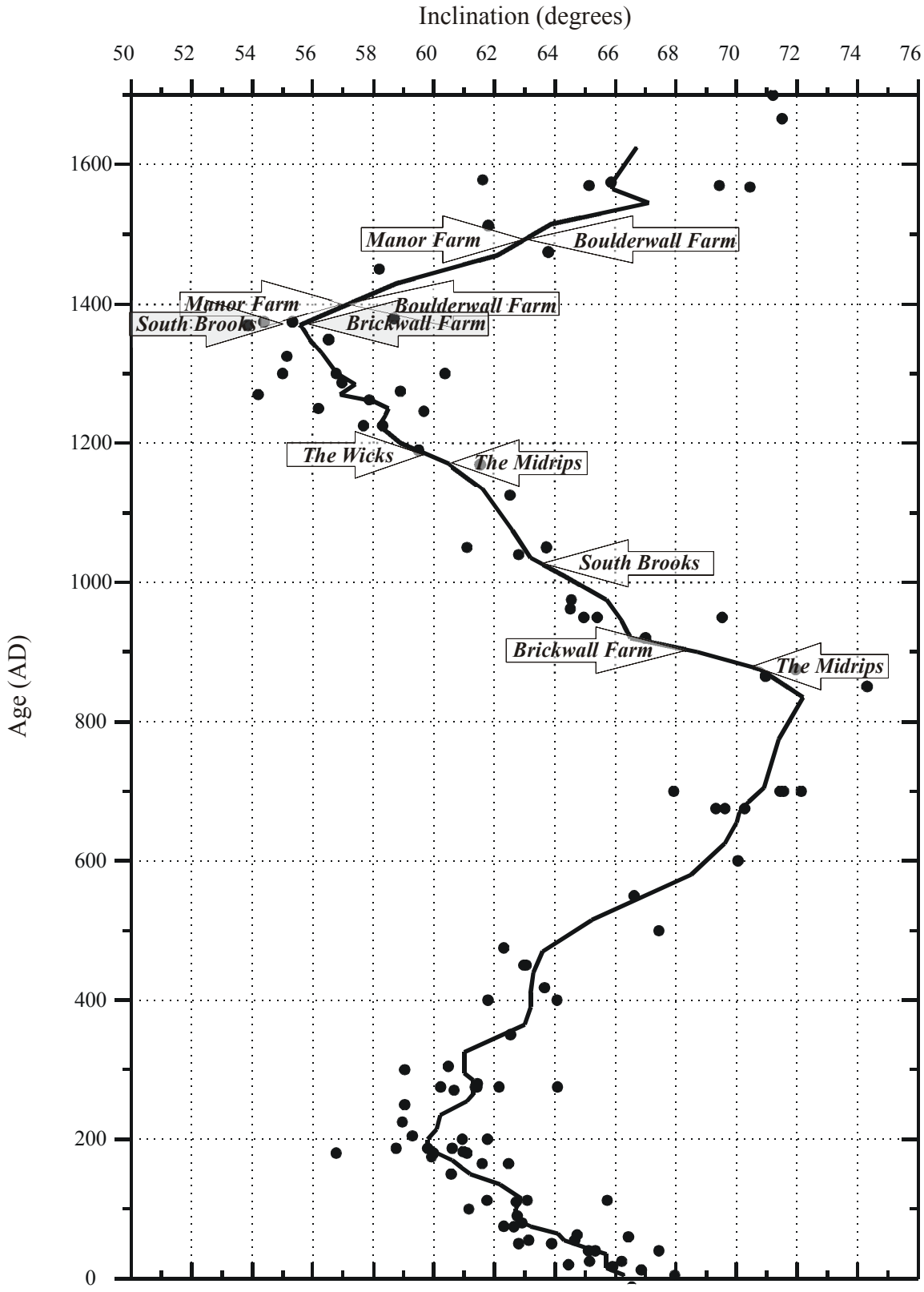

Figure 12 Smoothed inclination from the Paris calibration data (Le Goff *et al* 2002) with bracketing ages indicated for each of the post-gravel marshland core sites apart from the Wicks where only one date was determined.

6.1. The Midrips and the Wicks

Palaeoinclination derived from the 3 uppermost cores (Table 2, Mid3 to Mid1) at the most westerly marshland site, the Midrips, are in the range 62° to 60° and decrease upwards, although the value of α_{95} derived from Mid3 is high. Comparing this with the Paris calibration data (Fig 12) suggests possible ages in the range 150 to 300 AD with the trend of falling inclination particularly well-defined between 150 and 200 AD. The period between 1100 and 1175 AD also matches the sample data trend of a slight decrease in palaeoinclination. In contrast, the deepest core, Mid4, generated a well-constrained (high k and N; low α_{95}) palaeoinclination of around 70° which suggests dates in the ranges 600 to 700 AD or 875 AD and effectively eliminates the period 150 to 300 AD from the upper cores. Given the consistent up-core trend of decreasing inclination the most suitable depositional period is between 875 and 1150 AD (Fig 12), with the possibility of a hiatus in deposition mid-core.

The two cores from the Wicks also provide palaeoinclinations of around 60° (Table 2) although the result from the upper core (W2) should be treated with some caution (low N, high α_{95}). Nevertheless this places the depositional period at the Midrips at the younger end (*c* 1175 to 1200 AD, Fig 12) of that obtained from the Wicks which is intuitively consistent with the eastward younging trend across Dungeness. However, there is no evidence here of a deeper, older phase of deposition.

6.2. South Brooks

In contrast to the two westerly sites above, South Brooks (and Brickwall Farm – see below) show a strongly defined trend of palaeoinclination decreasing sharply upwards. In just 2m of core, the palaeoinclination falls from 64° to 47° at South Brooks (Table 2, SB3 to SB1). The only section of the Paris Master Curve to which this trend can be fitted over the past 2000 years is between 1025 and *c* 1375 AD (Fig 12). Palaeoinclination from SB1 (47°) in fact falls outside of the range of the Paris data but the strong inclination trend in this date range, together with the scatter in both the sample (SB1, high α_{95}) and the calibration data around 1375 AD (Fig 12), suggest that selected depositional period is reasonable.

6.3. Brickwall Farm

Results from Brickwall Farm (Table 2, Fig 12) are closely comparable to those at South Brooks with a strong up-core trend of decreasing inclination from around 68° to 51°. A further similarity is that whilst the three deeper sample cores generated relatively well-constrained palaeoinclinations the shallowest (Brick1) sample produced a high value of α_{95} and palaeoinclination outside the Paris calibration curve range. The relatively poorly constrained nature of results from the shallowest sample cores is common throughout the six marshland sites. A depositional period covering 900 to 1375 AD (Fig 12) is proposed here with the younger end of the range again being supported by the strong trend in palaeoinclination and the scatter of both sample and calibration data.

6.4. Manor Farm

At Manor Farm the trend in inclination is now reversed from the previous two sites as it increases up-core (Table 2, Fig 12). Results from the replicate Manor Farm cores are in good agreement with each other and all six mean palaeoinclinations are well constrained. There appears to be a contrast between the deeper cores (MF3 and MF6) whose mean inclination is 57° to 59° and the four shallower cores where the range is 63° to 65°, although in the latter case there a slight reversal of the trend from MF2 to MF1 and MF5 to MF4. However, overlap of the α_{95} cones of confidence of the mean inclinations from the two upper cores (Table 2, Fig 11b: MF1,2 and MF4,5 respectively) in each borehole indicates that these 2 upper values are not distinguishable at the 95% confidence level and can be averaged (Butler 1992; Tauxe 2002). Consequently, the general trend is best fitted to the period between 1400 and *c* 1525 AD (although 200 to 500 AD would also be possible but is discounted here on the basis of the eastward younging trend and the reasonable evidence for deposition in the period 950

to 1400 AD to the west at South Brooks and Brickwall Farm). This period, the fifteenth and sixteenth centuries AD, is relatively poorly defined in the Paris calibration data and it may be suggested that the true PSV during this period is more complex, as evidenced by the slight kink in the curve around 1550 AD which mimics the sample data MF2 to MF1 and MF5 to MF4 (Table 2, Fig 12).

6.5. Boulderwall Farm

Ignoring Bould3 (very low k, high α_{95}) the trend in palaeoinclination (Table 2), as at Manor Farm, is for a strong increase up-core from around 54° at depth (Bould2 and Bould4) to 63° in the upper core (Bould1). Again the period commencing around 1350 to 1400 AD up to 1500 AD is suggested with the same caveats attached to the period of minimum inclination values around 1400 AD as expressed above (Fig 12).

6.6. A chronostratigraphic model for post-gravel sedimentation

In order to determine the statistical likelihood that there is indeed any palaeosecular variation recorded in these sediments both through time at each site, and spatially across the study area, palaeoinclination at each site, and the associated α_{95} error bars can be compared (Fig 11). Any two samples whose mean values are enclosed by their respective α_{95} cones of confidence cannot be distinguished at the 95% probability level (Butler 1992; Tauxe 2002). The four western sites are shown separately (Fig 11a) to the two eastern sites (Fig 11b) for clarity – this division being supported by the differing up-core trends in inclination discussed above, indicating two distinct periods of sedimentation despite the common range of inclinations recorded. Statistically distinct inclinations are recorded from the deeper samples at the Midrips, South Brooks and Brickwall Farm. Near-surface samples from the Midrips and the Wicks are not distinguishable from the mid-core data at South Brooks and Brickwall Farm; this supports the broad interpretation of the data summarised by the placement of the isochrons in Figure 13. Less clear is the distinction of the uppermost samples at the four western marshland sites and this is a reflection of the high values of α_{95} caused, as we suggested previously, by sampling of the more slowly accreting mottled silts of unit 2 at the top of the respective piston cores. Nevertheless, the uppermost samples of the Midrips and the Wicks are not statistically different, neither are those from South Brooks or Brickwall Farm. The trend of falling inclination up-core is well-defined at all four sites (Fig 11a).

To the east (Fig 11b) the deeper samples at Manor Farm are distinct from those above but not from the deepest sediment recovered at Boulderwall Farm. Similarly the uppermost sediments at Manor Farm are not statistically different from each other, nor from the uppermost Boulderwall sediments. Previous lithostratigraphic evidence (Plater 1992) supports the conclusion implied by the PSV dates that there was a distinct break in deposition, possibly related to the emplacement of a significant shingle ridge which separated the sedimentation at Manor and Boulderwall Farms from the area to the west. Sample Bould3 is not plotted as it is distinct amongst the results presented here in having not only a relatively high α_{95} but also a low value of Fisher's k statistic.

In summary, we propose a broad chronostratigraphic model (Fig 13) which sees a general eastward younging trend upon which is superimposed a three phase post-gravel marshland depositional history at each site:

- The immediate post-gravel phase of marshland deposition appears to be temporally, if not lithostratigraphically, distinct from the main body of the laminated units 2 and 3, but it appears that only a relatively thin layer of this initial period of sedimentation was preserved. Only the Wicks marshland stratigraphy failed to record distinctly older basal deposits.
- Statistically indistinguishable palaeoinclination results from the mid-core samples of units 2 and 3 support a period of rapid sedimentation associated with the tidal rhythmites.

- Poorly constrained palaeodirections from the uppermost samples reflect the likelihood of a rapid slow down in sedimentation following the end of tidal rhythmite deposition and consequently the possibility for recording a distinct PSV record within these cores, and/or the potential for overprinting of the DRM in cores which recovered relatively large amounts of the heavily mottled unit 4 (see Fig 8 to compare sampling elevations of PSV cores with litho- and magnetostratigraphic zones and note, for example, that the well-constrained Manor Farm PSV data are restricted to magnetostratigraphic zone 1).

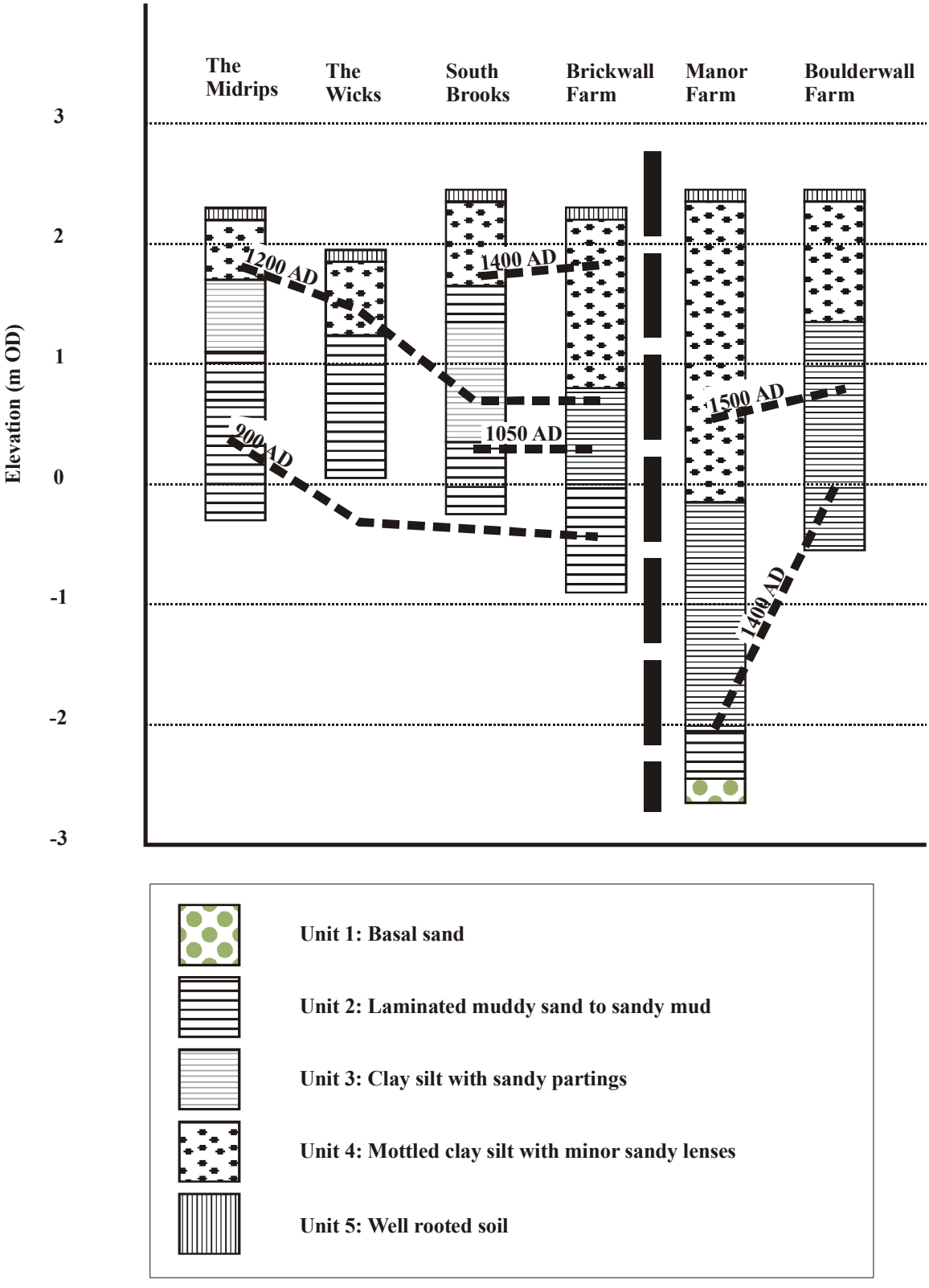

Figure 13 Schematic representation of post-gravel marshland chronostratigraphy based on a interpretation of the PSV dates given in Table 2. Timelines are plotted at mid-core elevation for each sample date and rounded to the nearest 50 years for clarity.

7. Discussion of PSV chronology

The PSV ages determined for the Dungeness marshland sediments are indicative of rapid back-barrier tidal sedimentation, ie accumulation of the tidal rhythmites, during a period which commenced over 1100 years ago and extended to at least 500 years ago (Fig 13). Although these ages seem young in the context of the OSL chronology for the shoreface sand body underlying the gravel in this region, which dates the sub-gravel sands between Broomhill and Denge Marsh to 4500–1000 years ago (Roberts and Plater 2005), it is clear that this sand body was a precursor to gravel deposition. Similarly, the radiocarbon age from *in situ* paired *Cerastoderma edule* shells in a laminated sequence from Manor Farm confirms a period of marsh sediment deposition *c* 1200–1000 cal years BP (Beta-160060/61 in Plater *et al* 2002). Whilst the disparity between the ^{14}C and PSV ages may be attributed to an unknown lock-in depth for the NRM, thus introducing a temporal offset between the time of deposition and the acquisition of the PSV signal, one may equally argue the significance of a poorly constrained reservoir effect on the radiocarbon age. Certainly, set within a sequence of late Holocene foreland progradation, and the marked changes in coastline which culminated in the storms of the thirteenth century, a period of marsh sedimentation following changing coastal morphology about 1200–450 years ago is in good general agreement. In addition, an eastward 'younging' trend in the PSV ages corresponds well with the eastward progradation of Dungeness.

A further positive aspect of this research is the apparent success of the technique in determining the age of minerogenic sediments where both the nature of sedimentation and the post-depositional environment count against it. As has become clear during the progress of the work, tidal rhythmite analysis confirms tidal sedimentation rates of the order of 0.2 to 1m/yr. In such circumstances, even a 3.5m long sediment core like that obtained from Manor Farm is unlikely to preserve a record of PSV for a period much longer than *c* 10–20 years. Consequently, matching the sequence of PSV preserved in the sediment record with a Master curve is problematic. This has been overcome by obtaining mean whole core values for inclination, which are then fitted to the archaeomagnetic calibration curve taking account of both trends in inclination up-core and the well-established eastward-younging of sediments across Dungeness. Indeed, the fact that inclination tends to be in good agreement in the middle of the sequence at each site, in that the α_{95} confidence intervals of the individual cores mean values often overlap, eg (and in particular) the uppermost 2m at Manor Farm, is a further confirmation of rapid marsh sediment accumulation.

Those cores with distinct mean inclinations may have sampled either the basal few centimetres of the sequence overlying the gravel, which was often lithologically somewhat distinct, typically coarser (SB3, Brick4, MF6) but sometimes noticeably muddier (Mid4, Bould4) than the overlying sediments (Fig 9), or alternatively, extended above the top of the laminated tidal rhythmites (units 2 and 3, Fig 13) into the mottled unit 2 (SB1, Brick1, Bould3). In the case of the former, it is not unreasonable to envisage that sediments immediately overlying the gravel represent an initial period of sedimentation in which extensive tidal rhythmite *preservation* (Stupples and Plater forthcoming) was not possible and so the basal few centimetres of the sample core is older than the majority of the overlying units 2 and 3. The latter group, especially Bould3, generated the highest values of α_{95} and this observation supports the lithological evidence of a dramatic reduction in sedimentation rates in moving from the tidal rhythmites of units 2 and 3 (*c* 0.5m/y) to the mottled unit 4 (cm to mm/y) in that the mottled units have the potential to record a genuine PSV due to their much longer depositional period. In both instances whole core mean palaeoinclinations are skewed by these effects but a higher resolution sampling regime would be required to unequivocally identify these older and younger sediments respectively. Additionally, the lower precision of the shallowest samples may be driven by the inclusion of sediments from magnetostratigraphic zone 2 (Fig 8) where the mottled appearance indicates significant post-depositional overprinting of the DRM. Scatter may also increase as a function of particle size – the concentration of magnetic minerals in the finer silty fraction has already

been mentioned and so the inclusion of an unusually sand-dominated sample in the PSV data may reduce the precision of the mean core direction obtained.

The PSV method used here has proved applicable to sediments where there is a clear, but variable, overprint from post-depositional diagenesis. Cleaning steps are effective in removing this overprint and in determining the hard remanence NRM, which has been shown to be less susceptible to overprinting than the soft remanence. Furthermore, the laminated nature of the sediments is indicative of changing tidal flow velocity and water depth related to the diurnal inequality, spring-neap cycle and equinoctial tides (amongst others). This is a clear illustration of a mechanical sorting and sediment processing signal on the nature of sedimentation – which would work against alignment of magnetic particles in the ambient magnetic field. From our results, however, PSV should be considered as an effective means for dating back-barrier marsh and lagoonal sediments where both depositional sedimentary and post-depositional geochemical processes influence the recording and preservation of the PSV record.

8. Conclusions

PSV ages are indicative of rapid marsh sedimentation during the period 875 to 1525 AD. Coupled with an apparent eastward-younging trend in marshland sedimentation, these chronological data agree well with evidence of late Holocene foreland progradation and storm-induced changes in coastline.

The PSV approach has been successful even though a rapid rate of sedimentation severely limited the potential extent and resolution of any palaeosecular variation record in inclination (and where declination data were unavailable). Mean core values, coupled with a consideration of broad up-core trends of palaeoinclination, and supporting chronostratigraphic, archaeological and historical evidence at each site, enabled effective dating with reference to the Paris calibration curve.

Despite clear evidence of diagenetic and pedogenetic overprinting of the NRM and sedimentary evidence of tidal current influences on sedimentation, a cleaned PSV record may be obtained from back-barrier and marsh sediments to provide a chronology for late Holocene coastal minerogenic sequences.

Acknowledgements
The authors should like to acknowledge the collaboration and support of the following: Antony Long (Durham), Martyn Waller (Kingston), Helen Roberts (Aberystwyth), Ed Schofield (Aberdeen), Damien Laidler (Durham), Kate Elmore (Liverpool), Simon Turner (Liverpool), Tim Rolph (Newcastle, Australia), Brian Banks (English Nature), Jon Hickes (MOD), Major O'Reilly (MOD), Simon Busuttil (RSPB), Pete Akers (RSPB), Luke Barber (Archaeology South-East), Melvyn and Dean Stupple (Strata Investigation Services), Bob Jude (Liverpool), Hilda Hull (Liverpool), Alan Henderson (Liverpool), David Hume (Durham), and Alex Bayliss (English Heritage). We are also grateful for the detailed comments of the three anonymous referees which have greatly improved the final report.

References

Abrahamsen, N, 1995 Palaeomagnetic investigation, *Aarhus Geoscience,* **5**, 55–63

Aitken, M J, 1970 Dating by archaeomagnetic and thermoluminescent methods, *Phil Trans Roy Soc,* **A269**, 77–88

Aitken, M J, 1974 *Physics and Archaeology,* 2 edn, Clarendon Press (Oxford)

Aitken, M J, 1990 *Science-based Dating in Archaeology,* Longman Archaeological Series, Longman (London)

Aitken, M J, 1999 Archaeological dating using physical phenomena, *Rep on Progress in Physics,* **62**, 1333–76

Aitken, M J, Hawley, H N, and Weaver, G H, 1963 Magnetic dating: further archaeomagnetic measurements in Britain, *Archaeometry,* **6,** 76–80

As, J A, and Zijderveld, J D A, 1958 Magnetic cleaning of rocks in palaeomagnetic research, *Geophysical J Roy Astronomical Soc,* **1**(4), 308–19

Barber, L, 1998a An early Romano-British salt-working site at Scotney Court, *Archaeologia Cantiana,* **118**, 327–53

Barber, L, 1998b Medieval rural settlement and economy at Lydd, in *Romney Marsh: Environmental Change and Human Occupation in a Coastal Lowland* (eds J Eddison, M Gardiner, and A Long), Oxford University Committee for Archaeology Monograph, **46**, 89–108, Oxford

Barendregt, R W, 1998 Palaeomagnetic Dating Methods, in *Dating Methods for Quaternary Deposits* (eds N W Rutter and N R Catto), GEOtext **2**, Geological Association of Canada, 29–49, St John's, Newfoundland

Batt, C M, 1997 The British archaeomagnetic calibration curve: an objective treatment, *Archaeometry*, **39**, 153–68

Batt, C M, 1998 Where to draw the line? The Calibration of Archaeomagnetic Dates, *Physics and Chemistry of the Earth*, **23,** 991–5

Bloemendal, J, Oldfield, F, and Thompson, R, 1979 Magnetic measurements used to assess sediment influx at Llyn Goddionduon, *Nature*, **280**, 50–3

Borradaile, G J, Lagroix, F, Maher, L, Stewart, J D, Lane, T, Linford, N, and Linford, P, 1999 Attempts to Date Salt-making Activity in Iron Age Britain using Magnetic Inclinations, *J Archaeol Sci*, **26**, 1377–89

Boyle, R, 1691 *Experimenta et Observationes Physicae,* London

Butler, R F, 1992 *Paleomagnetism: Magnetic Domains to Geologic Terranes,* Blackwell Scientific (Boston)

Clark, A J, 1979 Archaeomagnetic Dating, in *Three Surrey hillforts: excavations at Anstiebury, Holmbury and Hascombe 1972–1977* (ed FH Thompson), *Antiq J*, **59**, 245–318

Clark, A J, Tarling, D H, and Noël, M, 1988 Developments in Archaeomagnetic Dating in Britain, *J Archaeol Sci,* **15**, 645–67

Dekkers, M J, 1997 Environmental magnetism: an introduction, *Geologie en Mijnbouw,* **76**, 163–82

Eddison, J, 1983 The evolution of the barrier beaches between Fairlight and Hythe, *Geogr J,* **149**, 39–75

Fassbinder, J W, Stanjek, H, and Vali, H, 1990 Occurrence of bacterial magnetite in soils from archaeological sites, *ArchaeoPolona,* **31**, 117–28

Fisher, RA, 1953 Dispersion on a sphere, *Proc Roy Soc London,* **A217**, 295–305

Folgheraiter, G, 1899a Sur les variations seculaires de l'inclinaison magnetique dans l'antiquite, *Journal de Physique,* **8**, 5–16

Folgheraiter, G, 1899b Sur les variations seculaires de l'inclinaison magnetique dans l'antiquite, *Archives Scientifiques de Physique Naturelle,* **8**, 660

Gallet, Y, Genevey, A, and Le Goff, M, 2002 Three millennia of directional variation of the Earth's magnetic field in western Europe as revealed by archaeological artefacts, *Physics of the Earth and Planetary Interiors,* **131**, 81–9

Gogorza, C S G, Sinito, A M, and Vilas, J F, 2000 Geomagnetic variations over the last 6500 years as recorded by sediments from the lakes of south Argentina, *Geophysical J Int,* **143**, 787–98

Granar, L, 1958 Magnetic measurements on Swedish varved sediments, *Arkiv for Geofysik,* **3**, 1-40

Greensmith, J T, and Gutmanis, J C, 1990 Aspects of the late Holocene depositional history of the Dungeness area, Kent, *Proc Geologists' Assoc,* **101**, 225–37

Hounslow, M W, 2003 *PMAG Tools version 3.2*, Available free from http://geography.lancs.ac.uk/cemp/resources/software.htm#paleomag, M.Hounslow@lancaster.ac.uk

Huttunen, P, and Stober, J, 1980 Dating of palaeomagnetic records from Finnish lake sediment cores using pollen analysis, *Boreas,* **9**, 192–202

Ising, G, 1943 On the magnetic properties of varved clay, *Ark Mat Astron Fys,* **29A**, 1–37

King, J W, and Channell, J E T, 1991 Sedimentary magnetism, environmental magnetism and magnetostratigraphy, *Rev Geophysics, Supplement,* 358–70

King, J W, Banerjee, S K, Marvin, J, and Ozdemir, O, 1982 A comparison of different magnetic records for determining the relative grain size of magnetite in natural materials: some results from lake sediments, *Earth and Planetary Sci Letters,* **59**, 404–19

Kotilainen, A T, Saarinen, T, and Winterhalter, B, 2000 High-resolution paleomagnetic dating of sediments deposited in the central Baltic Sea during the last 3000 years, *Marine Geology,* **166**, 51–64

Le Goff, M, Gallet, Y, Genevey, A, and Warme, N, 2002 On archaeomagnetic secular variation curves and archaeomagnetic dating, *Physics of the Earth and Planetary Interiors*, **134**, 203–11

Lewis, W V, 1932 The formation of Dungeness Foreland, *Geogr J,* **80**, 309–24

Lewis, W V, and Balchin, W G V, 1940 Past sea-levels at Dungeness, *Geogr J,* **96**, 258–85

Linford, P, and Welch, C, 2004 Archaeomagnetic analysis of glassmaking sites at Bagot's Park in Staffordshire, England, *Physics of the Earth and Planetary Interiors,* **147**, 209–21

Long A J, Plater, A J, Waller, M P, and Innes, J B, 1996 Holocene coastal sedimentation in the Eastern English Channel: New data from the Romney Marsh region, United Kingdom, *Marine Geology,* **136**, 97–120

Long, A J, and Hughes, P D M, 1995 Mid- to late-Holocene evolution of the Dungeness foreland, UK, *Marine Geology,* **124**, 253–71

Long, A J, and Innes, J B, 1995 The back-barrier and barrier depositional history of Romney Marsh, Walland Marsh and Dungeness, Kent, England, *J Quaternary Sci,* **10**, 267–83

Long, A J, Dix, J C, Lloyd Jones, D, Roberts, D H, Croudace, I W, Cundy, A B, Roberts, A, and Shennan, I, 2002 *Bridgwater Bay – long term stability study,* University of Durham for West Somerset District Council

Løvlie, R, Svendsen, J I, and Mangerud, J, 1981 High-latitude Holocene paleosecular variationand magneto-stratigraphic correlation between two lakes in Spitzbergen (78^{o}N), *Physics of the Earth and Planetary Interiors,* **67**, 348–61

Mackereth, F J H, 1971 On the variation in the direction of the horizontal magnetization in lake sediments, *Earth and Planetary Sci Letters,* **12**, 332–8

Maher, B A, 1986 Characterization of soils by mineral magnetic measurements, *Physics of the Earth and Planetary Interiors,* **42**, 76–92

Maher, B A, 1988 Magnetic properties of some synthetic sub-micron magnetite, *Geophysical J,* **94**, 83–96

Maher, B A, 1997 Palaeomagnetic (secular variation) analysis of Holocene intertidal sediments from North Norfolk and the Humber, *LOIS Land-Ocean Interaction Study*, 2nd Annual Meeting, Hull 18–20th March 1997 NERC

Maher, B A, and Hallam, D F, 2005 Magnetic carriers and remanence mechanisms in magnetite-poor sediments of Pleistocene age, southern North Sea margin, *J Quaternary Sci*, **20**, 79–94

Malin, S R C, and Bulland, E, 1981 The direction of the Earth's magnetic field at London, 1570-1975, *Phil Trans Roy Soc,* **299**, 357–423

Manley, W F, MacLean, B, Kerwin, M W, and Andrews, J T, 1993 Magnetic susceptibility as a Quaternary correlation tool: examples from Hudson Strait sediment cores, eastern Canadian Arctic, *Current Research, Part D - Geological Survey of Canada,* **93**(1), 137–45

Matthews, J A, Bridges, E M, Caseldine, C J, Luckman, A J, Owen, G, Perry, A H, Shakesby, R A, Walsh, R P D, Whittaker, R J, and Willis, K J, (eds) 2000 *The Encyclopaedic Dictionary of Environmental Change*, 409–10, Arnold (London)

McFadden, P L, and Reid, A B, 1982 Analysis of paleomagnetic inclination data, *Geophysical J Roy Astronomical Soc*, **69**, 307–19

McNish, A G, and Johnson, E A, 1938 Magnetization of unmetamorphosed varves and marine sediments, *Terr Magn Atmos Elect,* **53**, 349–60

Melloni, M, 1853 Du magnetisme des roches, *Comptes Rendus de l'Academie Scientifique de Paris,* **37**, 966–8

Mercanton, P L, 1918 Etat magnetique de quelques terres cuites prehistoriques, *Comptes Rendus de l'Academie Scientifique de Paris,* **166**, 681–949

Morner, N-A, and Sylwan, CA, 1987 Detailed palaeomagnetic record for the last 6300 years from varved lake deposits in northern Sweden, in *Geomagnetism and Geoelectricity* (eds F J Lowes, D W Collinson, J H Parry, S K Runcorn, D C Tozer, and A Soward), NATO ASI Series C: Mathematical and Physical Sciences **261**, 63–70

Needham, S, 1988 A group of Early Bronze Age axes from Lydd, in *Romney Marsh: Evolution, Occupation and Reclamation* (eds J Eddison and C Green), Oxford University Committee for Archaeology Monograph **24**, 77–82, Oxford

Nichol, S L, Augustinus, P C, Gregory, M R, Creese, R, and Horrocks, M, 2000 Geomorphic and sedimentary evidence of human impact on the New Zealand coastal landscape, *Physical Geog,* **21**(2), 109–32

Noel, M, and Batt, C M, 1990 A method for correcting geographically separated remanence directions for the purposes of archaeomagnetic dating, *Geophysical J Int*, **102**, 753–6

Nolan, S R, Bloemendal, J, Boyle, J F, Jones, R T, Oldfield, F, and Whitney, M, 1999 Mineral magnetic and geochemical records of late glacial climatic change from two northwestern European carbonate lakes, *J Paleolimnology,* **22**, 97–107

Ojala, A, and Saarinen, T, 2002 Paleosecular variation of the Earth's magnetic field during the last 10,000 years based on the annually laminated sediment of Lake Nautajarvi, central Finland, *The Holocene,* **12**, 391–400

Oldfield, F, 1991 Environmental Magnetism - a personal perspective, *Quaternary Sci Rev,* **10**, 73–85

Oldfield, F, 1999 The rock magnetic identification of magnetic mineral and magnetic grain size assemblages, in *Environmental magnetism: a practical guide* (eds J Walden, F Oldfield, and J P Smith), Technical Guide No 6, 98–112, Quaternary Research Association (London)

Oldfield, F, and Yu, L, 1994 The influence of particle size variations on the magnetic properties of sediments from the north-eastern Irish Sea, *Sedimentology,* **41**, 1093–1108

Oldfield, F, Dearing, J A, Thompson, R, and Garret-Jones, S E, 1978 Some magnetic properties of lake sediments and their possible links with erosion rates, *Polskie Archiv fur Hydrobiologie,* **25**, 321–31

Peck, J A, Kong, J W, Colman, S M, and Kravchinski, V A, 1994 A rock-magnetic record from Lake Baikal, Siberia: Evidence for Late Quaternary climate change, *Earth and Planetary Sci Letters,* **122**, 221–38

Petersen, N, von Dobeneck, T, and Vali, H, 1986 Fossil bacterial magnetite in deep-sea sediments from the south Atlantic Ocean, *Nature,* **320**, 611–5

Plater, A, Stupples, P, Roberts, H, and Owen, C, 2002 The evidence for Late Holocene foreland progradation and rapid tidal sedimentation from the barrier and marsh sediments of Romney

Marsh and Dungeness: a geomorphological perspective, in *Romney Marsh: coastal and landscape change through the Ages* (eds A Long, S Hipkin, and H Clarke), Oxford University School for Archaeology Monograph **56**, 40–57, Oxford

Plater, A J, 1992 The late Holocene evolution of Denge Marsh, southeast England: a stratigraphic, sedimentological and micropalaeontological approach, *The Holocene,* **2**, 63–70

Plater, A J, and Long, A J, 1995 The morphology and evolution of Denge Beach and Denge Marsh, in *Romney Marsh: the debatable ground* (ed J Eddison), Oxford University Committee for Archaeology Monograph **41**, 8–36, Oxford

Plater, A J, Long, A J, Spencer, C D, and Delacour, R A P, 1999 The stratigraphic record of sea-level change and storms during the last 2000 years: Romney Marsh, southeast England, *Quaternary Int,* **55**, 17–27

Ridgway, J, Andrews, J E, Ellis, S, Horton, B P, Innes, J B, Knox, R W O'B, McArthur, J J, Maher, B A, Metcalfe, S E, Mitlehner, A, Parkes, A, Rees, J G, Samways, G M, and Shennan, I, 2000 Analysis and interpretation of Holocene sedimentary sequences in the Humber Estuary, in *Holocene Land - Ocean Interaction and Environmental Change around the North Sea* (eds I Shennan and J Andrews), Geological Society, Special Publication **166**, 9–39, London,

Roberts, A P, and Turner, G M, 1993 Diagenetic formation of ferrimagnetic iron sulphide minerals in rapidly deposited marine sediments, South Island, New Zealand, *Earth and Planetary Sci Letters,* **115**, 257–73

Roberts, H M, and Plater, A J, 2005 *Optically stimulated luminescence (OSL) dating of sands underlying the gravel beach ridges of Dungeness and Camber, SE England, UK*, CfA Rep, **27/2005**

Robinson, S G, 1982 Two applications of mineral-magnetic techniques to deep-sea sediment studies, *Geophysical J Royal Astronomical Soc,* **69**, 294

Robinson, S G, 1986 The late Pleistocene palaeoclimatic record of North Atlantic deep-sea sediments revealed by mineral-magnetic measurements, *Physics and the Earth and Planetary Interiors,* **42**, 22–47

Rother, K, 1989 Petro- und palaeomagnetische Untersuchungen an jungquartaren Sedimenten der Ostsee, *Veroffentlichungen des Zentralinstituts furPhysik der Erde,* **109**

Saarinen, T, 1994 Palaeomagnetic study of the Holocene sediments of Lake Paijanne (Central Finland) and Lake Paanajarvi (Northwest Russia), *Geolog Survey of Finland Bulletin,* **376**

Saarinen, T, 1998 High-resolution palaeosecular variation in northern Europe during the last 3200 years, *Physics of the Earth and Planetary Interiors,* **106**, 299–309

Saarinen, T, 1999 Palaeomagnetic dating of Late Holocene sediment in Fennoscandia, *Quatnerary Sci Reviews,* **18**(7), 889–97

Shuey, R T, Cole, E R, and Mikulich, M J, 1970 Geographic Correction of Archaeomagnetic Data, *J Geomagnetism and Geoelectricity*, **22**, 485–9

Smith, J, 1999 An introduction to the magnetic properties of natural materials, in *Environmental Magnetism: a practical guide* (eds J Walden, F Oldfield, and J P Smith), Technical Guide No 6, 5–25, Quaternary Res Assoc (London)

Snowball, I, and Sandgren, P, 2002 Geomagnetic field variations in northern Sweden during the Holocene quantified from varved sediments, and their implications for cosmogenic nuclide production rates, *The Holocene,* **12**(5), 517–30

Snowball, I, and Thompson, R, 1988 The occurrence of greigite in sediments from Loch Lomond, *J Quaternary Sci,* **3**, 121–5

Snowball, I, Sandgren, P, and Petterson, G, 1999 The mineral magnetic properties of an annually laminated Holocene lake-sediment sequence in northern Sweden, *The Holocene,* **9**, 353–62

Snowball, I F, 1991 Magnetic hysteresis properties of greigite (Fe_2S_3) and a new occurrence in Holocene sediments from Swedish Lappland, *Physics of the Earth and Planetary Interiors,* **68**, 32–40

Snowball, I F, 1994 Bacterial magnetite and the magnetic properties of sediments in a Swedish lake, *Earth and Planetary Sci Letters,* **126**, 129–42

Snowball, I F, Zillen, L, and Sandgren, P, 2002b Biogenic magnetite in Swedish varved lake sediments and its potential as a biomarker of environmental change, *Quaternary Int,* **18**, 13-19

Snowball, I F, Zillen, L, and Gaillard, M-J, 2002a Rapid early-Holocene environmental changes in northern Sweden based on studies of two varved lake-sediment sequences, *The Holocene,* **12**, 7–16

Spencer, C D, 1997 *The Holocene evolution of Romney Marsh: a record of sea-level change in a back-barrier environment,* Unpublished PhD thesis, University of Liverpool

Stober, J C, and Thompson, R, 1977 Palaeomagnetic secular variation studies of Finnish lake sediments and the carriers of remanence, *Earth and Planetary Sci Letters,* **37**, 139–49

Stober, J C, and Thompson, R, 1979 Magnetic remanence acquisition in Finnish lake sediments, *Geophysical J Royal Astronomical Soc,* **57** 727–39

Stoner, J S, Channell, J E T, and Hillaire-Marcel, C, 1996 The magnetic signature of rapidly deposited detrital layers from the deep Labrador Sea: relationship to North Atlantic Heinrich layers, *Palaeooceanography,* **11**(3), 309–25

Stupples, P, 2002a Tidal cycles preserved in late Holocene tidal rhythmites, the Wainway Channel, Romney Marsh, south-east England, *Marine Geologogy,* **182**, 231–46

Stupples, P, 2002b *Late Holocene intertidal sedimentation: a lithostratigraphic approach to palaeoenvironmental reconstruction in the Wainway Channel, Romney Marsh, southeast England*, Unpublished PhD Thesis, Manchester Metropolitan University

Stupples, P, and Plater, A J, forthcoming Controls on the temporal and spatial resolution of tidal signal preservation in late-Holocene tidal rhythmites, Romney Marsh, Southeast England, *Int J Earth Sci*

Tarling, D H, 1983 *Palaeomagnetism,* Chapman and Hall (London)

Tarling, D H, and Dobson, M J, 1995 Archaeomagnetism: An Error Assessment of Fired Material Observations in the British Directional Database, *J Geomagnetism and Geoelectricity,* **47**, 5–18

Tauxe, L, 2002 *Paleomagnetic Principles and Practise,* Kluwer Academic Publishers (Dordrecht, The Netherlands)

Thompson, R, 1973 Palaeolimnology and palaeomagnetism, *Nature,* **242**, 182–4

Thompson, R, and Edwards, K J, 1982 A Holocene palaeomagnetic record and a geomagnetic master curve from Ireland, *Boreas,* **11**, 335–49

Thompson, R, and Oldfield, F, 1986 *Environmental Magnetism,* George Allen & Unwin (London)

Thompson, R, and Turner, G M, 1985 Icelandic Holocene palaeolimno-magnetism, *Physics of the Earth and Planetary Interiors,* **38**, 250–61

Thompson, R, Battarbee, R W, O'Sullivan, P E, and Oldfield, F, 1975 Magnetic susceptibility of lake sediments, *Limnology and Oceanography,* **20**, 687–98

Tolonen, K, Siiriainen, A, and Thompson, R, 1975 Prehistoric erosion of sediment in Lake Lojvarvi, S Finland and its paleomagnetic dating, *Ann Bot Fennici,* **12**, 161–4

Turner, G M, 1987 A 5000 year geomagnetic palaeosecular variation record from western Canada, *Geophysical J Roy Astronomical Soc,* **91**, 103–21

Turner, G M, and Thompson, R, 1979 Behaviour of the Earth's magnetic field as recorded in the sediment of Loch Lomond, *Earth and Planetary Sci Letters,* **42,** 412–26

Turner, G M, and Thompson, R, 1981 Lake sediment record of the geomagnetic secular variation in Britain during Holocene times, *Geophysical J Roy Astronomical Soc,* **65**, 703–25

Turner, G M, and Thompson, R, 1982 Detransformation of the British geomagnetic secular variation record for Holocene times, *Geophysical J Roy Astronomical Soc,* **70**, 789–92

Verosub, K L, and Roberts, A P, 1995 Environmental magnetism: Past, present and future, *J Geophysical Res,* **100**, 2175–92

Walden, J, Oldfield, F, and Smith, J P, (eds) 1999 *Environmental Magnetism: a practical guide,* Technical Guide No 6, Quaternary Res Assoc (London)

Wheeler, A J, Oldfield, F, and Orford, J D, 1999 Depositional and post-depositional controls on magnetic signals from salt marshes on the north-west coast of Ireland, *Sedimentology,* **46**, 545–58

Yamazaki, T, Abdeldayem, A L, and Ikehara, K, 2003 Rock-magnetic changes with reduction diagenesis in Japan Sea sediments and preservation of geomagnetic secular variation in inclination during the last 30,000 years, *Earth Planets and Space*, **55**, 327–40

Zijderveld, J D A, 1976 AC demagnetisation of rocks: analysis of results, in *Methods in Palaeomagnetism* (eds D W Collinson, K M Creer and S K Runcorn), Developments in Solid Earth Geophysics, **3**, NATO Advanced Study Institute on Palaeomagnetic Methods, 254–86, Elsevier (Amsterdam)

Appendix I: Palaeomagnetic Secular Variation Data

Site	The Midrips TR 00466 18271 Elevation 2.306 m OD											
Core	Mid1			Mid2			Mid3			Mid4		
Elevation (m OD)	2.31 to 1.31			1.31 to 0.31			1.94 to 0.94			0.94 to -0.06		
	Cm from top	Dec (°)	Inc (°)	Cm from top	Dec (°)	Inc (°)	Cm from top	Dec (°)	Inc (°)	Cm from top	Dec (°)	Inc (°)
	06-08	36.1	61.8	05-07	23.5	57.0	05-07	261.9	67.7	02-04	153.9	38.8
	12-14	55.2	61.0	10-12	25.5	56.5	08-10	281.6	59.0	05-07	82.1	62.2
	16-18	45.8	60.7	14-16	28.9	57.8	11-13	219.5	70.0	07-09	37.4	71.2
	21-23	42.0	58.3	19-21	64.4	65.0	14-16	244.5	76.1	09-11	58.6	71.5
	26-28	34.4	69.3	24-26	45.7	67.4	26-28	292.3	70.6	12-14	86.0	74.7
	31-33	25.0	60.7	29-31	28.6	78.2	33-35	305.2	61.2	14-16	62.2	72.5
	41-43	18.0	66.3	34-36	33.2	56.7	43-45	285.0	59.6	19-21	42.2	74.7
	46-48	61.5	52.8	39-41	44.5	57.5	48-50	263.6	46.2	22-24	56.9	74.3
	51-53	35.7	76.5	43-45	16.5	61.0	53-55	304.5	32.3	24-26	20.5	60.8
	61-63	5.5	43.9	48-50	25.8	59.8	58-60	205.5	71.3	26-28	34.6	71.6
				53-55	24.3	58.8				29-31	38.6	67.8
				60-62	23.3	63.8				31-33	43.2	76.3
				65-67	30.0	72.2				33-35	49.3	73.3
				70-72	26.3	73.0				36-38	35.6	69.5
										38-40	35.3	69.9
										41-43	37.0	66.2
										43-45	28.0	76.6
										45-47	27.3	68.7
										47-49	41.5	74.4
										50-52	29.9	63.7
										52-54	29.3	69.3
										55-57	21.3	69.3
										57-59	13.6	73.7
										59-61	22.1	72.9
										62-64	27.3	75.8
										64-66	32.0	73.6
										67-69	42.3	80.3
										69-71	22.2	76.6
										71-73	22.1	72.9
										74-76	12.9	68.3
										76-78	40.4	65.7
										78-80	0.6	67.8
										81-83	5.8	68.9
										83-85	21.8	71.0
										86-88	19.0	71.4
										88-90	13.6	70.4
										90-92	191.9	66.5

Site	The Wicks TR 00888 18004 Elevation 1.936 m OD					
Core	W1			W2		
Elevation (m OD)	1.19 to 0.19			1.94 to 0.94		
	Cm from top	Dec (°)	Inc (°)	Cm from top	Dec (°)	Inc (°)
	05-07	356.7	61.6	07-09	30.7	58.7
	15-17	359.2	56.2	10-12	38.6	50.9
	24-26	351.9	67.1	17-19	148.9	58.7
	34-36	1.7	61.3	22-24	56.3	71.3
	44-46	5.1	60.0	27-29	22.1	57.7
	48-50	354.5	59.8	37-39	35.2	52.9
	53-55	349.8	66.3	41-43	84.8	-24.1
	63-65	348.4	65.5	51-53	73.7	69.1
	72-74	345.0	63.0			
	81-83	346.9	61.6			

Site	South Brooks TR 02786 17815 Elevation 2.450 m OD								
Core	SB1			SB2			SB3		
Elevation (m OD)	1.75 to 0.75			1.25 to 0.25			0.75 to -0.25		
	Cm from top	Dec (°)	Inc (°)	Cm from top	Dec (°)	Inc (°)	Cm from top	Dec (°)	Inc (°)
	05-07	4.4	29.4	10-12	357.6	50.7	05-07	45.4	65.5
	10-12	15.5	27.4	15-17	325.4	66.6	12-14	47.4	65.0
	15-17	352.5	48.8	19-21	16.5	52.2	19-21	49.3	68.0
	20-22	337.8	58.6	29-31	18.4	64.5	27-29	42.0	63.4
	25-27	8.3	55.3	34-36	18.7	59.3	34-36	32.7	67.3
	30-32	0.8	60.5	38-40	358.3	55.7	41-43	25.8	59.9
	35-37	342.3	54.5	48-50	354.7	56.0	48-50	32.7	57.2
	40-42	30.5	66.6	52-54	347.1	66.9	62-64	30.9	63.6
	45-47	347.9	47.7	57-59	347.8	58.3	70-72	25.8	69.7
	50-52	354.2	35.0	62-64	348.7	49.8	77-79	17.4	66.0
	55-57	22.7	51.1	71-73	29.2	67.6	84-86	5.2	63.4
	59-61	353.3	54.3						

Site	Brickwall Farm TR 05050 18290 Elevation 2.298 m OD											
Core	Brick1			Brick2			Brick3			Brick4		
Elevation (m OD)	1.8 to 0.8			0.8 to -0.2			1.15 to 0.15			0.15 to -0.85		
	Cm from top	Dec (°)	Inc (°)	Cm from top	Dec (°)	Inc (°)	Cm from top	Dec (°)	Inc (°)	Cm from top	Dec (°)	Inc (°)
	05-07	355.5	72.9	05-07	335.8	60.5	05-07	340.6	58.4	05-07	9.5	68.8
	15-17	321.7	39.8	14-16	1.1	60.4	15-17	353.7	62.1	15-17	359.8	70.6
	20-22	352.2	56.8	24-26	353.1	61.8	24-26	23.0	59.9	24-26	359.0	70.5
	25-27	345.9	66.6	33-35	357.3	63.3	34-36	342.5	64.5	33-35	7.3	73.3
	34-36	282.4	-7.4	43-45	339.7	64.3	43-45	351.3	56.9	43-45	359.7	64.0
	39-41	311.1	32.3	47-49	350.1	66.4	46-48	352.4	56.5	52-54	9.7	70.8
	44-46	312.7	35.3	52-54	334.3	64.0	52-54	355.4	58.1	62-64	3.3	69.3
	54-56	250.9	57.1	62-64	342.3	70.7	62-64	347.6	59.9	69-71	0.5	57.4
	58-60	297.3	56.4	71-73	340.7	68.8	71-73	347.7	53.6	83-85	25.3	55.8
	63-65	302.3	64.7	76-78	351.3	61.7	76-78	353.2	65.2	87-89	8.0	52.1

Site	Manor Farm TR 05928 18077 Elevation 2.464 m OD								
Core	MF1			MF2			MF3		
Elevation (m OD)	0.96 to -0.40			-0.04 to -1.04			-1.04 to -2.04		
	Cm from top	Dec (°)	Inc (°)	Cm from top	Dec (°)	Inc (°)	Cm from top	Dec (°)	Inc (°)
	05-07	338.5	71.1	05-07	13.3	70.6	05-07	9.1	66.3
	15-17	16.1	62.0	12-14	17.2	70.8	14-16	15.50	61.9
	24-26	18.2	62.4	24-26	25.3	65.3	24-26	13.70	62.7
	34-36	4.0	64.0	33-35	16.9	64.2	33-35	15.80	56.2
	39-41	15.2	68.6	38-40	23.8	68.7	38-40	13.30	61.0
	43-45	1.4	62.4	43-45	37.8	72.2	43-45	18.30	58.6
	53-55	9.1	57.0	52-54	24.8	68.3	52-54	6.40	58.9
	63-65	357.6	70.5	62-64	11.8	68.1	62-64	4.4	60.7
	72-74	1.0	63.5	71-73	12.3	58.3	72-74	4.9	59.8
	82-84	9.7	63.7	81-83	11.5	58.7	81-83	354.1	64.4
	MF4			MF5			MF6		
	0.46 to -0.54			-0.54 to -1.54			-1.54 to -2.54		
	Cm from top	Dec (°)	Inc (°)	Cm from top	Dec (°)	Inc (°)	Cm from top	Dec (°)	Inc (°)
	05-07	11.3	62.5	05-07	13.2	60.5	05-07	34.8	63.3
	14-16	10.4	59.2	14-16	20.5	70	14-16	33.1	65.7
	24-26	25.5	67.8	24-26	21.8	67.6	19-21	35.1	63.9
	33-35	12.2	66.8	33-35	21.1	68.6	24-26	38.2	61.2
	38-40	42.0	76.7	38-40	28.5	66.7	33-35	40	56.8
	43-45	19.9	69.2	43-45	28.7	67.3	38-40	35.3	55.9
	52-54	18.0	65.4	52-54	26.2	68.3	43-45	27.4	59.1
	62-64	3.0	62.3	62-64	21.2	68.6	52-54	31.8	54.7
	71-73	331.4	58.3	71-73	15	67.2	57-59	11.9	48.8
	80-82	323.0	54.6	81-83	14.9	61.4	62-64	12.5	56

Site	Boulderwall Farm TR 06181 19231 Elevation 2.438 m OD											
Core	Bould1			Bould2			Bould3			Bould4		
Elevation (m OD)	1.34 to 0.34			0.34 to -0.16			1.84 to 0.84			0.84 to -0.16		
	Cm from top	Dec (°)	Inc (°)	Cm from top	Dec (°)	Inc (°)	Cm from top	Dec (°)	Inc (°)	Cm from top	Dec (°)	Inc (°)
	02-04	14.5	66.7	06-08	76.8	79.0	03-05	254.5	44.7	00-02	356.1	57.6
	05-07	338.0	82.0	08-10	124.9	59.2	18-20	28.3	34.3	02-04	0.9	57.0
	07-09	26.6	51.9	10-12	119.3	59.7	21-23	126.5	35.0	05-07	4.4	47.9
	10-12	11.7	71.1	13-15	83.6	71.4	23-25	74.7	59.4	07-09	2.9	55.9
	12-14	0.2	76.0	16-18	83.3	66.1	28-30	14.4	50.7	09-11	4.2	50.5
	15-17	355.0	63.7	18-20	106.8	65.3	31-33	69.5	71.6	12-14	351.0	56.8
	17-19	5.2	70.8	21-23	81.2	54.1	34-36	53.9	58.3	14-16	350.7	50.6
	19-21	16.4	48.1	24-26	81.9	61.2	39-41	328.6	51.9	17-19	347.2	48.1
	22-24	10.6	73.1	33-35	60.5	44.8	42-44	318.7	17.0	19-21	344.9	55.2
	24-26	0.3	54.9	36-38	62.4	42.6	52-54	68.5	67.6	22-24	348.1	51.4
	27-29	33.4	72.0	38-40	61.9	42.0	55-57	21.8	61.3	24-26	336.8	49.9
	29-31	24.8	66.0	41-43	68.5	44.8	57-59	353.7	67.2	26-28	338.0	48.9
	32-34	14.3	66.6	43-45	59.3	59.0	60-62	33.3	53.8	29-31	350.6	51.6
	34-36	7.7	72.5				62-64	48.9	62.9	31-33	349.5	54.0
	36-38	2.5	49.8				64-66	24.5	26.9	33-35	355.6	57.6
	39-41	5.0	57.3				67-69	350.8	22.8	36-38	347.0	56.1
	41-43	19.2	64.0				69-71	2	3.1	38-40	345.9	56.9
	44-46	7.1	66.5							41-43	348.8	55.8
	46-48	355.7	62.5							43-45	341.6	59.8
	48-50	359.9	53.2							45-47	341.4	51.2
	51-53	10.7	60.8							48-50	337.9	63.7
	53-55	351.0	73.4							50-52	342.7	57.7
	56-58	343.6	70.4							53-55	334.3	51.5
	58-60	357.0	56.5							55-57	339.1	54.2
	60-62	357.6	60.9							57-59	341.5	58.6
	63-65	350.5	65.8							60-62	340.1	60.4
	65-67	352.1	67.4							62-64	337.1	62.1
	68-70	5.5	57.9							65-67	356.0	64.2
	70-72	3.1	64.1							67-69	3.3	53.5
	72-74	359.0	67.5							70-72	351.9	58.4
	75-77	3.2	68.8							72-74	1.2	54.4
	77-79	355.3	66.5							74-76	356.2	55.6
	80-82	4.5	63.4							77-79	346.0	62.6
	82-84	2.5	61.7							79-81	348.0	51.2
	85-87	353.0	61.5							82-84	356.7	64.3
	87-89	356.8	64.3							84-86	0.3	54.1
	89-91	355.8	67.0							86-88	353.7	46.4

Appendix II: Environmental Magnetic Property Data

Environmental magnetism data: The Midrips

Sample Name	Elevation m OD	Mass g	χ_{kappa} 10^{-8} m^3kg^{-1}	χ_{lf} 10^{-8} m^3kg^{-1}	χ_{hf} 10^{-8} m^3kg^{-1}	FD %	SIRM 10^{-5} Am^2kg^{-1}	χ_{arm} 10^{-8} m^3kg^{-1}	χ_{arm}/SIRM 10^{-3} mA^{-1}	SIRM/χ_{lf} 10^{-3} mA^{-1}	χ_{arm}/χ_{lf} no units
Mid1	0.02	11.46	18.51	16.58	16.19	2.37	697.55	260.56	0.37	42.08	15.72
Mid2	0.04	11.49	18.12	16.40	16.06	2.12	677.20	319.04	0.47	41.28	19.45
Mid3	0.06	10.15	12.99	11.48	11.14	3.00	297.12	263.60	0.89	25.88	22.96
Mid4	0.09	11.00	12.77	11.45	11.09	3.17	240.84	229.79	0.95	21.03	20.06
Mid5	0.11	10.72	10.37	9.24	9.00	2.53	167.40	95.16	0.57	18.13	10.30
Mid6	0.13	10.76	10.08	8.83	8.55	3.16	161.31	173.69	1.08	18.27	19.67
Mid7	0.15	10.69	9.94	8.66	8.38	3.24	177.89	207.57	1.17	20.55	23.98
Mid8	0.18	10.96	11.48	10.17	9.85	3.14	219.98	295.28	1.34	21.62	29.02
Mid9	0.20	10.66	11.65	10.22	9.94	2.75	219.87	257.67	1.17	21.51	25.21
Mid10	0.22	10.25	10.48	9.12	8.87	2.67	190.14	203.43	1.07	20.85	22.31
Mid11	0.25	9.95	10.94	9.54	9.34	2.11	188.41	156.93	0.83	19.74	16.44
Mid12	0.27	9.85	12.52	11.02	10.61	3.69	284.53	247.59	0.87	25.82	22.47
Mid13	0.29	11.02	12.43	11.03	10.93	0.82	328.95	221.66	0.67	29.84	20.10
Mid14	0.31	11.56	15.67	14.01	13.75	1.85	598.69	199.67	0.33	42.73	14.25
Mid15	0.34	9.86	16.26	14.40	14.14	1.76	577.22	299.37	0.52	40.09	20.79
Mid16	0.32	9.90	13.21	11.56	11.31	2.18	361.24	226.09	0.63	31.24	19.55
Mid17	0.34	9.66	24.29	21.63	21.32	1.44	1256.86	261.46	0.21	58.11	12.09
Mid18	0.36	10.47	19.69	17.63	17.29	1.90	865.97	270.70	0.31	49.13	15.36
Mid19	0.39	10.28	13.71	12.21	11.82	3.19	429.40	242.21	0.56	35.17	19.84
Mid20	0.41	10.50	13.92	12.52	12.05	3.80	420.32	243.06	0.58	33.57	19.41
Mid21	0.43	10.62	14.47	12.95	12.57	2.91	425.46	237.69	0.56	32.85	18.35
Mid22	0.46	10.15	14.10	12.47	12.17	2.37	443.10	202.94	0.46	35.54	16.28
Mid23	0.48	11.06	13.50	12.03	11.71	2.63	433.71	188.49	0.43	36.07	15.67
Mid24	0.50	10.71	14.70	13.03	12.94	0.72	495.22	174.04	0.35	38.00	13.36
Mid25	0.53	11.07	14.58	13.01	12.74	2.08	493.42	202.94	0.41	37.92	15.60
Mid26	0.55	11.77	15.29	13.63	13.34	2.18	561.21	234.44	0.42	41.16	17.20
Mid27	0.57	10.75	17.96	16.10	15.68	2.60	787.19	231.82	0.29	48.90	14.40
Mid28	0.60	11.09	17.86	16.01	15.65	2.25	781.17	228.71	0.29	48.80	14.29
Mid29	0.62	11.17	17.11	15.40	15.00	2.62	703.85	219.36	0.31	45.69	14.24
Mid30	0.64	9.49	16.41	14.38	13.96	2.93	652.92	213.13	0.33	45.40	14.82
Mid31	0.67	10.47	17.97	16.14	15.71	2.66	779.76	235.83	0.30	48.30	14.61
Mid32	0.69	11.15	23.44	21.25	20.72	2.53	1287.54	260.48	0.20	60.58	12.26
Mid33	0.71	10.54	27.16	24.62	24.00	2.50	1532.19	279.99	0.18	62.23	11.37
Mid34	0.74	10.44	27.26	24.72	24.14	2.33	1533.99	275.52	0.18	62.06	11.15
Mid35	0.76	11.41	15.04	13.54	12.93	4.53	537.73	191.09	0.36	39.72	14.11
Mid36	0.78	10.67	17.63	15.84	15.28	3.55	688.43	196.27	0.29	43.46	12.39
Mid37	0.81	11.42	12.93	11.65	11.13	4.51	359.65	143.74	0.40	30.87	12.34
Mid38	0.83	11.17	13.27	11.81	11.54	2.27	392.56	131.24	0.33	33.23	11.11
Mid39	0.85	10.15	18.01	16.11	15.87	1.53	748.45	203.22	0.27	46.44	12.61
Mid40	0.88	11.30	51.64	47.07	46.41	1.41	3390.86	360.95	0.11	72.04	7.67
Mid41	0.90	11.24	19.64	17.67	17.27	2.27	880.52	187.44	0.21	49.84	10.61
Mid42	0.92	10.99	35.07	31.94	31.39	1.71	2054.27	241.13	0.12	64.33	7.55
Mid43	0.95	10.69	17.53	15.67	15.39	1.79	680.53	110.96	0.16	43.43	7.08
Mid44	0.97	11.30	19.67	17.80	17.40	2.24	896.29	125.71	0.14	50.37	7.06
Mid45	0.99	10.68	17.20	15.45	15.07	2.42	614.08	94.87	0.15	39.75	6.14
Mid46	1.02	10.13	14.94	13.28	13.03	1.86	385.75	62.57	0.16	29.06	4.71
Mid47	1.04	11.14	11.71	10.32	10.05	2.61	248.61	44.33	0.18	24.09	4.30
Mid48	1.06	11.42	10.02	8.80	8.67	1.49	188.05	33.84	0.18	21.36	3.84
Mid49	1.09	10.75	9.49	8.28	8.19	1.12	133.84	26.54	0.20	16.16	3.21
Mid50	1.11	11.37	12.43	11.04	10.82	1.99	325.64	44.48	0.14	29.50	4.03
Mid51	1.13	11.04	9.02	7.88	7.70	2.30	95.35	20.19	0.21	12.10	2.56
Mid52	1.15	10.55	8.75	7.63	7.44	2.48	75.74	17.68	0.23	9.93	2.32
Mid53	1.18	11.86	8.72	7.67	7.42	3.30	80.17	19.14	0.24	10.45	2.49
Mid54	1.20	10.62	8.38	7.29	7.11	2.58	67.71	15.79	0.23	9.28	2.16

Sample Name	Elevation m OD	Mass g	χ_{kappa} 10^{-8} m^3kg^{-1}	χ_{lf} 10^{-8} m^3kg^{-1}	χ_{hf} 10^{-8} m^3kg^{-1}	FD %	SIRM 10^{-5} Am^2kg^{-1}	χ_{arm} 10^{-8} m^3kg^{-1}	χ_{arm}/SIRM 10^{-3} mA^{-1}	SIRM/χ_{lf} 10^{-3} mA^{-1}	χ_{arm}/χ_{lf} no units
Mid55	1.22	11.11	8.22	7.20	7.11	1.25	76.05	16.43	0.22	10.56	2.28
Mid56	1.25	12.25	8.30	7.27	7.14	1.69	67.59	14.83	0.22	9.30	2.04
Mid57	1.27	11.67	8.34	7.28	6.98	4.12	68.50	13.44	0.20	9.40	1.85
Mid58	1.29	11.17	11.03	9.67	9.14	5.56	79.75	24.27	0.30	8.24	2.51
Mid59	1.32	11.66	8.25	7.29	6.90	5.29	33.21	8.40	0.25	4.55	1.15
Mid60	1.35	10.49	9.39	8.15	7.91	2.92	38.62	9.31	0.24	4.74	1.14
Mid61	1.38	11.47	9.57	8.42	8.15	3.11	42.11	10.31	0.24	5.00	1.23
Mid62	1.41	10.83	9.62	8.41	8.36	0.55	37.98	9.88	0.26	4.52	1.18
Mid63	1.43	9.95	10.03	8.69	8.69	0.00	34.22	9.10	0.27	3.94	1.05
Mid64	1.46	10.10	10.46	9.21	9.16	0.54	31.85	9.24	0.29	3.46	1.00
Mid65	1.49	10.31	11.13	9.80	9.80	0.00	31.18	10.75	0.34	3.18	1.10
Mid66	1.52	9.57	11.22	9.77	9.61	1.60	28.36	9.60	0.34	2.90	0.98
Mid67	1.55	9.79	10.71	9.35	9.14	2.19	21.83	9.58	0.44	2.34	1.03
Mid68	1.58	10.60	9.77	8.58	8.54	0.55	20.27	8.83	0.44	2.36	1.03
Mid69	1.61	9.34	13.04	11.24	10.86	3.33	20.72	11.47	0.55	1.84	1.02
Mid70	1.63	9.82	10.47	9.12	9.02	1.12	19.99	11.07	0.55	2.19	1.21
Mid71	1.81	10.96	10.31	9.03	9.03	0.00	21.32	7.42	0.35	2.36	0.82
Mid72	1.98	10.56	11.09	9.80	9.32	4.83	33.12	23.35	0.71	3.38	2.38
Mid73	2.15	11.10	12.04	10.63	10.45	1.69	58.82	80.42	1.37	5.53	7.56
Mid74	2.29	10.13	17.31	18.40	15.20	17.43	153.79	103.73	0.67	8.36	5.64

Sample Name	Elevation m OD	HIRM 10^{-5} Am^2kg^{-1}	Hard %	ARM 10^{-5} Am^2kg^{-1}	SIRM/ARM no units	'Soft' 10^{-5} Am^2kg^{-1}	IRM_{-20} %	IRM_{-30} %	IRM_{-40} %	IRM_{-50} %	IRM_{-100} %	IRM_{-300} %
Mid1	0.02	8.08	1.16	20.74	33.63	73.73	10.57	18.18	25.87	38.32	80.54	98.84
Mid2	0.04	12.05	1.78	25.40	26.67	79.76	11.78	18.64	26.13	39.21	80.01	98.22
Mid3	0.06	9.75	3.28	20.98	14.16	39.32	13.23	20.67	31.33	41.92	81.27	96.72
Mid4	0.09	9.17	3.81	18.29	13.17	35.86	14.89	23.32	36.39	45.66	83.47	96.19
Mid5	0.11	5.87	3.51	7.57	22.10	25.25	15.08	24.36	36.68	48.35	82.68	96.49
Mid6	0.13	8.85	5.48	13.83	11.67	25.10	15.56	28.35	36.50	48.69	81.37	94.52
Mid7	0.15	9.90	5.56	16.52	10.77	31.58	17.75	25.50	37.12	51.56	82.51	94.44
Mid8	0.18	12.05	5.48	23.50	9.36	32.76	14.89	23.74	34.18	47.61	81.44	94.52
Mid9	0.20	11.80	5.37	20.51	10.72	33.74	15.35	24.32	33.88	48.06	81.45	94.63
Mid10	0.22	9.96	5.24	16.19	11.74	27.02	14.21	23.98	35.67	45.70	81.42	94.76
Mid11	0.25	10.88	5.77	12.49	15.08	29.69	15.76	24.25	34.38	46.54	79.84	94.23
Mid12	0.27	11.76	4.13	19.71	14.44	39.89	14.02	23.14	33.01	44.48	81.35	95.87
Mid13	0.29	9.99	3.04	17.64	18.64	41.37	12.58	18.98	31.02	43.26	81.80	96.96
Mid14	0.31	8.58	1.43	15.89	37.67	69.13	11.55	20.77	31.60	42.39	83.07	98.57
Mid15	0.34	11.20	1.94	23.83	24.22	66.59	11.54	18.03	30.28	40.97	79.93	98.06
Mid16	0.32	12.11	3.35	18.00	20.07	43.71	12.10	19.99	29.61	39.98	78.54	96.65
Mid17	0.34	7.25	0.58	20.81	60.39	146.28	11.64	19.08	28.49	40.53	81.11	99.42
Mid18	0.36	9.41	1.09	21.55	40.19	91.12	10.52	16.10	25.82	35.79	81.86	98.91
Mid19	0.39	10.13	2.36	19.28	22.27	48.17	11.22	16.60	26.25	38.14	79.99	97.64
Mid20	0.41	8.13	1.93	19.35	21.73	37.28	8.87	17.76	26.88	37.26	79.66	98.07
Mid21	0.43	10.95	2.57	18.92	22.49	41.14	9.67	17.40	25.69	35.05	78.38	97.43
Mid22	0.46	9.99	2.25	16.15	27.43	47.34	10.68	18.18	26.08	38.06	81.60	97.75
Mid23	0.48	8.83	2.04	15.00	28.91	49.46	11.40	19.51	27.83	38.97	81.15	97.96
Mid24	0.50	5.05	1.02	13.85	35.75	55.77	11.26	21.12	30.58	43.82	84.19	98.98
Mid25	0.53	8.26	1.67	16.15	30.55	58.44	11.84	20.26	29.79	41.69	82.60	98.33
Mid26	0.55	8.76	1.56	18.66	30.07	50.84	9.06	17.04	26.03	39.57	80.87	98.44
Mid27	0.57	6.76	0.86	18.45	42.66	75.09	9.54	17.18	24.84	38.17	80.17	99.14
Mid28	0.60	5.07	0.65	18.20	42.91	70.92	9.08	14.57	25.13	35.22	79.76	99.35
Mid29	0.62	5.58	0.79	17.46	40.31	70.81	10.06	17.67	26.28	39.26	81.57	99.21
Mid30	0.64	6.08	0.93	16.97	38.49	65.68	10.06	16.52	26.64	37.38	81.82	99.07
Mid31	0.67	10.31	1.32	18.77	41.54	79.23	10.16	15.79	26.23	34.95	82.16	98.68
Mid32	0.69	11.02	0.86	20.73	62.10	95.07	7.38	15.61	24.44	34.46	81.42	99.14

Sample Name	Elevation m OD	HIRM 10^{-5} Am^2kg^{-1}	Hard %	ARM 10^{-5} Am^2kg^{-1}	SIRM/ARM no units	'Soft' 10^{-5} Am^2kg^{-1}	IRM_{-20} %	IRM_{-30} %	IRM_{-40} %	IRM_{-50} %	IRM_{-100} %	IRM_{-300} %
Mid33	0.71	10.78	0.70	22.29	68.75	134.61	8.79	17.10	25.51	36.77	83.93	99.30
Mid34	0.74	9.35	0.61	21.93	69.95	113.67	7.41	16.60	25.33	33.81	83.29	99.39
Mid35	0.76	11.55	2.15	15.21	35.35	56.40	10.49	17.34	26.89	37.71	79.96	97.85
Mid36	0.78	14.32	2.08	15.62	44.06	68.33	9.93	16.46	27.22	37.99	82.31	97.92
Mid37	0.81	12.34	3.43	11.44	31.43	37.32	10.38	18.21	26.54	40.64	81.55	96.57
Mid38	0.83	12.72	3.24	10.45	37.58	39.43	10.04	16.95	26.82	39.15	80.39	96.76
Mid39	0.85	14.51	1.94	16.18	46.27	63.81	8.53	16.67	22.84	34.49	79.54	98.06
Mid40	0.88	8.93	0.26	28.73	118.02	354.41	10.45	17.00	25.70	38.51	82.66	99.74
Mid41	0.90	9.44	1.07	14.92	59.02	75.16	8.54	16.29	22.94	34.91	82.02	98.93
Mid42	0.92	1.48	0.07	19.19	107.03	176.74	8.60	17.68	25.21	40.15	85.35	99.93
Mid43	0.95	9.10	1.34	8.83	77.05	63.28	9.30	16.47	23.99	36.27	81.47	98.66
Mid44	0.97	7.98	0.89	10.01	89.57	88.76	9.90	17.13	25.18	38.57	82.81	99.11
Mid45	0.99	13.23	2.15	7.55	81.31	53.71	8.75	14.95	23.25	33.98	78.72	97.85
Mid46	1.02	12.75	3.31	4.98	77.45	34.01	8.82	17.39	23.29	35.80	80.66	96.69
Mid47	1.04	9.69	3.90	3.53	70.45	30.71	12.35	20.93	30.62	42.32	79.57	96.10
Mid48	1.06	9.64	5.13	2.69	69.81	19.30	10.26	16.77	27.65	37.03	77.32	94.87
Mid49	1.09	10.41	7.78	2.11	63.34	15.24	11.38	18.75	23.77	35.74	72.97	92.22
Mid50	1.11	-2.26	-0.69	3.54	91.97	41.38	12.71	20.14	33.16	46.32	84.71	100.69
Mid51	1.13	10.07	10.56	1.61	59.34	12.54	13.16	19.53	28.44	36.82	71.30	89.44
Mid52	1.15	10.52	13.89	1.41	53.83	9.81	12.95	19.93	29.52	37.87	65.39	86.11
Mid53	1.18	10.83	13.51	1.52	52.61	11.12	13.87	21.45	30.19	39.14	66.64	86.49
Mid54	1.20	9.79	14.46	1.26	53.87	9.56	14.11	20.83	28.39	36.89	64.45	85.54
Mid55	1.22	9.51	12.51	1.31	58.15	9.80	12.89	20.88	26.70	35.64	67.52	87.49
Mid56	1.25	9.87	14.60	1.18	57.25	9.07	13.42	20.03	26.09	36.74	65.05	85.40
Mid57	1.27	9.72	14.19	1.07	64.01	9.06	13.23	20.03	26.20	35.71	65.97	85.81
Mid58	1.29	7.60	9.53	1.93	41.28	12.93	16.21	25.71	34.55	41.77	72.04	90.47
Mid59	1.32	9.21	27.73	0.67	49.67	5.18	15.59	21.75	28.40	34.30	49.43	72.27
Mid60	1.35	10.09	26.13	0.74	52.09	6.32	16.37	24.06	28.99	36.25	50.26	73.87
Mid61	1.38	10.99	26.10	0.82	51.29	7.07	16.80	25.68	30.14	36.56	51.70	73.90
Mid62	1.41	10.72	28.24	0.79	48.30	6.02	15.84	22.72	27.93	33.41	48.65	71.76
Mid63	1.43	9.17	26.80	0.72	47.23	5.28	15.43	22.01	28.32	33.87	49.63	73.20
Mid64	1.46	8.01	25.14	0.74	43.29	4.67	14.68	22.76	29.39	36.67	50.73	74.86
Mid65	1.49	7.16	22.95	0.86	36.42	5.01	16.07	23.75	30.76	36.42	52.48	77.05
Mid66	1.52	5.63	19.85	0.76	37.10	5.35	18.86	27.91	36.02	41.40	56.70	80.15
Mid67	1.55	3.68	16.84	0.76	28.62	3.82	17.52	27.44	36.39	42.89	59.96	83.16
Mid68	1.58	3.28	16.21	0.70	28.83	3.70	18.27	26.96	34.49	42.88	60.22	83.79
Mid69	1.61	2.77	13.37	0.91	22.70	5.53	26.70	35.56	44.50	50.46	66.25	86.63
Mid70	1.63	3.26	16.33	0.88	22.68	3.90	19.50	29.58	37.81	44.79	61.73	83.67
Mid71	1.81	4.43	20.80	0.59	36.09	3.69	17.30	25.26	33.23	39.20	55.92	79.20
Mid72	1.98	5.89	17.79	1.86	17.82	7.28	21.98	30.30	40.84	47.21	61.87	82.21
Mid73	2.15	7.80	13.25	6.40	9.19	15.48	26.32	37.94	49.04	55.01	72.33	86.75
Mid74	2.29	8.14	5.29	8.26	18.62	56.37	36.65	46.69	61.02	67.14	85.29	94.71

Environmental magnetism data: The Wicks

Sample Name	Elevation m OD	Mass g	χ_{kappa} 10^{-8} m^3kg^{-1}	χ_{lf} 10^{-8} m^3kg^{-1}	χ_{hf} 10^{-8} m^3kg^{-1}	FD %	SIRM 10^{-5} Am^2kg^{-1}	χ_{arm} 10^{-8} m^3kg^{-1}	χ_{arm}/SIRM 10^{-3} mA^{-1}	SIRM/χ_{lf} 10^{-3} mA^{-1}	χ_{arm}/χ_{lf} no units
W1	0.20	14.16	8.81	8.05	7.80	3.07	238.36	125.91	0.53	29.61	15.64
W2	0.22	12.14	9.54	8.57	8.16	4.81	263.07	126.42	0.48	30.70	14.75
W3	0.24	9.23	10.61	9.21	8.72	5.29	330.99	114.09	0.34	35.94	12.39
W4	0.26	9.35	9.70	8.34	8.13	2.56	275.81	117.56	0.43	33.07	14.10
W5	0.29	11.09	9.99	8.92	8.61	3.54	284.76	147.20	0.52	31.91	16.49
W6	0.31	12.93	10.87	9.82	9.39	4.33	321.81	160.74	0.50	32.77	16.37
W7	0.33	13.26	11.87	10.75	10.37	3.51	413.76	167.50	0.40	38.50	15.59
W8	0.35	12.26	12.27	11.13	10.69	4.03	439.64	188.60	0.43	39.49	16.94
W9	0.38	12.26	12.76	11.62	11.17	3.86	486.82	181.30	0.37	41.88	15.60
W10	0.40	13.74	10.43	9.39	8.99	4.26	305.48	128.04	0.42	32.53	13.63
W11	0.42	13.12	12.07	10.93	10.48	4.18	445.29	176.58	0.40	40.72	16.15
W12	0.44	11.58	10.16	9.20	8.81	4.23	320.98	97.17	0.30	34.90	10.57
W13	0.47	12.88	11.44	10.40	9.90	4.85	466.64	123.79	0.27	44.85	11.90
W14	0.49	12.16	13.56	12.29	11.88	3.34	476.92	195.51	0.41	38.79	15.90
W15	0.51	11.89	23.90	21.91	21.40	2.30	1445.83	354.12	0.24	66.00	16.17
W16	0.53	11.45	15.58	14.06	13.84	1.55	721.01	230.64	0.32	51.29	16.41
W17	0.56	12.42	12.98	11.71	11.43	2.41	449.18	201.79	0.45	38.36	17.23
W18	0.58	12.38	17.03	15.51	14.94	3.65	793.01	266.86	0.34	51.13	17.21
W19	0.60	12.20	20.44	18.65	18.16	2.64	1141.75	335.34	0.29	61.21	17.98
W20	0.62	13.17	18.51	16.90	16.40	2.92	1018.46	280.26	0.28	60.27	16.59
W21	0.65	11.07	12.13	10.89	10.52	3.32	420.31	179.08	0.43	38.61	16.45
W22	0.67	13.72	10.88	9.87	9.44	4.43	304.64	154.02	0.51	30.85	15.60
W23	0.69	12.05	12.39	11.12	10.75	3.36	357.61	197.04	0.55	32.16	17.72
W24	0.71	12.09	14.83	13.44	12.98	3.38	579.53	243.54	0.42	43.13	18.13
W25	0.74	13.15	9.87	8.86	8.48	4.29	242.09	116.50	0.48	27.32	13.15
W26	0.76	13.66	10.53	9.56	9.12	4.60	254.77	138.33	0.54	26.66	14.47
W27	0.78	13.06	12.33	11.18	10.80	3.42	346.28	171.09	0.49	30.97	15.30
W28	0.80	11.42	10.04	8.94	8.63	3.43	246.10	102.69	0.42	27.54	11.49
W29	0.83	13.38	9.18	8.19	7.89	3.65	221.06	67.87	0.31	27.01	8.29
W30	0.85	14.12	8.80	7.93	7.61	4.02	180.62	62.35	0.35	22.77	7.86
W31	0.87	10.86	10.46	9.35	8.93	4.43	289.68	70.84	0.24	30.99	7.58
W32	0.89	11.48	7.61	6.62	6.40	3.29	155.93	45.13	0.29	23.55	6.82
W33	0.92	14.16	7.05	6.28	6.00	4.49	140.34	34.96	0.25	22.34	5.56
W34	0.94	11.66	8.11	7.12	6.91	3.01	166.67	41.28	0.25	23.40	5.80
W35	0.96	12.81	7.08	6.21	5.97	3.77	144.85	32.04	0.22	23.34	5.16
W36	0.98	13.08	6.58	5.85	5.51	5.88	122.28	29.33	0.24	20.90	5.01
W37	1.01	11.74	6.53	5.58	5.45	2.29	114.06	23.56	0.21	20.44	4.22
W38	1.03	13.77	4.89	4.25	4.10	3.58	88.94	16.90	0.19	20.91	3.97
W39	1.05	14.17	3.28	2.83	2.65	6.48	77.09	11.46	0.15	27.23	4.05
W40	1.07	13.13	3.60	3.01	3.01	0.00	47.26	7.25	0.15	15.71	2.41
W41	1.10	14.15	3.57	3.00	2.97	1.18	52.71	8.49	0.16	17.54	2.82
W42	1.14	13.08	4.39	3.67	3.63	1.04	51.13	8.31	0.16	13.93	2.26
W43	1.17	14.34	4.40	3.77	3.73	0.93	41.89	7.96	0.19	11.12	2.11
W44	0.95	13.51	6.51	5.59	5.52	1.32	137.89	28.35	0.21	24.67	5.07
W45	0.98	14.34	7.04	6.31	6.00	4.97	130.85	29.04	0.22	20.73	4.60
W46	1.00	15.05	5.88	5.25	4.98	5.06	105.22	23.51	0.22	20.04	4.48
W47	1.03	15.81	4.45	3.92	3.86	1.61	78.96	13.97	0.18	20.13	3.56
W48	1.06	16.87	3.49	3.02	2.93	2.94	73.69	11.78	0.16	24.37	3.90
W49	1.08	12.56	3.24	2.71	2.55	5.88	58.88	8.83	0.15	21.75	3.26
W50	1.11	13.59	2.86	2.32	2.25	3.17	46.46	5.90	0.13	20.04	2.54
W51	1.14	15.89	2.79	2.33	2.30	1.35	35.96	5.14	0.14	15.45	2.21
W52	1.16	13.04	3.98	3.38	3.34	1.14	39.46	5.60	0.14	11.69	1.66
W53	1.19	12.70	2.94	2.40	2.32	3.28	26.23	4.91	0.19	10.92	2.04
W54	1.22	12.71	3.23	2.67	2.64	1.47	26.25	5.67	0.22	9.82	2.12
W55	1.24	12.49	2.54	2.00	1.92	4.00	20.94	3.75	0.18	10.46	1.87
W56	1.27	12.34	3.59	3.00	2.96	1.35	26.52	7.38	0.28	8.85	2.46

Sample Name	Elevation m OD	Mass g	χ_{kappa} 10^{-8} m^3kg^{-1}	χ_{lf} 10^{-8} m^3kg^{-1}	χ_{hf} 10^{-8} m^3kg^{-1}	FD %	SIRM 10^{-5} Am^2kg^{-1}	χ_{arm} 10^{-8} m^3kg^{-1}	χ_{arm}/SIRM 10^{-3} mA^{-1}	SIRM/χ_{lf} 10^{-3} mA^{-1}	χ_{arm}/χ_{lf} no units
W57	1.30	12.85	3.80	3.19	3.11	2.44	30.31	5.41	0.18	9.50	1.70
W58	1.32	13.29	3.20	2.63	2.56	2.86	22.12	4.51	0.20	8.40	1.71
W59	1.35	14.38	3.40	2.85	2.82	1.22	21.79	4.19	0.19	7.64	1.47
W60	1.38	13.08	3.05	2.56	2.41	5.97	18.40	3.49	0.19	7.18	1.36
W61	1.40	13.88	3.07	2.56	2.41	5.63	18.58	4.21	0.23	7.26	1.64
W62	1.43	12.27	5.91	5.05	5.05	0.00	31.63	6.95	0.22	6.26	1.38
W63	1.46	12.21	6.76	6.02	5.86	2.72	32.15	7.59	0.24	5.34	1.26
W64	1.48	10.67	7.31	6.33	6.28	0.74	32.96	7.71	0.23	5.21	1.22
W65	1.51	11.70	8.20	7.18	7.14	0.60	36.49	8.95	0.25	5.08	1.25
W66	1.54	11.95	8.06	7.12	7.07	0.59	32.44	8.43	0.26	4.56	1.18
W67	1.56	10.75	8.47	7.44	7.40	0.62	29.09	8.25	0.28	3.91	1.11
W68	1.59	9.90	9.28	8.03	7.98	0.63	31.68	9.70	0.31	3.94	1.21
W69	1.62	10.82	10.47	9.25	9.06	2.00	38.90	11.53	0.30	4.21	1.25
W70	1.64	10.73	10.47	9.32	9.04	3.00	29.67	12.55	0.42	3.18	1.35
W71	1.67	10.45	9.25	8.23	7.99	2.91	24.75	12.84	0.52	3.01	1.56
W72	1.70	10.56	8.21	7.10	7.05	0.67	20.90	9.89	0.47	2.94	1.39
W73	1.72	10.47	8.23	7.12	7.12	0.00	18.09	7.81	0.43	2.54	1.10
W74	1.75	10.64	8.27	7.14	7.10	0.66	19.22	5.81	0.30	2.69	0.81
W75	1.78	11.33	8.52	7.46	7.37	1.18	20.84	6.31	0.30	2.79	0.85
W76	1.80	10.60	9.02	7.88	7.97	-1.20	24.96	11.78	0.47	3.17	1.50
W77	1.83	10.47	9.19	8.07	7.93	1.78	29.11	9.65	0.33	3.61	1.20
W78	1.86	10.23	7.55	6.55	6.35	2.99	30.08	6.22	0.21	4.59	0.95
W79	1.88	6.50	8.36	7.07	6.92	2.17	40.42	7.34	0.18	5.71	1.04

Sample Name	Elevation m OD	HIRM 10^{-5} Am^2kg^{-1}	Hard %	ARM 10^{-5} Am^2kg^{-1}	SIRM/ARM no units	'Soft' 10^{-5} Am^2kg^{-1}	IRM_{-20} %	IRM_{-30} %	IRM_{-40} %	IRM_{-50} %	IRM_{-100} %	IRM_{-300} %
W1	0.20	12.75	5.35	10.02	23.78	30.80	12.92	21.03	29.99	38.69	78.04	94.65
W2	0.22	10.64	4.04	10.06	26.14	31.13	11.83	18.21	27.06	36.24	77.98	95.96
W3	0.24	10.84	3.28	9.08	36.44	32.68	9.87	17.00	23.90	34.08	76.14	96.72
W4	0.26	11.80	4.28	9.36	29.47	30.45	11.04	16.73	27.28	36.53	76.42	95.72
W5	0.29	11.59	4.07	11.72	24.30	29.74	10.44	16.54	23.43	33.00	77.76	95.93
W6	0.31	13.39	4.16	12.79	25.15	28.71	8.92	17.16	21.95	33.25	77.00	95.84
W7	0.33	16.17	3.91	13.33	31.03	38.09	9.20	13.76	21.44	31.78	74.62	96.09
W8	0.35	15.76	3.59	15.01	29.28	41.96	9.54	14.58	23.42	29.80	76.88	96.41
W9	0.38	16.81	3.45	14.43	33.73	45.22	9.29	15.75	23.36	29.50	76.41	96.55
W10	0.40	14.21	4.65	10.19	29.97	31.26	10.23	16.56	25.60	33.28	77.08	95.35
W11	0.42	23.99	5.39	14.06	31.68	48.60	10.91	16.01	25.97	32.08	75.45	94.61
W12	0.44	19.24	6.00	7.73	41.50	35.92	11.19	16.75	25.68	34.01	75.11	94.00
W13	0.47	23.35	5.00	9.85	47.36	50.43	10.81	14.76	22.90	29.31	75.31	95.00
W14	0.49	22.64	4.75	15.56	30.64	56.66	11.88	17.74	25.38	33.63	76.17	95.25
W15	0.51	52.41	3.63	28.19	51.29	126.15	8.72	13.13	20.26	28.33	75.13	96.37
W16	0.53	34.71	4.81	18.36	39.27	78.60	10.90	16.77	23.78	32.26	75.93	95.19
W17	0.56	28.06	6.25	16.06	27.96	54.20	12.07	19.57	27.15	36.22	76.28	93.75
W18	0.58	38.99	4.92	21.24	37.33	94.83	11.96	16.33	23.45	32.86	74.76	95.08
W19	0.60	52.59	4.61	26.69	42.77	120.39	10.54	15.92	21.22	29.52	75.27	95.39
W20	0.62	42.92	4.21	22.31	45.65	100.21	9.84	15.31	21.66	29.11	76.46	95.79
W21	0.65	10.53	2.50	14.25	29.49	36.52	8.69	15.24	24.27	32.42	77.98	97.50
W22	0.67	11.54	3.79	12.26	24.85	29.74	9.76	17.44	25.39	36.44	77.61	96.21
W23	0.69	12.33	3.45	15.68	22.80	37.43	10.47	18.36	23.67	36.04	78.99	96.55
W24	0.71	13.14	2.27	19.39	29.89	44.42	7.66	15.08	22.61	30.89	78.29	97.73
W25	0.74	7.26	3.00	9.27	26.11	24.07	9.94	16.24	26.89	34.32	78.83	97.00
W26	0.76	9.01	3.54	11.01	23.14	24.90	9.77	19.65	27.53	36.49	79.09	96.46
W27	0.78	12.14	3.51	13.62	25.43	31.74	9.17	17.36	24.11	34.88	76.50	96.49
W28	0.80	8.17	3.32	8.17	30.11	23.02	9.35	20.33	29.22	39.76	80.04	96.68
W29	0.83	6.31	2.86	5.40	40.92	24.17	10.93	20.06	30.32	39.65	80.77	97.14
W30	0.85	8.50	4.71	4.96	36.39	21.24	11.76	18.54	28.67	35.88	76.51	95.29

Sample Name	Elevation m OD	HIRM 10^{-5} Am^2kg^{-1}	Hard %	ARM 10^{-5} Am^2kg^{-1}	SIRM/ARM no units	'Soft' 10^{-5} Am^2kg^{-1}	IRM_{-20} %	IRM_{-30} %	IRM_{-40} %	IRM_{-50} %	IRM_{-100} %	IRM_{-300} %
W31	0.87	10.98	3.79	5.64	51.37	26.18	9.04	14.67	25.04	31.89	77.05	96.21
W32	0.89	9.30	5.96	3.59	43.41	17.03	10.92	19.11	26.46	38.09	76.17	94.04
W33	0.92	8.72	6.22	2.78	50.43	19.31	13.76	21.69	28.84	38.89	77.79	93.78
W34	0.94	9.97	5.98	3.29	50.73	18.60	11.16	18.39	25.56	35.42	75.98	94.02
W35	0.96	8.08	5.58	2.55	56.80	19.24	13.28	21.55	29.52	40.41	77.67	94.42
W36	0.98	7.79	6.37	2.33	52.37	16.57	13.56	21.56	29.97	40.34	76.89	93.63
W37	1.01	7.94	6.96	1.88	60.83	13.82	12.12	18.75	29.47	36.83	77.55	93.04
W38	1.03	5.45	6.13	1.35	66.10	9.22	10.37	16.42	24.60	32.30	72.67	93.87
W39	1.05	3.40	4.41	0.91	84.49	10.35	13.43	20.79	29.61	42.84	79.94	95.59
W40	1.07	4.97	10.52	0.58	81.85	7.24	15.31	24.14	34.43	44.71	73.50	89.48
W41	1.10	4.43	8.41	0.68	78.02	8.82	16.73	27.13	35.28	44.87	75.87	91.59
W42	1.14	4.87	9.53	0.66	77.31	10.71	20.94	32.95	42.17	47.34	75.61	90.47
W43	1.17	4.28	10.22	0.63	66.15	13.46	32.12	42.20	50.41	56.28	76.95	89.78
W44	0.95	7.13	5.17	2.26	61.10	18.42	13.36	19.22	29.96	39.40	77.51	94.83
W45	0.98	9.31	7.12	2.31	56.61	13.74	10.50	20.29	26.89	37.94	74.15	92.88
W46	1.00	7.28	6.92	1.87	56.22	12.33	11.72	17.85	27.84	33.92	73.92	93.08
W47	1.03	5.97	7.57	1.11	70.99	10.40	13.18	19.43	29.84	37.71	74.09	92.43
W48	1.06	3.79	5.15	0.94	78.59	9.72	13.19	21.66	31.17	40.26	77.62	94.85
W49	1.08	3.49	5.93	0.70	83.73	7.99	13.57	20.79	31.44	41.52	76.85	94.07
W50	1.11	3.27	7.04	0.47	98.91	5.76	12.39	21.28	32.35	42.68	75.59	92.96
W51	1.14	3.46	9.63	0.41	87.92	5.80	16.14	23.96	34.78	44.14	72.20	90.37
W52	1.16	6.19	15.68	0.45	88.59	7.20	18.23	25.43	34.64	42.21	66.35	84.32
W53	1.19	4.79	18.24	0.39	67.13	4.93	18.78	26.42	34.85	42.77	63.55	81.76
W54	1.22	4.49	17.09	0.45	58.15	5.29	20.16	29.21	38.44	46.56	65.52	82.91
W55	1.24	3.47	16.58	0.30	70.19	4.77	22.77	29.70	39.87	47.13	67.52	83.42
W56	1.27	5.06	19.07	0.59	45.14	6.10	22.99	30.61	39.15	41.96	62.61	80.93
W57	1.30	5.81	19.15	0.43	70.39	6.18	20.39	26.93	37.00	43.65	62.47	80.85
W58	1.32	4.40	19.89	0.36	61.66	4.47	20.21	27.35	38.32	44.02	61.76	80.11
W59	1.35	4.93	22.62	0.33	65.36	4.30	19.73	26.99	34.55	40.84	57.52	77.38
W60	1.38	4.43	24.06	0.28	66.24	3.43	18.64	25.94	33.34	39.57	54.60	75.94
W61	1.40	3.92	21.10	0.33	55.47	3.01	16.21	26.42	33.19	39.44	57.20	78.90
W62	1.43	6.73	21.28	0.55	57.17	5.29	16.74	25.43	30.55	37.99	55.87	78.72
W63	1.46	7.72	24.01	0.60	53.23	5.07	15.76	24.17	29.20	35.40	51.25	75.99
W64	1.48	7.86	23.84	0.61	53.74	5.13	15.55	20.79	31.20	36.66	51.98	76.16
W65	1.51	8.60	23.57	0.71	51.23	5.80	15.88	24.16	31.59	37.24	52.15	76.43
W66	1.54	8.26	25.46	0.67	48.36	4.76	14.67	22.46	27.17	35.45	50.04	74.54
W67	1.56	8.07	27.75	0.66	44.28	3.99	13.71	21.87	28.04	32.68	48.38	72.25
W68	1.59	7.74	24.44	0.77	41.01	5.11	16.14	23.94	30.66	36.32	51.02	75.56
W69	1.62	8.89	22.86	0.92	42.39	7.36	18.92	28.40	34.50	39.25	53.90	77.14
W70	1.64	5.73	19.32	1.00	29.70	5.94	20.01	29.81	36.63	43.56	59.55	80.68
W71	1.67	3.58	14.46	1.02	24.21	5.36	21.65	28.45	39.90	45.95	62.44	85.54
W72	1.70	3.30	15.80	0.79	26.54	3.72	17.81	27.54	36.77	44.13	61.15	84.20
W73	1.72	2.67	14.75	0.62	29.09	3.28	18.15	29.01	37.15	43.29	61.64	85.25
W74	1.75	3.12	16.22	0.46	41.55	3.60	18.73	26.88	34.59	40.67	59.02	83.78
W75	1.78	3.97	19.04	0.50	41.46	3.97	19.07	27.14	34.13	41.16	57.22	80.96
W76	1.80	4.45	17.84	0.94	26.63	4.88	19.53	29.76	38.23	44.70	60.80	82.16
W77	1.83	5.63	19.33	0.77	37.89	5.67	19.48	29.09	36.57	42.72	59.14	80.67
W78	1.86	5.80	19.29	0.50	60.74	6.32	21.01	29.05	36.13	41.81	59.12	80.71
W79	1.88	5.17	12.80	0.58	69.15	10.62	26.27	38.30	48.60	53.81	72.32	87.20

Environmental magnetism data: South Brooks

Sample Name	Elevation m OD	Mass g	χ_{kappa} 10^{-8} m^3kg^{-1}	χ_{lf} 10^{-8} m^3kg^{-1}	χ_{hf} 10^{-8} m^3kg^{-1}	FD %	SIRM 10^{-5} Am^2kg^{-1}	χ_{arm} 10^{-8} m^3kg^{-1}	χ_{arm}/SIRM 10^{-3} mA^{-1}	SIRM/χ_{lf} 10^{-3} mA^{-1}	χ_{arm}/χ_{lf} no units
SB1	-0.23	14.31	12.28	11.01	10.73	2.54	440.60	111.71	0.25	40.03	10.15
SB2	-0.20	8.84	16.17	13.64	13.47	1.24	709.30	130.23	0.18	52.02	9.55
SB3	-0.17	11.50	12.73	11.17	11.04	1.17	535.35	105.68	0.20	47.91	9.46
SB4	-0.14	12.03	10.30	9.23	8.98	2.70	322.89	83.35	0.26	34.99	9.03
SB5	-0.11	13.23	9.44	8.50	8.35	1.78	310.81	73.06	0.24	36.55	8.59
SB6	-0.08	7.85	11.52	9.61	9.55	0.66	306.15	68.98	0.23	31.84	7.18
SB7	-0.05	8.48	11.95	10.32	10.14	1.71	256.34	69.97	0.27	24.84	6.78
SB8	-0.02	10.32	10.74	9.40	9.10	3.09	225.64	67.14	0.30	24.02	7.15
SB9	0.01	12.34	10.49	9.32	9.07	2.61	207.55	82.33	0.40	22.28	8.84
SB10	0.04	12.53	10.07	9.02	8.78	2.65	226.15	89.84	0.40	25.07	9.96
SB11	0.07	9.28	17.43	15.63	15.15	3.10	414.36	168.08	0.41	26.51	10.75
SB12	0.09	11.71	17.14	15.50	15.20	1.93	583.93	160.08	0.27	37.68	10.33
SB13	0.12	11.76	18.76	16.92	16.84	0.50	670.56	174.19	0.26	39.62	10.29
SB14	0.15	12.65	16.86	15.30	15.03	1.81	672.67	150.76	0.22	43.96	9.85
SB15	0.18	12.94	13.29	11.98	11.59	3.23	519.14	116.78	0.22	43.34	9.75
SB16	0.21	12.37	14.08	12.73	12.33	3.17	578.26	120.26	0.21	45.42	9.45
SB17	0.24	12.04	16.44	14.87	14.54	2.23	668.19	153.36	0.23	44.93	10.31
SB18	0.27	13.49	13.88	12.56	12.34	1.77	554.65	121.39	0.22	44.16	9.66
SB19	0.30	11.77	8.25	7.05	6.84	3.01	269.19	67.35	0.25	38.16	9.55
SB20	0.33	12.89	7.81	6.82	6.63	2.84	219.88	64.76	0.29	32.22	9.49
SB21	0.36	14.07	7.52	6.65	6.43	3.21	204.86	63.90	0.31	30.82	9.61
SB22	0.38	10.49	8.32	7.05	6.91	2.03	217.01	71.90	0.33	30.77	10.20
SB23	0.41	12.68	10.53	9.43	9.23	2.09	313.95	94.63	0.30	33.30	10.04
SB24	0.44	9.74	9.89	8.42	8.52	-1.22	219.28	88.60	0.40	26.05	10.53
SB25	0.47	11.58	9.71	8.59	8.42	2.01	193.90	83.99	0.43	22.56	9.77
SB26	0.50	9.54	10.23	8.91	8.54	4.12	169.10	76.80	0.45	18.98	8.62
SB27	0.53	12.28	8.90	7.82	7.69	1.56	154.72	76.09	0.49	19.80	9.74
SB28	0.56	11.91	8.46	7.43	7.26	2.26	144.44	77.07	0.53	19.44	10.37
SB29	0.59	10.69	9.20	8.00	7.96	0.58	140.29	79.41	0.57	17.53	9.92
SB30	0.62	11.59	10.37	9.19	8.89	3.29	153.13	81.88	0.53	16.66	8.91
SB31	0.65	10.63	10.86	9.55	9.17	3.94	157.59	82.14	0.52	16.50	8.60
SB32	0.67	10.44	10.52	9.20	9.01	2.08	139.41	73.02	0.52	15.16	7.94
SB33	0.70	10.85	10.56	9.17	8.94	2.51	141.42	75.97	0.54	15.43	8.29
SB34	0.73	12.01	10.40	9.28	8.95	3.59	136.47	69.41	0.51	14.70	7.48
SB35	0.76	10.06	8.29	7.26	6.96	4.11	83.32	46.07	0.55	11.48	6.35
SB36	0.79	9.54	8.34	7.08	7.08	0.00	75.35	41.17	0.55	10.65	5.82
SB37	0.82	10.52	9.05	7.89	7.89	0.00	70.92	30.77	0.43	8.99	3.90
SB38	0.85	9.86	9.05	7.71	7.71	0.00	79.57	26.54	0.33	10.33	3.44
SB39	0.88	10.61	8.88	7.68	7.50	2.45	65.30	15.94	0.24	8.50	2.07
SB40	0.91	9.92	8.98	7.61	7.61	0.00	62.93	15.59	0.25	8.27	2.05
SB41	0.94	9.71	8.87	7.67	7.62	0.67	58.72	13.61	0.23	7.65	1.77
SB42	0.97	10.79	8.24	7.14	7.14	0.00	53.86	12.42	0.23	7.55	1.74
SB43	1.00	11.17	9.62	8.51	8.19	3.68	50.45	12.32	0.24	5.93	1.45
SB44	1.03	10.20	8.70	7.50	7.40	1.31	39.37	10.23	0.26	5.25	1.36
SB45	1.06	10.32	7.57	6.54	6.35	2.96	34.95	9.41	0.27	5.35	1.44
SB46	1.09	9.76	8.16	6.97	6.81	2.21	40.36	10.80	0.27	5.79	1.55
SB47	1.11	10.30	8.92	7.72	7.52	2.52	40.98	11.08	0.27	5.31	1.44
SB48	1.14	10.28	8.52	7.34	7.39	-0.66	38.56	9.91	0.26	5.25	1.35
SB49	1.17	11.83	9.06	7.99	7.86	1.59	49.69	12.11	0.24	6.22	1.52
SB50	1.20	11.29	10.16	8.99	8.85	1.48	54.10	12.94	0.24	6.02	1.44
SB51	1.23	12.25	8.22	7.22	7.02	2.82	40.29	9.76	0.24	5.58	1.35
SB52	1.26	12.58	7.64	6.68	6.64	0.60	36.83	8.58	0.23	5.51	1.28
SB53	1.29	10.95	8.89	7.67	7.63	0.60	38.54	9.68	0.25	5.02	1.26
SB54	1.32	10.95	9.07	7.85	7.94	-1.16	39.90	9.45	0.24	5.08	1.20
SB55	1.35	10.72	9.99	8.72	8.72	0.00	48.52	12.21	0.25	5.56	1.40
SB56	1.38	11.34	10.07	8.86	8.73	1.49	44.70	11.33	0.25	5.04	1.28

Sample Name	Elevation m OD	Mass g	χ_{kappa} 10^{-8} m^3kg^{-1}	χ_{lf} 10^{-8} m^3kg^{-1}	χ_{hf} 10^{-8} m^3kg^{-1}	FD %	SIRM 10^{-5} Am^2kg^{-1}	χ_{arm} 10^{-8} m^3kg^{-1}	χ_{arm}/SIRM 10^{-3} mA^{-1}	SIRM/χ_{lf} 10^{-3} mA^{-1}	χ_{arm}/χ_{lf} no units
SB57	1.41	11.97	9.14	8.10	7.98	1.55	45.70	11.49	0.25	5.64	1.42
SB58	1.44	12.18	9.24	8.17	8.09	1.01	48.75	11.53	0.24	5.96	1.41
SB59	1.47	11.10	7.99	6.94	6.80	1.95	40.94	9.25	0.23	5.90	1.33
SB60	1.50	12.14	8.87	7.74	7.66	1.06	38.78	10.38	0.27	5.01	1.34
SB61	1.53	12.09	10.39	9.14	9.14	0.00	46.70	15.51	0.33	5.11	1.70
SB62	1.56	10.42	8.90	7.68	7.68	0.00	42.11	21.46	0.51	5.48	2.79
SB63	1.59	9.86	10.49	9.18	9.03	1.66	46.42	31.97	0.69	5.05	3.48
SB64	1.61	12.39	9.29	8.19	8.03	1.97	39.53	18.19	0.46	4.83	2.22
SB65	1.64	11.67	10.37	9.17	9.09	0.93	42.64	21.35	0.50	4.65	2.33
SB66	1.67	12.52	7.57	6.59	6.59	0.00	34.29	7.97	0.23	5.20	1.21
SB67	1.70	11.68	8.39	7.40	7.23	2.31	44.04	12.57	0.29	5.95	1.70
SB68	1.73	9.82	10.57	9.16	9.06	1.11	59.27	18.74	0.32	6.47	2.05
SB69	1.82	11.22	8.19	7.13	7.09	0.62	35.66	8.91	0.25	5.00	1.25
SB70	1.92	10.32	9.01	7.80	7.61	2.48	31.13	8.98	0.29	3.99	1.15
SB71	2.02	11.40	6.61	5.75	5.66	1.53	30.79	7.68	0.25	5.36	1.34
SB72	2.12	13.88	8.00	7.06	6.95	1.53	29.74	8.49	0.29	4.21	1.20
SB73	2.22	13.09	7.14	6.23	6.15	1.23	31.82	8.28	0.26	5.11	1.33
SB74	2.32	11.28	10.56	9.36	9.09	2.84	75.54	20.46	0.27	8.07	2.19

Sample Name	Elevation m OD	HIRM 10^{-5} Am^2kg^{-1}	Hard %	ARM 10^{-5} Am^2kg^{-1}	SIRM/ARM no units	'Soft' 10^{-5} Am^2kg^{-1}	IRM_{-20} %	IRM_{-30} %	IRM_{-40} %	IRM_{-50} %	IRM_{-100} %	IRM_{-300} %
SB1	-0.23	6.10	1.38	8.89	49.55	40.92	9.29	19.57	26.59	40.39	80.28	98.62
SB2	-0.20	-2.87	-0.40	10.37	68.42	72.10	10.17	16.43	26.47	36.78	78.81	100.40
SB3	-0.17	3.33	0.62	8.41	63.64	56.56	10.57	19.13	25.19	38.92	80.26	99.38
SB4	-0.14	4.34	1.35	6.64	48.66	39.46	12.22	19.72	29.28	39.07	79.75	98.65
SB5	-0.11	4.08	1.31	5.82	53.45	34.02	10.94	21.44	29.17	40.26	81.89	98.69
SB6	-0.08	7.60	2.48	5.49	55.75	26.31	8.59	14.94	23.41	29.64	74.62	97.52
SB7	-0.05	7.49	2.92	5.57	46.03	23.77	9.27	14.57	24.08	33.17	75.83	97.08
SB8	-0.02	7.85	3.48	5.34	42.22	22.75	10.08	16.23	27.13	37.32	75.89	96.52
SB9	0.01	8.39	4.04	6.55	31.67	30.24	14.57	22.51	31.28	38.67	76.97	95.96
SB10	0.04	6.72	2.97	7.15	31.62	32.59	14.41	22.65	28.69	39.75	78.38	97.03
SB11	0.07	12.72	3.07	13.38	30.97	42.84	10.34	17.28	26.71	33.47	77.73	96.93
SB12	0.09	12.37	2.12	12.74	45.83	57.43	9.83	15.03	22.25	32.71	74.19	97.88
SB13	0.12	11.26	1.68	13.87	48.36	52.60	7.84	15.70	21.92	32.46	74.84	98.32
SB14	0.15	9.11	1.35	12.00	56.05	60.41	8.98	14.04	23.13	32.38	76.54	98.65
SB15	0.18	8.42	1.62	9.30	55.85	38.89	7.49	15.44	22.72	31.07	76.16	98.38
SB16	0.21	8.60	1.49	9.57	60.41	46.13	7.98	13.85	21.60	31.30	74.52	98.51
SB17	0.24	9.70	1.45	12.21	54.74	42.74	6.40	11.78	18.97	28.44	75.14	98.55
SB18	0.27	7.83	1.41	9.66	57.40	43.47	7.84	14.37	20.88	31.02	75.35	98.59
SB19	0.30	2.20	0.82	5.36	50.21	24.89	9.25	18.08	28.59	39.27	82.85	99.18
SB20	0.33	5.36	2.44	5.16	42.65	25.41	11.56	19.78	28.65	36.15	79.14	97.56
SB21	0.36	4.89	2.39	5.09	40.27	20.64	10.07	17.42	26.45	37.31	80.67	97.61
SB22	0.38	4.91	2.26	5.72	37.92	24.52	11.30	18.03	26.61	36.98	81.69	97.74
SB23	0.41	6.99	2.23	7.53	41.68	32.09	10.22	15.61	24.35	33.41	79.93	97.77
SB24	0.44	7.56	3.45	7.05	31.09	24.67	11.25	18.01	28.65	38.12	79.45	96.55
SB25	0.47	7.64	3.94	6.69	29.00	24.37	12.57	18.31	27.37	38.96	79.68	96.06
SB26	0.50	7.61	4.50	6.11	27.66	20.59	12.18	20.46	30.00	39.85	79.33	95.50
SB27	0.53	7.22	4.67	6.06	25.55	19.28	12.46	21.07	29.24	41.32	79.87	95.33
SB28	0.56	7.05	4.88	6.13	23.55	21.54	14.92	21.64	33.33	40.87	79.37	95.12
SB29	0.59	8.41	6.00	6.32	22.19	22.61	16.12	24.80	35.36	42.43	79.18	94.00
SB30	0.62	8.45	5.52	6.52	23.50	23.37	15.26	26.61	35.53	45.91	79.68	94.48
SB31	0.65	8.33	5.28	6.54	24.10	22.92	14.54	26.08	33.32	45.05	78.95	94.72
SB32	0.67	8.63	6.19	5.81	23.98	21.97	15.76	25.80	36.31	45.49	78.06	93.81
SB33	0.70	8.24	5.83	6.05	23.39	21.30	15.06	25.42	34.39	46.04	78.44	94.17
SB34	0.73	8.14	5.97	5.53	24.70	23.59	17.28	26.15	34.79	44.52	78.49	94.03
SB35	0.76	8.32	9.98	3.67	22.72	16.23	19.47	29.50	39.09	49.24	74.51	90.02
SB36	0.79	8.86	11.76	3.28	22.99	14.99	19.90	29.91	38.38	46.20	71.88	88.24

Sample Name	Elevation m OD	HIRM 10^{-5} Am^2kg^{-1}	Hard %	ARM 10^{-5} Am^2kg^{-1}	SIRM/ARM no units	'Soft' 10^{-5} Am^2kg^{-1}	IRM_{-20} %	IRM_{-30} %	IRM_{-40} %	IRM_{-50} %	IRM_{-100} %	IRM_{-300} %
SB37	0.82	9.99	14.09	2.45	28.95	14.10	19.88	29.08	38.11	45.72	68.70	85.91
SB38	0.85	10.07	12.65	2.11	37.66	14.38	18.07	26.81	35.96	44.63	69.27	87.35
SB39	0.88	7.62	11.66	1.27	51.47	10.07	15.42	23.44	29.57	39.54	67.93	88.34
SB40	0.91	8.28	13.16	1.24	50.72	10.55	16.76	23.88	31.15	39.05	65.57	86.84
SB41	0.94	7.68	13.07	1.08	54.19	8.72	14.86	22.70	31.00	36.65	63.32	86.93
SB42	0.97	8.84	16.41	0.99	54.48	9.15	16.99	24.68	32.89	38.35	60.83	83.59
SB43	1.00	10.20	20.22	0.98	51.45	11.04	21.88	29.91	35.90	42.53	58.73	79.78
SB44	1.03	8.62	21.90	0.81	48.35	6.91	17.55	28.04	33.24	39.04	55.79	78.10
SB45	1.06	7.79	22.30	0.75	46.64	6.64	19.01	25.30	32.68	38.51	55.31	77.70
SB46	1.09	8.45	20.95	0.86	46.95	8.00	19.83	26.06	34.17	39.87	57.28	79.05
SB47	1.11	8.55	20.86	0.88	46.46	8.22	20.05	28.19	34.21	41.35	57.39	79.14
SB48	1.14	8.00	20.75	0.79	48.87	6.80	17.64	27.51	35.03	41.04	57.29	79.25
SB49	1.17	10.34	20.80	0.96	51.54	9.60	19.32	29.71	36.51	41.82	58.67	79.20
SB50	1.20	12.05	22.27	1.03	52.53	10.84	20.04	29.34	35.43	40.05	55.60	77.73
SB51	1.23	9.49	23.55	0.78	51.86	7.56	18.77	27.66	34.37	39.01	54.47	76.45
SB52	1.26	8.87	24.09	0.68	53.95	6.04	16.40	24.46	31.02	38.23	53.46	75.91
SB53	1.29	9.22	23.93	0.77	50.00	7.25	18.81	26.51	32.71	37.15	52.22	76.07
SB54	1.32	9.57	24.00	0.75	53.02	7.78	19.51	27.25	33.24	37.66	53.81	76.00
SB55	1.35	10.99	22.65	0.97	49.91	9.81	20.22	27.69	34.86	39.76	55.22	77.35
SB56	1.38	10.98	24.56	0.90	49.56	8.88	19.87	27.18	32.36	37.80	51.79	75.44
SB57	1.41	11.31	24.75	0.91	49.97	9.09	19.89	26.95	33.79	38.67	52.84	75.25
SB58	1.44	12.22	25.06	0.92	53.13	8.53	17.51	26.65	32.60	36.56	51.82	74.94
SB59	1.47	10.24	25.01	0.74	55.59	7.00	17.09	26.26	32.25	36.30	51.23	74.99
SB60	1.50	10.44	26.92	0.83	46.94	6.90	17.81	22.95	29.48	35.18	49.75	73.08
SB61	1.53	12.36	26.47	1.23	37.82	8.56	18.33	24.85	31.78	36.78	50.49	73.53
SB62	1.56	9.90	23.51	1.71	24.65	7.29	17.33	25.24	31.05	37.65	54.28	76.49
SB63	1.59	10.78	23.23	2.55	18.24	8.46	18.23	24.10	33.08	39.15	54.91	76.77
SB64	1.61	10.20	25.81	1.45	27.30	6.55	16.58	22.62	29.60	36.45	51.83	74.19
SB65	1.64	10.97	25.73	1.70	25.09	6.82	15.99	24.49	31.01	36.28	51.34	74.27
SB66	1.67	9.30	27.12	0.63	54.06	5.64	16.46	25.05	30.06	35.71	50.91	72.88
SB67	1.70	11.10	25.21	1.00	44.03	7.53	17.10	25.14	33.82	38.33	53.75	74.79
SB68	1.73	12.18	20.56	1.49	39.73	14.03	23.67	31.92	40.59	46.40	61.18	79.44
SB69	1.82	10.53	29.54	0.71	50.28	5.43	15.24	22.43	27.73	34.11	48.32	70.46
SB70	1.92	9.55	30.67	0.71	43.55	4.64	14.90	22.49	28.77	32.90	48.11	69.33
SB71	2.02	7.22	23.46	0.61	50.37	5.42	17.59	25.24	31.95	37.20	53.27	76.54
SB72	2.12	8.06	27.12	0.68	44.02	5.06	17.03	24.70	31.18	35.53	50.42	72.88
SB73	2.22	7.48	23.50	0.66	48.29	5.60	17.59	26.40	33.32	38.01	54.65	76.50
SB74	2.32	7.50	9.93	1.63	46.38	21.82	28.89	40.19	51.45	59.79	77.83	90.07

Environmental magnetism data: Brickwall Farm

Sample Name	Elevation m OD	Mass g	χ_{kappa} 10^{-8} m^3kg^{-1}	χ_{lf} 10^{-8} m^3kg^{-1}	χ_{hf} 10^{-8} m^3kg^{-1}	FD %	SIRM 10^{-5} Am^2kg^{-1}	χ_{arm} 10^{-8} m^3kg^{-1}	χ_{arm}/SIRM 10^{-3} mA^{-1}	SIRM/χ_{lf} 10^{-3} mA^{-1}	χ_{arm}/χ_{lf} no units
BF1	-0.84	10.94	7.55	5.57	6.12	-9.84	74.23	45.69	0.62	13.32	8.20
BF2	-0.81	11.33	8.94	7.59	7.73	-1.74	126.11	170.50	1.35	16.61	22.45
BF3	-0.78	12.18	10.21	8.91	8.71	2.30	144.50	191.12	1.32	16.22	21.45
BF4	-0.74	11.20	11.27	9.82	9.82	0.00	159.35	215.37	1.35	16.23	21.93
BF5	-0.71	11.78	9.46	8.32	7.98	4.08	135.74	155.56	1.15	16.32	18.70
BF6	-0.68	12.33	9.02	7.99	7.79	2.54	128.91	144.18	1.12	16.13	18.04
BF7	-0.65	10.75	10.55	9.16	9.16	0.00	157.53	203.79	1.29	17.19	22.24
BF8	-0.61	12.32	10.11	8.89	8.52	4.11	148.94	220.28	1.48	16.76	24.79
BF9	-0.58	12.05	10.63	9.38	9.13	2.65	159.77	225.17	1.41	17.04	24.02
BF10	-0.55	9.99	12.02	10.56	10.16	3.79	206.90	269.94	1.30	19.58	25.55
BF11	-0.52	10.40	11.99	10.67	10.24	4.05	231.96	248.17	1.07	21.74	23.26
BF12	-0.48	11.82	13.51	12.01	11.67	2.82	407.09	257.46	0.63	33.89	21.44
BF13	-0.45	9.58	14.22	12.79	12.27	4.08	375.97	333.72	0.89	29.39	26.08
BF14	-0.42	11.09	14.65	13.07	13.12	-0.34	524.16	269.04	0.51	40.10	20.58
BF15	-0.39	10.83	21.11	18.97	18.69	1.46	1096.74	334.26	0.30	57.82	17.62
BF16	-0.35	9.75	23.14	20.82	20.31	2.46	1246.25	392.67	0.32	59.86	18.86
BF17	-0.32	9.65	21.61	19.11	18.54	2.98	1139.65	302.84	0.27	59.63	15.84
BF18	-0.29	10.34	15.44	13.78	13.30	3.51	520.87	286.97	0.55	37.80	20.83
BF19	-0.26	11.10	14.25	12.62	12.39	1.79	421.89	275.58	0.65	33.43	21.84
BF20	-0.22	10.50	17.63	15.72	15.19	3.33	577.84	336.00	0.58	36.77	21.38
BF21	-0.18	10.48	15.61	13.84	13.46	2.76	387.52	272.58	0.70	28.01	19.70
BF22	-0.14	10.87	22.60	20.23	19.59	3.18	712.26	428.27	0.60	35.20	21.17
BF23	-0.11	10.58	21.90	19.66	19.33	1.68	775.19	419.37	0.54	39.42	21.33
BF24	-0.07	10.25	21.42	18.83	18.83	0.00	805.51	411.77	0.51	42.77	21.86
BF25	-0.04	9.14	20.72	18.05	18.11	-0.30	676.56	451.02	0.67	37.48	24.99
BF26	0.00	10.72	17.38	15.68	15.40	1.79	490.03	373.08	0.76	31.26	23.80
BF27	0.03	10.46	18.09	16.30	15.82	2.93	523.47	367.83	0.70	32.11	22.57
BF28	0.07	10.16	13.92	12.36	11.96	3.19	309.82	290.03	0.94	25.07	23.47
BF29	0.10	11.04	11.95	10.47	10.28	1.73	221.49	232.59	1.05	21.16	22.22
BF30	0.14	10.46	9.51	8.13	8.17	-0.59	140.71	176.37	1.25	17.32	21.70
BF31	0.17	10.77	10.96	9.38	9.24	1.49	152.23	204.53	1.34	16.23	21.81
BF32	0.20	10.73	10.16	8.62	8.71	-1.08	127.09	188.80	1.49	14.74	21.90
BF33	0.24	9.77	9.64	7.78	7.99	-2.63	100.84	138.26	1.37	12.96	17.77
BF34	0.27	11.24	9.63	8.23	6.72	18.38	92.21	74.91	0.81	11.20	9.10
BF35	0.31	10.00	9.21	7.95	7.70	3.14	74.38	36.30	0.49	9.36	4.57
BF36	0.34	11.01	10.38	9.22	8.81	4.43	106.15	142.02	1.34	11.52	15.41
BF37	0.38	10.65	11.35	10.04	9.57	4.67	134.01	221.87	1.66	13.34	22.09
BF38	0.41	10.49	11.95	10.63	10.49	1.35	156.50	223.76	1.43	14.72	21.04
BF39	0.45	11.43	11.48	10.33	9.76	5.51	141.50	209.69	1.48	13.70	20.30
BF40	0.48	10.21	10.24	8.71	8.76	-0.56	103.56	122.59	1.18	11.88	14.07
BF41	0.52	10.31	10.28	8.88	9.02	-1.64	93.25	111.10	1.19	10.50	12.51
BF42	0.55	10.90	9.77	8.21	8.35	-1.68	101.80	145.65	1.43	12.39	17.73
BF43	0.59	10.81	9.97	8.32	8.51	-2.22	116.08	168.89	1.45	13.95	20.29
BF44	0.62	9.98	10.47	8.97	8.97	0.00	129.01	183.70	1.42	14.38	20.48
BF45	0.66	9.93	9.99	8.46	8.21	2.98	110.13	174.21	1.58	13.01	20.58
BF46	0.69	10.57	9.56	8.09	8.13	-0.58	114.58	188.61	1.65	14.17	23.32
BF47	0.73	10.60	9.96	8.58	8.35	2.75	118.26	171.68	1.45	13.78	20.00
BF48	0.76	10.96	10.89	9.45	9.27	1.93	118.65	161.33	1.36	12.56	17.08
BF49	0.80	10.80	10.00	8.52	8.28	2.72	94.28	84.06	0.89	11.07	9.87
BF50	0.85	9.69	9.62	8.20	8.05	1.89	81.70	40.79	0.50	9.96	4.97
BF51	0.89	10.47	9.14	7.88	7.64	3.03	72.29	26.95	0.37	9.18	3.42
BF52	0.94	10.87	8.05	6.85	6.85	0.00	61.56	18.71	0.30	8.98	2.73
BF53	0.99	11.24	7.52	6.50	6.32	2.74	55.31	18.82	0.34	8.51	2.90
BF54	1.04	9.53	7.35	5.88	6.04	-2.68	46.92	15.69	0.33	7.98	2.67
BF55	1.08	11.59	7.35	6.12	6.34	-3.52	41.21	16.74	0.41	6.73	2.73
BF56	1.13	12.40	7.27	6.25	6.37	-1.94	42.82	13.82	0.32	6.85	2.21

Sample Name	Elevation m OD	Mass g	χ_{kappa} 10^{-8} m^3kg^{-1}	χ_{lf} 10^{-8} m^3kg^{-1}	χ_{hf} 10^{-8} m^3kg^{-1}	FD %	SIRM 10^{-5} Am^2kg^{-1}	χ_{arm} 10^{-8} m^3kg^{-1}	χ_{arm}/SIRM 10^{-3} mA^{-1}	SIRM/χ_{lf} 10^{-3} mA^{-1}	χ_{arm}/χ_{lf} no units
BF57	1.18	12.11	7.93	7.18	6.65	7.47	47.95	15.65	0.33	6.68	2.18
BF58	1.23	12.14	7.91	6.88	6.75	1.80	50.11	13.26	0.26	7.29	1.93
BF59	1.27	12.38	8.16	7.07	7.23	-2.29	54.68	15.24	0.28	7.74	2.16
BF60	1.32	12.70	8.62	7.52	7.68	-2.09	48.37	16.28	0.34	6.43	2.16
BF61	1.37	12.03	7.85	6.69	6.77	-1.24	41.46	13.25	0.32	6.20	1.98
BF62	1.42	12.62	7.50	6.42	6.30	1.85	39.61	16.45	0.42	6.17	2.56
BF63	1.46	12.03	7.22	6.28	6.20	1.32	38.76	15.98	0.41	6.17	2.55
BF64	1.51	12.14	7.30	6.14	6.18	-0.67	39.41	13.03	0.33	6.42	2.12
BF65	1.56	11.58	7.42	6.17	6.13	0.70	37.97	16.12	0.42	6.15	2.61
BF66	1.61	13.06	7.37	6.39	6.39	0.00	39.88	16.64	0.42	6.24	2.60
BF67	1.66	13.63	7.27	6.31	6.27	0.58	40.14	12.68	0.32	6.36	2.01
BF68	1.70	11.58	7.88	6.78	6.78	0.00	43.34	18.16	0.42	6.39	2.68
BF69	1.75	13.37	8.67	7.63	7.37	3.43	57.23	21.00	0.37	7.50	2.75
BF70	1.87	11.75	8.93	7.74	7.66	1.10	44.16	16.15	0.37	5.70	2.09
BF71	1.97	11.79	10.14	8.69	8.52	1.95	59.99	28.20	0.47	6.90	3.24
BF72	2.07	11.60	19.66	17.42	17.07	1.98	209.01	84.19	0.40	12.00	4.83
BF73	2.17	11.49	20.03	17.97	17.45	2.91	213.35	80.03	0.38	11.87	4.45
BF74	2.27	10.47	19.83	17.86	17.29	3.21	206.68	87.64	0.42	11.57	4.91

Sample Name	Elevation m OD	HIRM 10^{-5} Am^2kg^{-1}	Hard %	ARM 10^{-5} Am^2kg^{-1}	SIRM/ARM no units	'Soft' 10^{-5} Am^2kg^{-1}	IRM_{-20} %	IRM_{-30} %	IRM_{-40} %	IRM_{-50} %	IRM_{-100} %	IRM_{-300} %
BF1	-0.84	7.42	9.99	3.64	20.41	16.12	21.71	31.28	40.92	48.90	75.42	90.01
BF2	-0.81	10.11	8.02	13.57	9.29	22.94	18.19	31.43	40.95	52.51	79.30	91.98
BF3	-0.78	12.02	8.32	15.21	9.50	27.92	19.32	31.06	41.96	55.11	79.69	91.68
BF4	-0.74	12.61	7.91	17.14	9.30	36.63	22.99	34.02	42.87	53.35	80.30	92.09
BF5	-0.71	10.62	7.83	12.38	10.96	25.48	18.77	32.26	40.93	52.04	79.65	92.17
BF6	-0.68	10.41	8.08	11.48	11.23	21.78	16.90	31.03	38.10	52.03	79.07	91.92
BF7	-0.65	11.26	7.15	16.22	9.71	32.65	20.73	29.04	40.56	49.62	79.93	92.85
BF8	-0.61	10.85	7.28	17.53	8.49	31.02	20.83	29.94	39.87	52.24	80.12	92.72
BF9	-0.58	11.48	7.18	17.92	8.91	29.38	18.39	31.06	41.53	49.10	80.15	92.82
BF10	-0.55	12.38	5.98	21.49	9.63	37.60	18.17	27.93	35.81	45.97	79.86	94.02
BF11	-0.52	11.18	4.82	19.75	11.74	35.18	15.17	23.81	33.45	42.44	79.07	95.18
BF12	-0.48	11.64	2.86	20.49	19.86	45.86	11.27	17.27	24.14	35.83	76.61	97.14
BF13	-0.45	10.07	2.68	26.56	14.15	45.64	12.14	20.04	27.35	38.10	78.55	97.32
BF14	-0.42	8.43	1.61	21.42	24.48	53.85	10.27	15.28	22.69	33.96	79.11	98.39
BF15	-0.39	12.62	1.15	26.61	41.22	81.23	7.41	12.07	20.61	30.36	76.71	98.85
BF16	-0.35	11.14	0.89	31.26	39.87	101.95	8.18	13.37	18.91	28.46	77.72	99.11
BF17	-0.32	4.69	0.41	24.11	47.28	92.92	8.15	12.45	18.49	26.94	76.61	99.59
BF18	-0.29	9.30	1.79	22.84	22.80	51.83	9.95	14.79	23.21	34.21	77.45	98.21
BF19	-0.26	11.23	2.66	21.94	19.23	47.62	11.29	18.10	24.35	35.39	78.00	97.34
BF20	-0.22	14.58	2.52	26.75	21.61	59.41	10.28	18.41	26.43	36.74	80.79	97.48
BF21	-0.18	12.48	3.22	21.70	17.86	52.79	13.62	23.17	31.03	43.33	81.49	96.78
BF22	-0.14	12.88	1.81	34.09	20.89	87.54	12.29	18.40	28.18	40.58	80.77	98.19
BF23	-0.11	14.33	1.85	33.38	23.22	80.05	10.33	18.19	25.79	35.39	78.30	98.15
BF24	-0.07	12.86	1.60	32.78	24.58	82.30	10.22	16.72	24.07	33.71	76.36	98.40
BF25	-0.04	12.45	1.84	35.90	18.85	69.63	10.29	16.92	24.17	32.21	75.58	98.16
BF26	0.00	12.76	2.60	29.70	16.50	55.79	11.39	18.54	26.00	36.13	77.32	97.40
BF27	0.03	12.20	2.33	29.28	17.88	60.69	11.59	18.59	25.99	34.33	75.92	97.67
BF28	0.07	9.31	3.00	23.09	13.42	45.01	14.53	21.64	32.50	42.18	80.92	97.00
BF29	0.10	10.38	4.69	18.51	11.96	35.56	16.05	23.82	34.97	46.57	81.94	95.31
BF30	0.14	8.32	5.92	14.04	10.02	25.41	18.06	26.65	40.65	48.32	82.33	94.08
BF31	0.17	9.87	6.49	16.28	9.35	30.61	20.11	31.12	42.32	52.38	80.71	93.51
BF32	0.20	9.38	7.38	15.03	8.46	27.85	21.92	30.07	43.97	54.60	81.26	92.62
BF33	0.24	9.36	9.28	11.01	9.16	23.04	22.85	35.24	43.58	55.10	78.23	90.72
BF34	0.27	8.74	9.47	5.96	15.46	21.02	22.79	34.84	44.62	52.10	76.80	90.53
BF35	0.31	6.65	8.94	2.89	25.74	14.41	19.37	31.65	43.15	53.30	76.50	91.06
BF36	0.34	9.02	8.50	11.31	9.39	24.94	23.50	35.79	46.57	54.88	78.91	91.50

Sample Name	Elevation m OD	HIRM 10^{-5} Am^2kg^{-1}	Hard %	ARM 10^{-5} Am^2kg^{-1}	SIRM/ARM no units	'Soft' 10^{-5} Am^2kg^{-1}	IRM_{-20} %	IRM_{-30} %	IRM_{-40} %	IRM_{-50} %	IRM_{-100} %	IRM_{-300} %
BF37	0.38	10.84	8.09	17.66	7.59	32.50	24.26	36.27	47.34	56.80	80.57	91.91
BF38	0.41	12.48	7.97	17.81	8.79	35.61	22.75	35.35	47.16	55.87	80.71	92.03
BF39	0.45	11.90	8.41	16.69	8.48	34.52	24.40	36.80	47.67	55.67	80.70	91.59
BF40	0.48	10.10	9.75	9.76	10.61	26.65	25.74	38.09	48.42	56.54	78.27	90.25
BF41	0.52	8.80	9.44	8.84	10.54	24.09	25.83	37.11	47.60	56.52	77.53	90.56
BF42	0.55	9.92	9.74	11.59	8.78	26.37	25.90	37.88	46.73	55.23	78.32	90.26
BF43	0.59	10.35	8.92	13.44	8.63	28.64	24.68	35.94	46.93	56.62	79.36	91.08
BF44	0.62	11.01	8.53	14.62	8.82	32.22	24.97	35.41	47.59	57.32	80.14	91.47
BF45	0.66	10.36	9.41	13.87	7.94	28.28	25.68	34.29	46.70	57.41	78.99	90.59
BF46	0.69	9.94	8.68	15.01	7.63	24.06	21.00	36.95	45.34	57.38	80.37	91.32
BF47	0.73	11.23	9.49	13.67	8.65	28.18	23.83	35.93	46.33	56.39	78.98	90.51
BF48	0.76	11.76	9.91	12.84	9.24	27.79	23.42	37.11	45.08	56.28	78.87	90.09
BF49	0.80	11.37	12.06	6.69	14.09	21.24	22.53	33.93	43.85	54.22	74.97	87.94
BF50	0.85	12.80	15.66	3.25	25.16	18.07	22.12	32.20	39.60	49.11	67.77	84.34
BF51	0.89	12.10	16.73	2.15	33.70	15.88	21.96	29.99	37.29	45.05	64.02	83.27
BF52	0.94	11.68	18.97	1.49	41.34	11.93	19.38	27.31	35.05	42.23	60.17	81.03
BF53	0.99	10.75	19.43	1.50	36.92	9.48	17.14	26.77	34.28	41.41	59.05	80.57
BF54	1.04	10.30	21.95	1.25	37.58	7.80	16.63	24.37	31.72	39.12	55.36	78.05
BF55	1.08	9.25	22.45	1.33	30.92	6.63	16.08	22.77	30.83	36.36	53.52	77.55
BF56	1.13	9.99	23.32	1.10	38.94	7.12	16.62	23.85	30.99	37.16	53.18	76.68
BF57	1.18	11.71	24.43	1.25	38.50	7.92	16.52	22.75	30.64	36.66	52.56	75.57
BF58	1.23	12.32	24.58	1.06	47.49	8.81	17.57	25.45	31.74	37.73	52.82	75.42
BF59	1.27	12.29	22.47	1.21	45.07	10.67	19.51	27.30	33.96	40.14	55.56	77.53
BF60	1.32	11.44	23.66	1.30	37.33	9.66	19.97	27.70	34.43	40.36	55.25	76.34
BF61	1.37	10.89	26.27	1.06	39.30	6.28	15.15	23.96	30.22	35.36	50.30	73.73
BF62	1.42	10.39	26.23	1.31	30.26	6.40	16.16	23.42	29.06	35.55	51.22	73.77
BF63	1.46	10.22	26.37	1.27	30.46	6.05	15.61	22.56	28.90	35.03	51.01	73.63
BF64	1.51	10.08	25.57	1.04	37.99	6.36	16.13	22.84	29.25	33.89	51.21	74.43
BF65	1.56	9.19	24.21	1.28	29.59	5.87	15.45	22.71	30.48	36.43	53.19	75.79
BF66	1.61	9.28	23.28	1.32	30.11	6.26	15.71	23.42	30.27	36.15	54.43	76.72
BF67	1.66	9.32	23.22	1.01	39.77	6.18	15.39	23.95	29.63	36.49	53.54	76.78
BF68	1.70	9.45	21.81	1.45	29.98	7.97	18.38	25.51	32.48	39.03	56.36	78.19
BF69	1.75	9.80	17.12	1.67	34.24	11.93	20.85	28.86	37.12	42.89	62.41	82.88
BF70	1.87	9.96	22.56	1.29	34.35	9.14	20.69	29.21	34.97	42.01	56.50	77.44
BF71	1.97	11.20	18.67	2.25	26.72	13.53	22.55	32.45	40.91	48.72	63.54	81.33
BF72	2.07	16.36	7.83	6.70	31.19	57.88	27.69	42.88	52.76	60.78	78.35	92.17
BF73	2.17	24.75	11.60	6.37	33.49	61.73	28.93	37.01	48.95	56.92	74.30	88.40
BF74	2.27	15.05	7.28	6.98	29.63	65.36	31.62	44.69	52.02	62.81	79.47	92.72

Environmental magnetism data: Manor Farm

Sample Name	Elevation m OD	Mass g	χ_{kappa} 10^{-8} m^3kg^{-1}	χ_{lf} 10^{-8} m^3kg^{-1}	χ_{hf} 10^{-8} m^3kg^{-1}	FD %	SIRM 10^{-5} Am^2kg^{-1}	χ_{arm} 10^{-8} m^3kg^{-1}	χ_{arm}/SIRM 10^{-3} mA^{-1}	SIRM/χ_{lf} 10^{-3} mA^{-1}	χ_{arm}/χ_{lf} no units
MF1	-2.34	13.99	2.92	2.25	2.25	0.00	101.49	17.38	0.17	45.07	7.72
MF2	-2.27	12.31	15.69	14.38	14.06	2.26	1004.97	118.67	0.12	69.87	8.25
MF3	-2.21	11.95	9.93	8.70	8.54	1.92	397.55	81.06	0.20	45.68	9.31
MF4	-2.16	12.35	7.18	6.19	6.11	1.31	152.07	88.07	0.58	24.55	14.22
MF5	-2.10	11.96	5.24	4.35	4.30	0.96	56.96	18.41	0.32	13.10	4.23
MF6	-2.05	10.01	8.23	6.99	6.99	0.00	128.25	28.97	0.23	18.35	4.14
MF7	-1.99	12.01	7.11	6.20	6.04	2.68	127.14	41.17	0.32	20.50	6.64
MF8	-1.94	11.80	7.53	6.57	6.31	3.87	137.32	63.51	0.46	20.91	9.67
MF9	-1.89	11.25	8.58	7.56	7.29	3.53	122.65	60.87	0.50	16.23	8.06
MF10	-1.83	12.15	7.16	6.21	6.13	1.32	101.25	39.23	0.39	16.30	6.31
MF11	-1.78	11.18	7.83	6.89	6.62	3.90	122.14	40.09	0.33	17.74	5.82
MF12	-1.72	9.37	10.18	8.96	8.75	2.38	124.74	45.97	0.37	13.91	5.13
MF13	-1.67	10.20	9.69	8.43	8.19	2.91	135.17	46.38	0.34	16.03	5.50
MF14	-1.61	10.06	10.90	9.55	9.50	0.52	112.82	48.80	0.43	11.82	5.11
MF15	-1.56	8.94	10.77	9.34	9.17	1.80	123.54	43.92	0.36	13.23	4.70
MF16	-1.49	10.69	9.00	7.86	7.67	2.38	130.00	39.26	0.30	16.54	5.00
MF17	-1.44	9.51	9.61	8.15	7.88	3.23	133.80	42.51	0.32	16.43	5.22
MF18	-1.38	10.54	8.64	7.50	7.40	1.27	103.05	41.78	0.41	13.74	5.57
MF19	-1.33	9.44	10.40	9.01	8.95	0.59	117.15	44.67	0.38	13.01	4.96
MF20	-1.27	9.11	9.72	8.40	8.18	2.61	100.73	43.63	0.43	12.00	5.20
MF21	-1.22	9.44	10.21	8.79	8.69	1.20	118.29	52.27	0.44	13.45	5.94
MF22	-1.16	9.98	14.70	13.02	12.82	1.54	165.50	104.90	0.63	12.71	8.06
MF23	-1.11	9.71	13.94	12.52	12.00	4.12	184.82	107.41	0.58	14.77	8.58
MF24	-1.05	9.61	13.22	11.56	11.45	0.90	162.75	95.29	0.59	14.08	8.25
MF25	-1.00	9.41	13.55	11.74	11.74	0.00	155.33	83.54	0.54	13.23	7.11
MF26	-0.94	9.98	12.18	10.57	10.52	0.47	157.10	83.69	0.53	14.86	7.92
MF27	-0.89	9.54	10.57	9.07	9.01	0.58	134.96	90.32	0.67	14.88	9.96
MF28	-0.83	9.67	11.39	9.98	9.72	2.59	153.05	130.69	0.85	15.34	13.10
MF29	-0.78	10.61	11.65	10.27	10.13	1.38	180.11	141.57	0.79	17.53	13.78
MF30	-0.72	9.98	12.79	11.28	10.88	3.56	206.06	176.22	0.86	18.27	15.63
MF31	-0.67	10.46	14.38	12.76	12.33	3.37	217.64	206.06	0.95	17.06	16.15
MF32	-0.61	10.00	14.36	12.75	12.35	3.14	317.80	234.39	0.74	24.93	18.39
MF33	-0.56	10.46	12.63	11.09	10.90	1.72	231.84	176.70	0.76	20.91	15.93
MF34	-0.48	11.16	12.44	11.11	10.98	1.21	224.85	191.29	0.85	20.23	17.21
MF35	-0.43	10.30	13.49	11.99	11.75	2.02	197.75	251.28	1.27	16.50	20.96
MF36	-0.38	10.54	11.16	9.82	9.59	2.42	183.01	218.23	1.19	18.63	22.21
MF37	-0.32	10.04	11.07	9.61	9.46	1.55	179.14	228.35	1.27	18.64	23.76
MF38	-0.27	11.06	10.89	9.63	9.45	1.88	177.92	246.42	1.39	18.48	25.60
MF39	-0.21	9.72	14.66	13.06	12.65	3.15	350.93	380.24	1.08	26.87	29.11
MF40	-0.16	10.96	12.19	10.81	10.58	2.11	255.68	281.02	1.10	23.65	25.99
MF41	-0.11	10.39	11.73	10.35	10.01	3.26	306.88	198.38	0.65	29.65	19.17
MF42	-0.05	missing									
MF43	0.00	10.60	24.51	22.36	21.89	2.11	1288.56	272.32	0.21	57.63	12.18
MF44	0.05	12.21	8.10	7.04	6.92	1.74	156.89	110.27	0.70	22.28	15.66
MF45	0.11	11.01	12.23	10.76	10.54	2.11	339.91	239.83	0.71	31.58	22.28
MF46	0.16	10.67	15.88	14.01	13.68	2.34	588.94	238.41	0.40	42.03	17.02
MF47	0.22	9.62	19.97	17.92	17.40	2.90	875.70	248.88	0.28	48.86	13.89
MF48	0.27	10.67	17.39	15.61	14.96	4.20	725.64	247.23	0.34	46.48	15.84
MF49	0.32	10.58	17.36	15.60	15.08	3.33	731.63	291.55	0.40	46.90	18.69
MF50	0.38	12.11	9.35	8.21	8.01	2.51	181.26	158.85	0.88	22.07	19.34
MF51	0.43	11.40	9.57	8.42	7.98	5.21	148.54	194.61	1.31	17.64	23.12
MF52	0.44	11.63	9.69	8.51	8.21	3.54	158.84	193.97	1.22	18.66	22.79
MF53	0.50	10.34	10.28	8.95	8.51	4.86	166.11	243.15	1.46	18.56	27.17
MF54	0.55	11.50	10.12	8.78	8.65	1.49	171.17	223.94	1.31	19.49	25.50
MF55	0.60	10.01	12.95	11.29	11.09	1.77	464.08	88.13	0.19	41.11	7.81
MF56	0.66	10.39	10.95	9.48	9.62	-1.52	219.92	49.99	0.23	23.20	5.27

Sample Name	Elevation m OD	Mass g	χ_{kappa} 10^{-8} m^3kg^{-1}	χ_{lf} 10^{-8} m^3kg^{-1}	χ_{hf} 10^{-8} m^3kg^{-1}	FD %	SIRM 10^{-5} Am^2kg^{-1}	χ_{arm} 10^{-8} m^3kg^{-1}	χ_{arm}/SIRM 10^{-3} mA^{-1}	SIRM/χ_{lf} 10^{-3} mA^{-1}	χ_{arm}/χ_{lf} no units
MF57	0.71	11.63	8.20	6.92	7.05	-1.86	129.38	44.32	0.34	18.69	6.40
MF58	0.77	11.03	11.99	10.43	10.43	0.00	263.49	55.74	0.21	25.27	5.35
MF59	0.82	9.75	9.89	8.26	8.41	-1.86	67.62	47.24	0.70	8.19	5.72
MF60	0.88	11.64	6.04	4.94	5.11	-3.48	45.69	21.63	0.47	9.25	4.38
MF61	0.93	12.26	6.64	5.55	5.63	-1.47	42.43	15.96	0.38	7.65	2.88
MF62	0.99	10.72	6.79	5.74	5.60	2.44	34.38	12.75	0.37	5.99	2.22
MF63	1.04	12.16	5.35	4.52	4.44	1.82	35.73	12.26	0.34	7.90	2.71
MF64	1.09	12.18	6.53	5.58	5.58	0.00	38.48	16.39	0.43	6.89	2.93
MF65	1.15	12.12	7.02	5.98	6.07	-1.38	37.39	15.97	0.43	6.25	2.67
MF66	1.20	11.12	8.32	7.15	7.11	0.63	50.20	25.21	0.50	7.02	3.52
MF67	1.26	11.76	7.60	6.59	6.51	1.29	41.91	21.34	0.51	6.36	3.24
MF68	1.36	12.46	7.19	6.26	6.14	1.92	39.50	18.23	0.46	6.31	2.91
MF69	1.46	12.33	8.47	7.42	7.30	1.64	49.91	27.71	0.56	6.72	3.73
MF70	1.56	11.35	9.48	8.33	8.15	2.12	49.77	31.20	0.63	5.98	3.75
MF71	1.66	11.30	8.95	7.83	7.61	2.82	48.78	28.37	0.58	6.23	3.62
MF72	1.74	11.00	9.20	7.82	7.77	0.58	45.47	25.76	0.57	5.82	3.29
MF73	1.84	10.00	9.37	7.95	7.95	0.00	44.92	15.50	0.35	5.65	1.95
MF74	1.94	9.52	9.36	7.93	7.93	0.00	34.65	14.09	0.41	4.37	1.78
MF75	2.04	9.16	9.85	8.41	8.30	1.30	53.10	17.29	0.33	6.32	2.06
MF76	2.14	10.23	13.50	11.73	11.73	0.00	113.49	38.15	0.34	9.68	3.25
MF77	2.24	10.89	13.57	11.99	11.76	1.92	118.09	49.35	0.42	9.85	4.12

Sample Name	Elevation m OD	HIRM 10^{-5} Am^2kg^{-1}	Hard %	ARM 10^{-5} Am^2kg^{-1}	SIRM/ARM no units	'Soft' 10^{-5} Am^2kg^{-1}	IRM_{-20} %	IRM_{-30} %	IRM_{-40} %	IRM_{-50} %	IRM_{-100} %	IRM_{-300} %
MF1	-2.34	2.36	2.32	1.38	73.37	10.93	10.77	18.35	23.38	36.00	79.35	97.68
MF2	-2.27	6.93	0.69	9.45	106.39	132.58	13.19	21.74	29.38	40.85	82.06	99.31
MF3	-2.21	-0.21	-0.05	6.45	61.61	44.26	11.13	19.00	25.57	40.40	83.49	100.05
MF4	-2.16	5.02	3.30	7.01	21.69	20.49	13.48	22.88	32.54	41.70	79.98	96.70
MF5	-2.10	3.15	5.53	1.47	38.88	9.28	16.29	25.70	36.34	48.36	79.69	94.47
MF6	-2.05	-5.42	-4.22	2.31	55.62	15.72	12.25	21.12	30.30	41.05	75.93	104.22
MF7	-1.99	1.63	1.28	3.28	38.80	16.68	13.12	20.82	31.58	41.80	77.87	98.72
MF8	-1.94	16.52	12.03	5.06	27.16	18.89	13.76	21.16	31.69	41.12	77.53	87.97
MF9	-1.89	13.11	10.69	4.85	25.31	18.19	14.83	21.83	32.77	46.74	77.91	89.31
MF10	-1.83	4.71	4.65	3.12	32.43	13.52	13.36	21.81	35.36	46.04	77.06	95.35
MF11	-1.78	4.40	3.60	3.19	38.28	15.28	12.51	23.94	30.70	44.42	77.42	96.40
MF12	-1.72	6.86	5.50	3.66	34.09	15.43	12.37	22.76	28.85	42.15	73.98	94.50
MF13	-1.67	5.45	4.03	3.69	36.62	17.71	13.10	22.75	32.42	42.70	76.69	95.97
MF14	-1.61	6.24	5.53	3.88	29.04	19.43	17.22	26.69	33.63	46.54	76.47	94.47
MF15	-1.56	6.53	5.29	3.50	35.34	14.23	11.52	23.81	29.17	40.34	73.95	94.71
MF16	-1.49	6.11	4.70	3.13	41.60	18.47	14.20	24.75	31.81	44.62	79.64	95.30
MF17	-1.44	4.74	3.54	3.38	39.54	21.30	15.92	28.91	37.47	51.33	81.91	96.46
MF18	-1.38	6.38	6.20	3.33	30.99	14.37	13.95	25.65	34.82	44.74	76.82	93.80
MF19	-1.33	6.82	5.82	3.56	32.95	16.62	14.18	20.77	29.66	41.90	73.50	94.18
MF20	-1.27	5.95	5.91	3.47	29.01	18.09	17.96	24.49	37.00	46.94	76.31	94.09
MF21	-1.22	6.49	5.49	4.16	28.43	22.12	18.70	25.56	39.90	48.13	79.27	94.51
MF22	-1.16	11.46	6.92	8.35	19.82	38.14	23.05	33.90	45.30	53.82	79.63	93.08
MF23	-1.11	11.04	5.97	8.55	21.62	37.94	20.53	29.79	37.96	50.78	78.47	94.03
MF24	-1.05	10.53	6.47	7.58	21.46	32.96	20.25	28.48	38.15	48.92	79.41	93.53
MF25	-1.00	9.13	5.88	6.65	23.36	28.67	18.46	29.74	39.60	48.82	76.94	94.12
MF26	-0.94	8.95	5.70	6.66	23.58	28.36	18.05	27.36	38.40	47.79	79.52	94.30
MF27	-0.89	7.70	5.71	7.19	18.77	25.74	19.07	29.51	39.55	49.43	79.52	94.29
MF28	-0.83	7.86	5.13	10.40	14.71	26.76	17.48	29.36	40.72	48.27	80.97	94.87
MF29	-0.78	8.37	4.65	11.27	15.98	31.47	17.47	31.43	42.46	50.43	82.14	95.35
MF30	-0.72	10.16	4.93	14.03	14.69	33.76	16.38	29.29	38.20	46.65	80.43	95.07
MF31	-0.67	9.82	4.51	16.40	13.27	44.30	20.36	30.25	39.22	51.33	79.71	95.49
MF32	-0.61	9.59	3.02	18.66	17.03	44.71	14.07	21.36	29.73	40.13	73.87	96.98
MF33	-0.56	7.54	3.25	14.07	16.48	42.03	18.13	29.98	38.51	54.11	84.06	96.75

Sample Name	Elevation m OD	HIRM 10^{-5} Am^2kg^{-1}	Hard %	ARM 10^{-5} Am^2kg^{-1}	SIRM/ARM no units	'Soft' 10^{-5} Am^2kg^{-1}	IRM_{-20} %	IRM_{-30} %	IRM_{-40} %	IRM_{-50} %	IRM_{-100} %	IRM_{-300} %
MF34	-0.48	9.71	4.32	15.23	14.77	43.40	19.30	29.98	39.98	49.32	79.42	95.68
MF35	-0.43	10.32	5.22	20.00	9.89	41.88	21.18	31.51	41.64	53.27	79.83	94.78
MF36	-0.38	9.13	4.99	17.37	10.54	32.27	17.63	26.35	36.35	46.53	76.61	95.01
MF37	-0.32	9.11	5.09	18.18	9.86	26.37	14.72	25.45	36.60	47.27	77.97	94.91
MF38	-0.27	9.52	5.35	19.62	9.07	32.64	18.35	28.38	37.08	49.40	80.68	94.65
MF39	-0.21	11.18	3.19	30.27	11.59	41.88	11.94	21.46	29.01	41.37	76.59	96.81
MF40	-0.16	8.82	3.45	22.37	11.43	40.25	15.74	26.21	34.92	47.42	78.84	96.55
MF41	-0.11	6.99	2.28	15.79	19.43	42.97	14.00	24.28	32.96	41.50	78.81	97.72
MF42	-0.05	missing										
MF43	0.00	14.20	1.10	21.68	59.44	108.67	8.43	14.67	24.39	30.75	74.27	98.90
MF44	0.05	9.00	5.74	8.78	17.87	25.50	16.25	24.62	34.67	43.05	77.98	94.26
MF45	0.11	10.12	2.98	19.09	17.81	41.68	12.26	19.15	25.28	36.47	77.81	97.02
MF46	0.16	7.82	1.33	18.98	31.03	53.01	9.00	18.81	26.35	33.58	76.15	98.67
MF47	0.22	-10.38	-1.19	19.81	44.20	115.85	13.23	20.76	30.01	43.12	87.77	101.19
MF48	0.27	9.83	1.36	19.68	36.87	70.22	9.68	18.33	27.25	36.70	80.17	98.64
MF49	0.32	15.43	2.11	23.21	31.53	63.85	8.73	16.90	22.25	35.53	80.26	97.89
MF50	0.38	8.54	4.71	12.64	14.33	26.19	14.45	26.71	36.78	47.64	82.70	95.29
MF51	0.43	9.51	6.40	15.49	9.59	28.53	19.21	29.31	37.56	51.37	80.24	93.60
MF52	0.44	10.66	6.71	15.44	10.29	30.76	19.37	28.59	36.23	48.95	80.70	93.29
MF53	0.50	11.33	6.82	19.35	8.58	31.81	19.15	28.79	38.17	47.94	81.24	93.18
MF54	0.55	11.88	6.94	17.83	9.60	28.37	16.57	28.65	38.23	47.16	80.54	93.06
MF55	0.60	11.38	2.45	7.02	66.15	52.75	11.37	18.43	26.69	38.71	82.78	97.55
MF56	0.66	10.67	4.85	3.98	55.27	28.78	13.09	23.31	35.12	46.71	82.17	95.15
MF57	0.71	10.34	7.99	3.53	36.67	17.00	13.14	24.23	32.71	42.99	75.39	92.01
MF58	0.77	11.65	4.42	4.44	59.38	42.09	15.97	26.63	37.98	51.15	85.13	95.58
MF59	0.82	12.41	18.35	3.76	17.98	10.66	15.76	24.83	34.60	43.60	65.21	81.65
MF60	0.88	10.56	23.10	1.72	26.54	7.91	17.31	22.82	32.13	38.63	57.59	76.90
MF61	0.93	10.06	23.71	1.27	33.40	7.19	16.95	24.81	31.90	38.93	56.64	76.29
MF62	0.99	7.28	21.17	1.01	33.88	6.12	17.82	25.30	32.20	38.10	57.80	78.83
MF63	1.04	8.70	24.34	0.98	36.61	5.55	15.53	22.83	30.26	36.76	52.70	75.66
MF64	1.09	9.23	23.99	1.30	29.50	6.25	16.24	22.99	28.79	35.85	54.35	76.01
MF65	1.15	9.36	25.04	1.27	29.42	6.17	16.51	22.54	30.36	36.24	53.42	74.96
MF66	1.20	9.91	19.74	2.01	25.02	10.04	20.00	28.89	38.44	44.62	60.71	80.26
MF67	1.26	10.21	24.37	1.70	24.67	6.56	15.65	24.16	31.27	38.04	53.91	75.63
MF68	1.36	10.15	25.68	1.45	27.21	5.94	15.03	23.94	31.34	37.49	52.34	74.32
MF69	1.46	11.81	23.67	2.21	22.62	9.24	18.52	26.56	33.64	39.46	55.06	76.33
MF70	1.56	12.22	24.54	2.48	20.04	8.87	17.83	25.35	32.74	39.12	53.80	75.46
MF71	1.66	12.23	25.08	2.26	21.60	8.70	17.83	25.57	31.06	37.88	53.87	74.92
MF72	1.74	11.08	24.37	2.05	22.17	8.83	19.41	26.12	34.12	40.00	54.63	75.63
MF73	1.84	8.64	19.24	1.23	36.40	9.83	21.87	32.10	39.58	46.50	61.41	80.76
MF74	1.94	7.98	23.04	1.12	30.89	6.71	19.37	25.67	34.61	39.51	54.88	76.96
MF75	2.04	8.59	16.18	1.38	38.59	11.51	21.68	28.73	39.07	46.41	63.91	83.82
MF76	2.14	11.12	9.80	3.04	37.37	31.39	27.66	39.18	48.37	54.11	74.52	90.20
MF77	2.24	13.03	11.04	3.93	30.06	30.25	25.61	35.23	44.78	55.14	73.35	88.96

Environmental magnetism data: Boulderwall Farm

Sample Name	Elevation m OD	Mass g	χ_{kappa} 10^{-8} m^3kg^{-1}	χ_{lf} 10^{-8} m^3kg^{-1}	χ_{hf} 10^{-8} m^3kg^{-1}	FD %	SIRM 10^{-5} Am^2kg^{-1}	χ_{arm} 10^{-8} m^3kg^{-1}	χ_{arm}/SIRM 10^{-3} mA^{-1}	SIRM/χ_{lf} 10^{-3} mA^{-1}	χ_{arm}/χ_{lf} no units
BW1	-0.05	7.29	16.48	15.22	14.81	2.70	224.55	326.69	1.45	14.75	21.46
BW2	-0.03	7.71	16.15	14.99	14.86	0.87	220.50	346.98	1.57	14.71	23.15
BW3	-0.01	9.25	15.03	13.73	13.68	0.39	210.81	367.18	1.74	15.35	26.74
BW4	0.01	11.88	9.75	8.79	8.63	1.91	148.14	201.07	1.36	16.85	22.87
BW5	0.03	9.60	8.99	8.33	7.97	4.38	128.18	150.27	1.17	15.38	18.03
BW6	0.06	12.07	8.74	8.08	7.71	4.62	135.58	147.49	1.09	16.78	18.25
BW7	0.08	10.57	8.58	7.81	7.67	1.82	143.60	181.45	1.26	18.39	23.24
BW8	0.10	10.92	8.20	7.51	7.28	3.05	137.85	159.16	1.15	18.35	21.19
BW9	0.12	11.90	10.21	9.37	9.12	2.69	271.98	163.82	0.60	29.03	17.49
BW10	0.14	11.21	12.16	11.42	10.79	5.47	347.01	203.65	0.59	30.39	17.84
BW11	0.16	10.64	11.78	10.90	10.48	3.88	316.97	214.50	0.68	29.07	19.67
BW12	0.18	9.33	11.88	10.98	10.55	3.90	252.50	248.91	0.99	22.99	22.66
BW13	0.20	9.68	14.67	13.74	13.07	4.89	345.42	369.78	1.07	25.15	26.92
BW14	0.23	10.02	13.14	12.18	11.73	3.69	274.66	343.02	1.25	22.55	28.17
BW15	0.25	10.47	12.89	12.03	11.46	4.76	265.44	317.16	1.19	22.06	26.36
BW16	0.27	11.16	12.30	11.34	10.94	3.56	224.38	298.24	1.33	19.79	26.30
BW17	0.29	10.26	10.97	10.13	9.74	3.85	179.87	250.97	1.40	17.75	24.77
BW18	0.31	11.11	10.70	9.95	9.54	4.07	162.98	233.75	1.43	16.38	23.49
BW19	0.33	10.96	11.33	10.54	10.13	3.90	162.73	281.19	1.73	15.44	26.68
BW20	0.35	12.28	10.48	9.69	9.28	4.20	235.72	210.02	0.89	24.33	21.67
BW21	0.37	10.55	16.47	15.41	14.84	3.69	569.66	287.91	0.51	36.97	18.68
BW22	0.40	7.31	15.25	14.30	13.47	5.74	311.99	280.26	0.90	21.82	19.60
BW23	0.42	10.44	17.37	16.18	15.56	3.85	519.26	278.88	0.54	32.08	17.23
BW24	0.44	9.21	20.55	19.39	18.30	5.60	836.10	283.29	0.34	43.12	14.61
BW25	0.46	10.04	18.77	17.59	16.99	3.40	670.26	254.82	0.38	38.11	14.49
BW26	0.48	10.91	17.55	16.36	15.86	3.08	620.26	268.15	0.43	37.91	16.39
BW27	0.50	11.04	22.74	21.43	20.93	2.33	1084.84	298.51	0.28	50.63	13.93
BW28	0.52	13.13	21.94	20.45	20.07	1.86	1133.68	263.88	0.23	55.43	12.90
BW29	0.54	11.73	13.07	11.72	11.72	0.00	388.05	239.07	0.62	33.11	20.40
BW30	0.57	12.70	10.66	9.21	9.37	-1.71	177.78	219.35	1.23	19.30	23.82
BW31	0.59	11.87	11.23	10.62	9.99	5.95	172.58	253.55	1.47	16.25	23.88
BW32	0.61	11.48	10.08	9.10	9.06	0.48	133.72	164.64	1.23	14.69	18.08
BW33	0.63	11.96	8.57	7.36	7.61	-3.41	86.82	40.76	0.47	11.80	5.54
BW34	0.65	12.65	8.28	7.95	7.28	8.46	95.43	41.82	0.44	12.01	5.26
BW35	0.67	12.26	8.35	7.34	7.50	-2.22	101.20	50.98	0.50	13.78	6.94
BW36	0.69	10.43	9.02	8.01	7.96	0.60	114.67	77.44	0.68	14.32	9.67
BW37	0.71	12.69	8.24	7.56	7.25	4.17	106.48	94.41	0.89	14.08	12.48
BW38	0.74	11.21	9.62	8.87	8.20	7.54	115.40	139.44	1.21	13.01	15.71
BW39	0.76	10.29	9.24	8.26	8.26	0.00	116.79	138.14	1.18	14.14	16.73
BW40	0.78	9.61	8.47	7.65	7.33	4.08	107.35	127.87	1.19	14.04	16.73
BW41	0.80	10.71	9.82	8.59	8.78	-2.17	138.51	212.18	1.53	16.13	24.70
BW42	0.82	10.23	10.66	9.77	9.53	2.50	142.73	225.75	1.58	14.60	23.10
BW43	0.84	11.16	11.30	10.53	10.17	3.40	152.79	264.90	1.73	14.51	25.16
BW44	0.86	12.01	10.00	9.29	8.91	4.04	136.77	215.90	1.58	14.73	23.25
BW45	0.88	10.07	9.26	8.74	8.20	6.25	128.63	182.04	1.42	14.72	20.83
BW46	0.91	11.68	9.22	8.47	8.26	2.53	126.44	170.88	1.35	14.92	20.17
BW47	0.93	11.64	9.58	9.41	8.51	9.59	134.43	191.35	1.42	14.29	20.34
BW48	0.85	11.69	7.59	8.59	6.76	21.39	63.15	26.80	0.42	7.35	3.12
BW49	0.88	11.73	6.87	7.16	6.10	14.88	60.74	25.95	0.43	8.48	3.62
BW50	0.91	10.91	8.34	6.92	7.42	-7.28	58.79	29.87	0.51	8.50	4.32
BW51	0.94	9.15	7.68	6.67	6.72	-0.82	50.81	22.28	0.44	7.62	3.34
BW52	0.96	10.21	8.65	8.48	7.79	8.09	52.17	21.85	0.42	6.16	2.58
BW53	0.99	9.55	7.87	5.34	7.12	-33.33	53.27	27.91	0.52	9.97	5.23
BW54	1.02	11.13	6.81	6.42	5.79	9.79	54.02	26.14	0.48	8.41	4.07
BW55	1.05	11.37	7.97	7.30	6.86	6.02	62.41	39.47	0.63	8.55	5.41
BW56	1.08	10.84	7.57	7.06	6.78	3.92	57.96	29.54	0.51	8.21	4.19

Sample Name	Elevation m OD	Mass g	χ_{kappa} 10^{-8} m^3kg^{-1}	χ_{lf} 10^{-8} m^3kg^{-1}	χ_{hf} 10^{-8} m^3kg^{-1}	FD %	SIRM 10^{-5} Am^2kg^{-1}	χ_{arm} 10^{-8} m^3kg^{-1}	χ_{arm}/SIRM 10^{-3} mA^{-1}	SIRM/χ_{lf} 10^{-3} mA^{-1}	χ_{arm}/χ_{lf} no units
BW57	1.11	10.42	7.16	6.53	6.38	2.21	52.85	17.03	0.32	8.10	2.61
BW58	1.13	12.05	6.05	5.52	5.27	4.51	48.22	12.43	0.26	8.74	2.25
BW59	1.16	11.69	6.36	7.27	5.56	23.53	47.38	14.06	0.30	6.52	1.93
BW60	1.19	11.73	6.45	6.14	5.67	7.64	43.47	11.11	0.26	7.08	1.81
BW61	1.22	11.85	6.76	6.33	5.99	5.33	47.63	13.40	0.28	7.53	2.12
BW62	1.25	10.75	6.62	6.19	5.82	6.02	43.13	14.62	0.34	6.97	2.36
BW63	1.27	12.40	6.33	5.93	5.49	7.48	50.33	19.68	0.39	8.49	3.32
BW64	1.30	11.34	6.89	6.39	6.08	4.83	47.59	15.65	0.33	7.45	2.45
BW65	1.33	11.74	8.24	7.88	7.33	7.03	42.82	16.76	0.39	5.43	2.13
BW66	1.36	11.24	8.76	8.18	8.00	2.17	39.25	12.70	0.32	4.80	1.55
BW67	1.39	11.95	7.33	6.90	6.73	2.42	39.25	12.56	0.32	5.69	1.82
BW68	1.47	13.47	5.90	5.53	5.27	4.70	41.25	19.40	0.47	7.46	3.51
BW69	1.54	12.78	6.70	6.30	5.98	4.97	42.39	15.19	0.36	6.73	2.41
BW70	1.61	11.44	5.79	5.55	5.07	8.66	37.11	13.51	0.36	6.68	2.43
BW71	1.68	12.79	6.27	5.98	5.63	5.88	41.23	16.20	0.39	6.89	2.71
BW72	1.75	13.56	6.10	5.86	5.46	6.92	38.97	13.78	0.35	6.65	2.35
BW73	1.82	12.37	9.70	9.18	8.81	3.96	80.72	32.02	0.40	8.80	3.49
BW74	1.96	13.77	7.18	6.90	6.46	6.32	47.47	18.35	0.39	6.88	2.66
BW75	2.06	11.99	8.89	8.55	8.17	4.39	58.17	29.71	0.51	6.81	3.48
BW76	2.16	12.65	14.44	13.91	13.12	5.68	134.59	62.54	0.46	9.67	4.50
BW77	2.26	12.46	14.22	13.69	13.00	4.99	143.50	70.43	0.49	10.48	5.15
BW78	2.41	11.72	16.41	15.95	6.57	58.82	184.89	63.35	0.34	11.59	3.97

Sample Name	Elevation m OD	HIRM 10^{-5} Am^2kg^{-1}	Hard %	ARM 10^{-5} Am^2kg^{-1}	SIRM/ARM no units	'Soft' 10^{-5} Am^2kg^{-1}	IRM_{-20} %	IRM_{-30} %	IRM_{-40} %	IRM_{-50} %	IRM_{-100} %	IRM_{-300} %
BW1	-0.05	13.24	5.90	26.00	8.64	56.48	25.15	36.92	46.97	56.72	83.95	94.10
BW2	-0.03	13.18	5.98	27.62	7.98	50.30	22.81	37.12	47.01	55.74	83.68	94.02
BW3	-0.01	13.33	6.33	29.23	7.21	48.58	23.04	36.78	46.30	57.56	83.53	93.67
BW4	0.01	9.28	6.27	16.01	9.26	28.65	19.34	32.15	39.88	51.46	82.18	93.73
BW5	0.03	7.97	6.22	11.96	10.72	25.03	19.53	33.52	46.84	53.57	81.97	93.78
BW6	0.06	8.49	6.27	11.74	11.55	23.63	17.43	32.11	39.63	49.87	81.21	93.73
BW7	0.08	7.19	5.01	14.44	9.94	25.58	17.81	27.33	41.90	52.74	83.06	94.99
BW8	0.10	6.57	4.76	12.67	10.88	25.63	18.59	28.61	38.59	47.61	83.46	95.24
BW9	0.12	5.97	2.20	13.04	20.86	36.25	13.33	20.20	29.17	36.55	78.42	97.80
BW10	0.14	7.95	2.29	16.21	21.41	39.59	11.41	20.63	29.85	38.31	80.21	97.71
BW11	0.16	6.69	2.11	17.07	18.56	41.58	13.12	20.88	28.62	38.48	82.51	97.89
BW12	0.18	9.11	3.61	19.81	12.74	33.34	13.20	24.33	31.50	42.77	80.88	96.39
BW13	0.20	10.51	3.04	29.43	11.74	49.74	14.40	22.76	29.65	41.15	79.02	96.96
BW14	0.23	8.69	3.16	27.30	10.06	45.42	16.54	24.98	32.70	43.24	80.73	96.84
BW15	0.25	9.73	3.66	25.25	10.51	44.03	16.59	25.29	34.78	43.53	81.11	96.34
BW16	0.27	9.90	4.41	23.74	9.45	38.13	17.00	27.42	35.18	47.80	81.13	95.59
BW17	0.29	9.05	5.03	19.98	9.00	35.56	19.77	30.16	40.62	48.55	82.07	94.97
BW18	0.31	8.30	5.09	18.61	8.76	33.83	20.76	30.22	43.39	52.16	83.06	94.91
BW19	0.33	9.39	5.77	22.38	7.27	35.92	22.07	30.09	44.29	51.37	82.43	94.23
BW20	0.35	8.64	3.67	16.72	14.10	36.24	15.37	24.20	30.52	40.87	80.26	96.33
BW21	0.37	7.85	1.38	22.92	24.86	52.93	9.29	17.52	25.45	35.44	79.06	98.62
BW22	0.40	10.34	3.31	22.31	13.98	44.98	14.42	22.26	31.15	38.99	78.71	96.69
BW23	0.42	9.17	1.77	22.20	23.39	58.86	11.33	18.61	26.39	35.58	78.75	98.23
BW24	0.44	10.66	1.28	22.55	37.08	69.69	8.33	14.77	25.11	33.73	79.28	98.72
BW25	0.46	8.39	1.25	20.28	33.04	60.97	9.10	16.52	26.05	35.39	80.34	98.75
BW26	0.48	9.17	1.48	21.35	29.06	64.03	10.32	15.65	22.54	33.08	76.23	98.52
BW27	0.50	7.12	0.66	23.76	45.66	87.53	8.07	15.30	20.74	32.54	77.72	99.34
BW28	0.52	7.62	0.67	21.00	53.97	90.71	8.00	15.30	24.04	30.70	82.37	99.33
BW29	0.54	9.63	2.48	19.03	20.39	48.79	12.57	18.25	30.12	39.45	82.45	97.52
BW30	0.57	9.49	5.34	17.46	10.18	30.55	17.18	29.80	37.90	47.85	82.24	94.66
BW31	0.59	10.07	5.83	20.18	8.55	37.76	21.88	30.25	42.42	52.44	82.70	94.17
BW32	0.61	10.03	7.50	13.11	10.20	29.64	22.17	30.33	42.73	51.89	78.97	92.50

Sample Name	Elevation m OD	HIRM 10^{-5} Am^2kg^{-1}	Hard %	ARM 10^{-5} Am^2kg^{-1}	SIRM/ARM no units	'Soft' 10^{-5} Am^2kg^{-1}	IRM_{-20} %	IRM_{-30} %	IRM_{-40} %	IRM_{-50} %	IRM_{-100} %	IRM_{-300} %
BW33	0.63	9.98	11.49	3.24	26.76	17.45	20.10	28.06	36.59	46.92	73.54	88.51
BW34	0.65	10.43	10.93	3.33	28.66	17.31	18.14	27.52	39.44	48.00	74.49	89.07
BW35	0.67	10.68	10.55	4.06	24.94	22.02	21.76	31.77	39.42	48.45	75.49	89.45
BW36	0.69	10.77	9.39	6.16	18.60	23.00	20.06	28.63	40.19	50.08	77.23	90.61
BW37	0.71	9.12	8.56	7.51	14.17	19.68	18.48	31.29	38.55	50.37	78.25	91.44
BW38	0.74	10.28	8.91	11.10	10.40	21.62	18.73	32.66	43.06	48.83	77.78	91.09
BW39	0.76	10.42	8.93	11.00	10.62	24.37	20.86	32.87	41.90	50.26	78.88	91.07
BW40	0.78	8.61	8.02	10.18	10.55	24.50	22.82	30.42	43.29	52.56	79.47	91.98
BW41	0.80	10.34	7.46	16.89	8.20	27.09	19.56	31.23	43.48	52.11	81.36	92.54
BW42	0.82	10.34	7.24	17.97	7.94	29.69	20.80	34.63	44.65	54.43	81.44	92.76
BW43	0.84	10.87	7.12	21.09	7.25	31.57	20.66	30.80	44.65	53.62	82.44	92.88
BW44	0.86	9.98	7.30	17.19	7.96	29.44	21.53	34.37	42.83	54.38	82.50	92.70
BW45	0.88	9.13	7.09	14.49	8.88	28.22	21.94	33.89	43.39	54.59	81.23	92.91
BW46	0.91	9.44	7.47	13.60	9.30	28.72	22.71	31.09	42.96	54.13	80.95	92.53
BW47	0.93	9.24	6.87	15.23	8.83	30.35	22.58	32.74	44.72	52.66	81.46	93.13
BW48	0.85	9.62	15.24	2.13	29.60	12.50	19.80	28.85	38.14	45.84	68.41	84.76
BW49	0.88	9.99	16.44	2.07	29.41	12.61	20.76	30.75	38.72	46.69	67.18	83.56
BW50	0.91	11.19	19.03	2.38	24.73	11.89	20.23	28.47	37.82	44.53	63.44	80.97
BW51	0.94	9.40	18.51	1.77	28.65	9.95	19.58	30.12	35.84	43.52	63.10	81.49
BW52	0.96	11.28	21.62	1.74	30.00	9.34	17.91	27.71	35.31	41.04	59.15	78.38
BW53	0.99	9.42	17.68	2.22	23.98	9.78	18.36	29.58	38.43	44.62	62.83	82.32
BW54	1.02	10.37	19.20	2.08	25.96	10.50	19.44	30.10	38.00	44.22	63.63	80.80
BW55	1.05	13.61	21.81	3.14	19.86	11.85	18.98	25.45	33.71	42.47	60.90	78.19
BW56	1.08	12.80	22.08	2.35	24.65	11.08	19.12	26.65	35.68	41.37	59.77	77.92
BW57	1.11	11.99	22.69	1.36	39.00	9.65	18.26	25.99	35.84	40.56	57.49	77.31
BW58	1.13	10.97	22.75	0.99	48.73	9.30	19.28	25.98	34.58	39.90	56.57	77.25
BW59	1.16	10.88	22.96	1.12	42.32	8.16	17.22	26.86	32.76	38.98	56.49	77.04
BW60	1.19	10.59	24.37	0.88	49.14	7.18	16.52	25.45	31.26	38.09	54.15	75.63
BW61	1.22	10.77	22.61	1.07	44.64	8.38	17.60	25.88	33.03	39.13	56.21	77.39
BW62	1.25	9.89	22.93	1.16	37.07	7.72	17.91	24.76	33.11	39.07	55.74	77.07
BW63	1.27	10.86	21.58	1.57	32.13	9.35	18.57	26.90	34.21	40.30	57.53	78.42
BW64	1.30	10.64	22.36	1.25	38.21	7.92	16.64	26.44	33.19	39.49	56.71	77.64
BW65	1.33	11.05	25.80	1.33	32.10	6.19	14.45	24.08	31.07	36.02	52.42	74.20
BW66	1.36	11.00	28.04	1.01	38.82	5.78	14.72	22.65	29.38	34.57	49.74	71.96
BW67	1.39	10.88	27.73	1.00	39.27	5.97	15.20	21.14	29.22	35.15	50.53	72.27
BW68	1.47	9.47	22.97	1.54	26.70	7.32	17.74	25.83	31.37	39.34	56.12	77.03
BW69	1.54	10.15	23.95	1.21	35.07	7.62	17.97	24.73	31.32	38.56	54.39	76.05
BW70	1.61	8.95	24.11	1.08	34.51	6.38	17.19	23.84	32.63	38.61	53.69	75.89
BW71	1.68	9.58	23.25	1.29	31.98	6.72	16.29	25.96	31.05	38.11	54.89	76.75
BW72	1.75	8.95	22.97	1.10	35.53	7.36	18.87	24.50	34.24	38.16	54.67	77.03
BW73	1.82	10.42	12.91	2.55	31.67	28.05	34.75	47.25	55.62	61.09	74.68	87.09
BW74	1.96	10.47	22.05	1.46	32.50	8.80	18.54	28.22	34.12	41.49	56.34	77.95
BW75	2.06	10.41	17.90	2.37	24.59	12.75	21.92	32.60	42.87	47.84	63.91	82.10
BW76	2.16	12.67	9.41	4.98	27.04	40.88	30.37	42.39	52.61	58.12	77.17	90.59
BW77	2.26	13.79	9.61	5.61	25.60	35.99	25.08	39.01	49.26	55.04	76.02	90.39
BW78	2.41	10.07	5.44	5.04	36.66	68.97	37.31	48.47	62.14	68.17	84.98	94.56